Contribution of Energy Metabolism to Cardiomyocyte Maturation

by

Kaya Lutchmi Persad

A thesis submitted in partial fulfillment of the requirements for the degree of

Master of Science

Medical Sciences – Pediatrics

University of Alberta

Abstract:

Proliferating cells, such as neonatal cardiomyocytes, have a high Warburg effect, which is a metabolic state in which there is high rates of glycolysis uncoupled from glucose oxidation under aerobic conditions. The Warburg effect is typically seen in cancerous cells and actively proliferating cells, such as fetal cardiomyocytes. In the newborn period there is a decreased proliferation of cardiomyocytes accompanied by a decrease in glycolysis. This is followed by the maturation of cardiomyocytes. This change in energy metabolism in the newborn heart may be due to changes in energy substrate availability, such as an increase in circulating ketone levels. Ketones have the potential to modify the Warburg effect, either through altering glycolysis or glucose oxidation. Ketones, such as β-hydroxybutyrate (BOHB), are not only a fuel source for the heart, but also have cell signaling properties, including the endogenous inhibition of histone deacetylases (HDAC). HDAC2 knockout and knockdown studies in animals and cell cultures are known to increase differentiation and reduce proliferation of cancerous cells. The objective of this study is to determine if the Warburg effect influences maturation of cardiomyocytes, and whether ketones, affect this process.

Objective 1: To determine if the Warburg effect influences maturation of cardiomyocytes, and whether ketones, which increase in the newborn period, affect this process.

Objective 2: To understand how ketones influence maturation and the Warburg effect in proliferating cardiomyocytes.

Hypothesis: Ketones will promote cardiomyocyte maturation through decreases in glycolysis, and the subsequent decrease of the Warburg effect, and/or due to an inhibition of HDAC2 signalling.

Methods: H9c2 cardiomyocytes were either proliferating or were differentiated (matured) for 7-days using 1uM trans-retinoic acid, in the presence or absence of 1 mM BOHB. The Warburg effect was then directly measured by assessing glycolysis and glucose oxidation. Ketone oxidation and fatty acid oxidation were also assessed. To assess if ketones were acting through metabolic pathways, siRNA was used to knockdown BOHB dehydrogenase 1 (BDH1) the first enzyme involved in BOHB oxidation, in proliferating H9c2 cardiomyocytes. Cells were then cultured in the presence or absence of 1 mM BOHB for 6 days, before assessing glycolysis, glucose oxidation, and ketone oxidation. To assess if ketones were acting through the endogenous inhibition of HDAC2, siRNA was used to knockdown HDAC2 in proliferating H9c2 cardiomyocytes. Cells were then cultured in the presence or absence of 1 mM BOHB for 6 days, before assessing glycolysis, glucose oxidation, and ketone oxidation.

Results: The Warburg effect was high in proliferating cardiomyocytes and was decreased by 78% with maturation. This was not due to an increase in glucose oxidation, but rather due to a decrease in glycolysis in proliferating versus matured cells. Ketones decreased the Warburg effect by 28%. This was due solely to a decrease in glycolysis and not glucose oxidation. Adding ketones to proliferating cells also increased markers of cardiomyocyte maturation such as SERCA2 and PGC-1α. Knocking down BDH1 did decrease ketone oxidation but was not accompanied by changes in glycolysis or glucose oxidative rates. Furthermore, ketones affected glycolysis similarly in BDH1 knockdown

cells compared to controls in that there was a decrease in the Warburg effect. The knockdown of HDAC2 lead to a increase in glycolysis and glucose oxidation, with reductions in ketone oxidation. The addition of ketones led to a decrease in glycolysis comparable to untreated controls.

Conclusion: Cardiomyocyte maturation is associated with a reduced Warburg effect, due exclusively to a decrease in glycolysis. Ketones contribute to the decrease in the Warburg effect, primarily by inhibiting glycolysis. The addition of BOHB increases maturation and decreases the Warburg effect in proliferating cardiomyocytes. BDH1 knockdown does not change the effects of ketones on glycolysis in proliferating cardiomyocytes. HDAC2 knockdown increases glycolysis in proliferating H9c2 cells, however this affect is abolished by the addition of ketones. This indicates that HDAC2 signaling may play a key role in ketones regulation of cardiomyocyte maturation. These results have potential implications in understanding the maturation of cardiomyocytes in the newborn period.

Preface

This thesis is an original work by Kaya Lutchmi Persad. None of the data in this thesis has previously been published. Some sections of the literature review were adapted from a review by Kaya L. Persad and Gary D. Lopaschuk: Energy Metabolism on Mitochondrial Maturation and Its Effects on Cardiomyocyte Cell Fate (1)

Acknowledgments

I would like to start by thanking my supervisor, Dr. Gary D. Lopaschuk for his support, mentorship, and guidance over the last two and half years. Thank you for giving me so many meaningful opportunities to grow and learn more in this field, to think outside of the box, and to develop my leadership and troubleshooting skills.

I would also like to thank my committee members, Dr. John R. Ussher and Dr. Jason R.B. Dyck for their time and thoughtful feedback on how to improve my research.

Thank you to my fellow lab members: Berna Güven, Qiuyu (Violet) Sun, Qutuba Karwi, Ezra Ketema, Kim Ho, Muhammad Ahsan, Kaleigh Wei, Sai Panidarapu, Donna Andre, Liyan Zhang, and Cory Wagg. I have had such a great time with all of you and I am so grateful for the opportunity to meet you all. A special thank you to Violet, Berna, and Qutuba for all of your support and friendship.

Thank you to my summer student and Pharmacology Honors project student Madeline Houncaren, and summer student Jalene Greenwood for their help and support for this project. I really enjoyed mentoring these two; thank you for working so diligently and helping me become a better mentor.

I would also like to thank my sources of funding through the University of Alberta, the Women's, and Children Health Research Initiative (WCHRI) through the Stollery Children's Hospital Foundation, and the Canadian Institutes for Health Research (CIHR).

Last but not least I would like to thank my family. Thank you to my parents, Sujata, and Rabindranath Persad; to my siblings: Amit, Neesha, and particularly my little brother Rohan (aka my therapist); and to the best dog, Mochi. I appreciate all of your love,

encouragement, and support throughout my life and during the challenges of doing my MSc degree. I don’t think that I could have done it without you!

Table of Contents

List of Tables

List of Figures

List of Abbreviations

Abbreviations	Definition
ACC	Acetyl CoA carboxylase
ATGL	Adipose triglyceride lipase
ATP	Adenosine triphosphate
BDH1	BOHB dehydrogenase 1
BOHB	β-hydroxybutyrate
BSA	Bovine serum albumin
CHD	Congenital heart defects
CPT-1	Carnitine palmitoyl transferase 1
ddH_2O	Double distilled water
DMEM	Dulbecco's Modified Eagle Medium
ECs	Endothelial cells
ESCs	Embryonic stem cells
ETC	Electron transport chain
F-1,6-BP	Fructose-1,6-bisphosphate
F-2,6-BP	Fructose-2,6-bisphosphatase
FBS	Fetal bovine serum
Foxo3a	Forkhead box O3
G6PD	Glucose 6 phosphate dehydrogenase
H_2SO_4	Sulfuric acid
HDAC	Histone deacetylase

hESCs	Human ESCs
hESC-CMs	hESC derived cardiomyocytes
HIF-1α	Hypoxia inducible factor 1-alpha
hiPSC-CMs	Human induced pluripotent stem cell derived cardiomyocytes
IDH	Isocitrate dehydrogenase
ISCs	Intestinal stem cells
KD	Ketogenic diet
KLF7	Kruppel Like Factor 7
LCAD	Long-chain acyl-CoA dehydrogenase
LT-HSCs	Long term hematopoietic stem cells
MCD	Malonyl-CoA decarboxylase
MCK	Muscle creatine kinase
MI	Myocardial infarction
MPC	Mitochondrial pyruvate carrier
mtDNA	Mitochondrial deoxyribose nucleic acid
NAD^+	Nicotinamide adenine dinucleotide
NADH	NAD^+ + Hydrogen
NADPH	NAD^+ phosphate
NMR	Nuclear magnetic resonance
PBS	Phosphate buffered saline
PDH	Pyruvate dehydrogenase
PDK	PDH kinase

PFK-1	Phosphofructokinase
PFKFB3	6-phosphofructo-2-kinase/Fructose-2,6-bisphosphate
PGC-1α	PPAR gamma coactivator `1 alpha
PKM2	Pyruvate kinase isoform M2
PPAR	Peroxisome proliferator activated receptor
PPI	Phosphatase inhibitors
PPP	Pentose phosphate pathway
PVDF	Polyvinylidene difluoride
RA	All-trans retinoic acid
RXR	Retinoid X receptor
SDS-PAGE	Sodium dodecyl sulfate polyacrylamide gel electrophoresis
SERCA2	Sarco/endoplasmic reticulum CA^{2+} ATPase
siRNA	Small interfering ribonucleic acid
TCA	Tricarboxylic acid

CHAPTER 1: Literature Review

**Some sections of this literature have been adapted from a review written by Kaya L. Persad and Gary D. Lopaschuk (1)*

In the newborn period the heart undergoes dramatic changes. The proliferation of cardiomyocytes is halted almost immediately after birth, and cardiac cells transition such that they experience physiological hypertrophy, multinucleation, and an increase the expression of sarcomeric proteins (2). These changes are required in order to support the heart's ability to constantly pump blood throughout the body. During this period of maturation, there are significant changes in energy metabolism. In the fetal period, the heart primarily relies on glycolysis to support proliferation; conversely, shortly after birth there is a decrease in glycolysis and a subsequent increased reliance on oxidative metabolism- mainly fatty acid oxidation (3). Given that the heart has limited energy stores, this switch in metabolism is crucial to provide the continuously beating heart with sufficient adenosine triphosphate (ATP) to meet the extensive energetic demands.

1.1 The Warburg effect

The Warburg effect is a metabolic state in which there are high rates of glycolysis uncoupled from glucose oxidation under aerobic conditions, leading to increased production of lactate (Figure 1.1).The Warburg effect is typically seen in cancerous cells and actively proliferating cells (4), but is also present in fetal proliferating cardiomyocytes (3) and hypertrophied myocardium (5). In cancer cells, a high Warburg effect promotes

their growth, survival, and proliferation. Given that stem cells have a high rate of glycolysis, even in the presence of oxygen, they also exhibit the Warburg effect (6–8). This is thought to be due to a low copy number of mitochondrial deoxyribose nucleic acid (mtDNA) within stem cells, leading to more immature mitochondria (6,9). Although the Warburg effect is inefficient in its ability to produce ATP, the carbons from glucose can be used for anabolic processes needed to support cell proliferation (10–12). Particularly, there is a greater synthesis of reducing equivalent in the pentose phosphate pathway (PPP), such as reduced nicotinamide adenine dinucleotide phosphate (NADPH), which is highly consumed during the synthesis of amino acids and nucleotides needed to replicate cellular content during division (11,13). Additionally, a characteristic of the Warburg effect is that the fate of pyruvate to lactate production is higher, leading to the regeneration of nicotinamide adenine dinucleotide (NAD^+) from NAD^+ + hydrogen (NADH), which further supports proliferation and allows for the continuation of glycolysis (11). When stem cells differentiate and mature, there is a reversal of the Warburg effect, as evidenced by a decrease in glycolysis and an increase in oxidative phosphorylation, as discussed above, in order to better support the needs of the differentiated cells (14) (Figure 1.1).

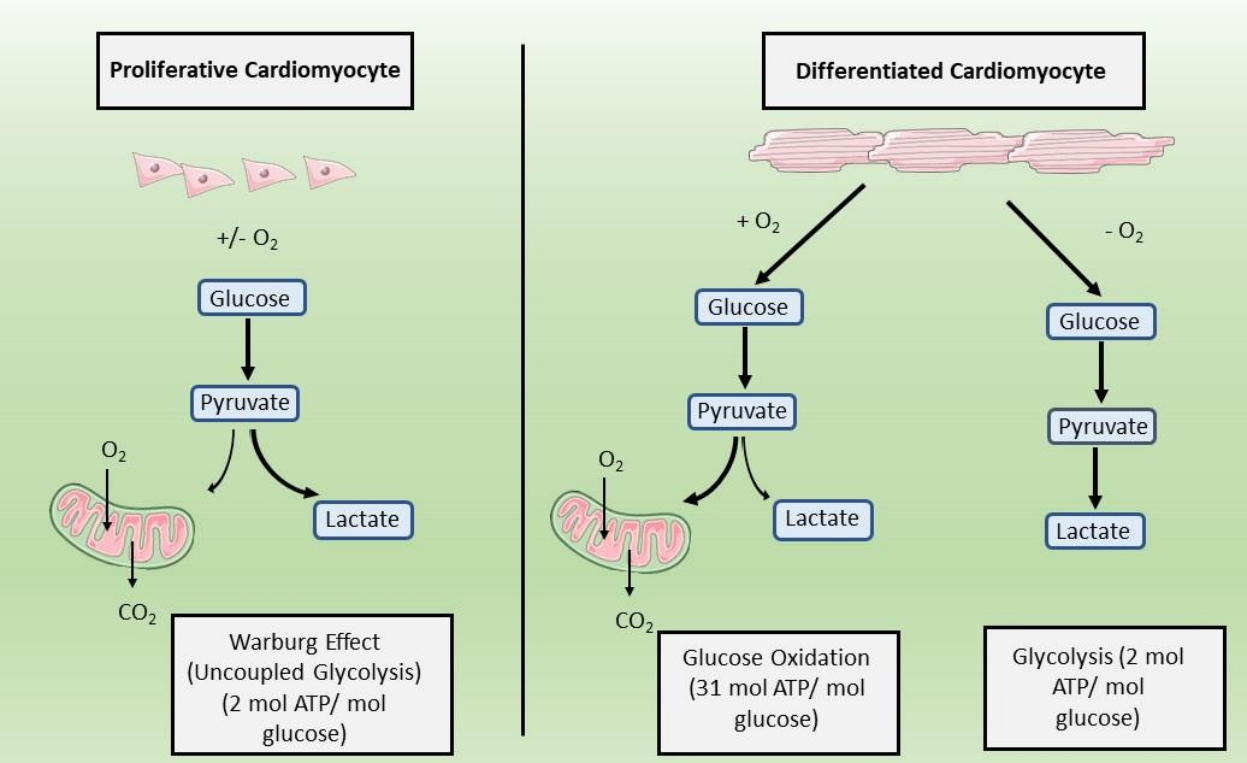

Figure 1.1 **The Warburg effect.** Graphic presentation of how glucose is metabolised under the conditions of the Warburg effect in proliferating cardiomyocytes such that there is a higher rate of glycolysis uncoupled from glucose oxidation regardless of oxygen availability. This is altered under conditions of differentiation such that there is an increase in glucose oxidation couple with glycolysis under aerobic conditions. Under aerobic conditions, glucose is only capable of being metabolized through glycolysis. Adenosine triphosphate (ATP). Oxygen (O_2). Carbon dioxide (CO_2).

1.2 Cardiac maturation

The fetal heart's metabolism reflects the Warburg effect, as there is a high dependency on glycolysis for energy production. This is largely due to the fact that in the later stages of fetal heart formation, cardiogenic cells rapidly proliferate to complete the development of the heart (15). This is mediated through hypoxia-inducible factor 1-alpha (HIF-1α) that

is generated due to the fetal heart's location within a low oxygen environment (16,17). To optimize the heart for strong, lifelong, and efficient pumping, fetal cardiomyocytes must undergo maturational changes. This involves changes in cell structure, gene expression, and importantly, cellular metabolism (18). As early as 7 days post-birth, there is a decrease in glycolysis such that it now only contributes to 10% of ATP production (as opposed to > 40% of ATP production in fetal life) (3,19). This reduction in glycolysis is indicative of a reduced Warburg effect. Interestingly, glucose oxidation still remains low during this time, most likely due to an increase in pyruvate dehydrogenase kinase (PDK) expression, which phosphorylates and inhibits pyruvate dehydrogenase (PDH) (3). As discussed previously, glucose oxidation does not fully mature in the heart until the infant is weaned from breast milk (20). Rather, the heart switches from primarily glycolytic metabolism to fatty acid oxidation immediately post birth (3). This switch is also seen in human induced pluripotent stem cells derived cardiomyocytes (hiPSC-CMs) (21). Exposure to high levels of glucose leads to an impaired differentiation into cardiomyocytes, seen in both human and mouse embryonic stem cells (ESCs) (22,23). Conversely, suppressing glucose levels supplements the differentiation and maturation of hiPSC-CMs (22). Together, this indicates the reliance that proliferating stem cells or immature cardiomyocytes have on the Warburg effect, and that this is reversed during differentiation and maturation. A key change indicative of cardiomyocyte maturation is the assembly of sarcomeres in cardiomyocytes, leading to increased expression of sarcomere proteins, such as sarco/endoplasmic reticulum Ca^{2+}-ATPase (SERCA2) and cardiac troponin T (24). The process of cardiomyocyte maturation occurs in the immediate

newborn period when cardiomyocytes lose their proliferative capacity but increase their contractile ability (18).

1.2.1 Role of mitochondrial biogenesis in the maturation of cardiomyocytes

1.2.1.1 Postnatal cardiomyocyte maturation

Cardiac energy demands are dynamic during developmental stages; as a result, mitochondrial number and function must change to support these changes in energy demand (25). During the early postnatal period, myocardial energy demand increases dramatically; as such there is an observed increase in the number of mitochondria in the cell and hence an increase in mitochondrial proteins (25,26). Cardiac mitochondria are characterized by their ability to efficiently produce ATP through oxidative metabolism (27). Increases in mitochondrial number and proteins are associated with increased mitochondrial biogenesis; this is mainly regulated through peroxisome proliferator-activated receptor (PPAR) gamma coactivator 1 alpha (PGC-1α) and PGC-1β, which seem to have over-lapping roles in the heart in the immediate postnatal stage (28). In mouse hearts, PGC-1α gene expression is increased directly after birth; this is observed before increases in mitochondrial biogenesis, or the switch of energy production from relying mainly on glucose to relying on fatty acids (29). If PGC-1α is overexpressed in primary rat neonatal ventricular cardiomyocytes, there is an increase in mitochondrial biogenesis and oxidative phosphorylation. If PGC-1α is overexpressed *in vivo* in transgenic mice there is an uncontrollable mitochondrial biogenesis, with the mice presenting with massive edema, increased heart size, and cardiomyopathy (29).

Therefore, it appears that there is a certain threshold of PGC-1α expression needed to properly regulate the heart's development. However, it is clear that an increase in PGC-1α is associated with a matured heart.

When PGC-1α or PGC-1β is knocked out in mice it was observed that, while the animals lived, there was a decrease in the growth of the heart and slow-twitch skeletal muscle, both of which have a high energy demand (30,31). If a PGC1α/β double knock out is produced, the mice die soon after birth, and they have smaller hearts, irregular rhythms and reduced cardiac output (28). Martin et al., (32) created a viable PGC1-α/β deficient mouse through the deletion of PGC-1β in the heart and skeletal muscle through the actions of Cre recombinase regulated by the muscle creatine kinase (MCK) promoter (MCK-Cre) with a generalized PGC-1α null background (PGC-1α$^{-/-\beta f/f/MCK\text{-}Cre}$). They showed that the loss of both PGC-1α and PGC-1β during postnatal development results in lethal cardiomyopathy due to defects in mitochondrial maturation and reduced expression of genes associated with mitochondrial dynamics (32). Additionally, these changes were associated with a decrease in mtDNA, and electron transport chain (ETC) complexes I and IV. Further, Martin et al., (32) demonstrated that the deletion of PGC-1α/β did not affect mitochondrial dynamics in adult mouse hearts. This demonstrates the importance of PGC-1α and PGC-1β in the newborn period, as this is where the most dramatic effects on mitochondrial maturation and biogenesis are seen.

1.2.1.2 Stem cells

Stem cells are non-specialized cells, which under certain conditions, can mature into cells with a specific function, including differentiating to cardiomyocytes. In the mature cardiomyocyte, mitochondria take up a significant amount of cell space, occupying 20-40% of cell volume (33). During prolonged culture of hiPSC-CMs there is an increase in mitochondrial biogenesis, as well as increases in membrane potential and ETC complex activity (34). In line with this increase in mitochondrial biogenesis, within hiPSC-CMs there is a significant upregulation of PGC-1α, which promotes a more mature metabolism consistent with cardiomyocytes (35). ZLN005, a chemical which increases PGC-1α gene expression, will promote the maturation of cardiomyocytes derived from human embryonic stems cells (hESCs) (36). This indicates the importance of PGC-1α activation in a stem cells ability to differentiate into a cardiomyocyte.

1.2.2 Metabolic changes during cardiomyocyte maturation

In the following section the roles of glycolysis, glucose oxidation, fatty acid oxidation, and ketone oxidation in the regulation of cell maturation will be discussed. While the focus is on their influence on cardiomyocyte maturation, discussion of other cell types, such as a cancer cells, will be included as this may ultimately inform our understanding of cardiomyocyte maturation.

1.2.2.1Glucose metabolism

1.2.2.1.1 Glycolysis

High rates of glycolysis are a common characteristic of proliferating cells, including fetal cardiomyocytes, stem cells, and tumor cells. The high glycolytic rates are an alternative source of energy, or ATP, production for proliferating cells that have an immature mitochondrial morphology, decreased mitochondrial respiration and lower oxidative reserve capacity compared to differentiated cells (6,7,37,38). During differentiation of cells, such as maturation of cardiomyocytes following birth, there is a dramatic decrease in glycolysis as mitochondrial oxidative metabolism increases (3) (Figure 1.2). In contrast, increases in glycolytic enzymes are observed during nuclear reprogramming toward a more pluripotent or stem like state (6,39). In long-term hematopoietic stem cells (LT-HSCs) there are high levels of glycolytic intermediates (i.e., fructose-1,6-bisphosphate (F-1,6-BP), and pyruvate), which are the products of the rate limiting steps of glycolysis (40). LT-HSCs also have a high expression of PDK2 and 4, enzymes which phosphorylate and inactivates PDH, essentially enhancing the Warburg effect by uncoupling glycolysis from glucose oxidation (41). Although glycolysis is a much less efficient way to generate ATP compared to glucose oxidation, it does allow for ATP to be generated quickly and in the absence of oxygen (42). Proliferating cells are not limited by ATP production as glycolytic cells are able to maintain a high ATP/ADP ratio, even during division (10,43). However, high rates of glycolysis are advantageous to rapidly dividing cells, as it allows for the maintenance of intermediates required for the biosynthesis of cellular content for the daughter cells (11,44). PPP intermediates, such as ribose-5-phosphate, provide the carbons for purine and pyrimidine nucleotides, amino acid, and triacylglycerol/lipid synthesis (44). The premature inhibition of glycolysis in stem cells can lead to cell death, whereby stimulating glycolysis through the inhibition of oxidative phosphorylation

maintains the stemness of a cell and reduces its ability to differentiate (7,45). During the maturation of cardiomyocytes from the fetal to the newborn period, a switch from glycolysis to oxidative phosphorylation is required for proper development (3,46). In order to support the ATP needs of differentiated cells, there is an upregulation in tricarboxylic acid (TCA) cycle enzymes and ETC subunits (8,47).

Pyruvate Kinase isoform M2 (PKM2), 6-phosphofructo-2-kinase/Fructose-2,6-bisphosphate (PFKFB3), and glucose-6-phosphate dehydrogenase (G6PD) have been identified as key regulators of the Warburg effect in proliferating cells (Figure 1.2). Pyruvate kinase dephosphorylates phosphoenolpyruvate during glycolysis, producing ATP and pyruvate. As discussed previously, anabolic metabolism is integral to proliferative capacity. PKM2 is mainly expressed in proliferating cells, however it has lower enzymatic activity compared to PKM1 which is mainly expressed in adult cells (43,48). In proliferating cells, PKM2 exist in a dimer conformation, which has a lower enzymatic activity and promotes an increase in anabolic metabolism, through the PPP, which subsequently allows for the synthesis of biomolecules necessary for proliferation (49). PKM2 can shift into an active tetrameric conformation by upstream F-1,6-BP (50). As such, small molecule activators of PKM2 have been studied as a way to induce the active tetrameric conformation of PKM2, which resemble the effects of PKM1 substitution studies, leading to decreased tumorgenicity (43,51). Studies in which PKM2 is activated to its tetrameric conformation were shown to lead to a decrease in the cells ability to proliferate (51–53). PKM2 also seems to play a role in the fate of pyruvate, as it can be reduced to lactate or oxidized to acetyl-CoA for further pyruvate oxidation. Increased

PKM2 activity leads to an increase in the amount of pyruvate being used for mitochondrial oxidative metabolism, and a reduced production of lactate (43). This may be due to an increase in PKM2 binding to Mfn2, which promotes mitochondrial fusion, through mTOR, which subsequently leads to an increase in oxidative phosphorylation and a decrease in glycolysis (54). During cardiomyocyte development, PKM2 appears to have a significant role, as it is highly expressed during development and immediately after birth, although it is replaced by PKM1 in the adult cardiomyocyte (55). As such, more research regarding the role of PKM2 in cardiomyocyte proliferation and differentiation is necessary.

The role of PFKFB3 in cell fate has been mainly studied in the context of cancer and angiogenesis (the process of forming new blood vessels). PFKFB3 is responsible for an increased synthesis of fructose-2,6-bisphosphatase (F-2,6-BP), which allosterically regulates phosphofructkinase-1 (PFK-1) (56–58). PFK-1 catalyzes a key rate limiting step of glycolysis, the conversion of fructose-6-phosphate to F-1,6-BP (59). PFKFB3 is associated with an increase in glycolysis within cancer cells, as seen by increases in PFKFB3 expression and phosphorylation (60). It has been shown that F-2,6-BP, is upregulated in cancerous cells, associated with stimulation of glycolysis, and its depletions can suppress cell survival and proliferation (61,62). As such, the inhibition of PFKFB3, and the subsequent decrease in F-2,6-BP, has been examined with findings indicating that the inhibition of PFKFB3 reduces glycolysis, slows tumor growth and induces cell death (60,63,64). PFKFB3 has also been studied in endothelial cells (ECs) during angiogenesis, as they consume high levels of glucose and exhibit the Warburg effect, as they are highly glycolytic, even in the presence of oxygen (65,66). When

PFKFB3 is silenced in ECs, there is a reduction in vessel sprouting/proliferation due an inability to produce energy through glycolysis (65). These bodies of evidence make PFKFB3 an interesting target of the Warburg effect, and further research should be done in understanding its role in the maturing and differentiating cardiomyocyte.

As previously described, elevated levels of anabolic metabolism and the biosynthesis of cellular content is required for rapidly dividing and proliferating cells. The PPP is critical in this process. G6PD shunts glucose from the glycolytic pathway to the PPP, were it leads the production of ribose and NADPH. These products are critical for biosynthesis and anabolic metabolism. Knockdown of G6PD decreases cancer cell proliferation and glycolysis, while reducing the tumorigenic properties of gastric cancer cells (67). In non-cancerous cells, reduced G6PD activity blocks regular proliferation and can lead to deficiencies in growth and development, or potentially death, in animal models (68–71). Increasing PPP activity has been associated with increased and more aggressive tumor malignancy (72). G6PD is regulated by the NADPH/$NADP^+$ ratio, such that a reduction in NADPH activates G6PD (73). Importantly, along with leading to the production of important components for proliferation, NADPH is essential in protecting cells from oxidative stress, as described by Yang et al., (74). Briefly, NADPH is a potent antioxidant, and the knockout of G6PD leaves embryonic stem cells highly sensitized to oxidants, such as diamide, ultimately resulting in increased cell death (75). NADPH is essential to the proper functioning of the major components of the antioxidant system, the glutathione system, catalase, and superoxide dismutase, either through NAPDHs reductive properties, or through allosteric binding (76). In the cardiomyocyte, the

pentose/G6PD/NADPH/ glutathione pathway seems to have a cardioprotective mechanism, as it protects against ROS-induced injury, and deficiencies in G6PD lead to increased myocardial infarction (MI) induced damage in animal models (77,78). Indeed, in hypertrophied cardiomyocytes, which typically reflect a more fetal like metabolic system (46), there is a decrease in G6PD expression (79). Moreover, restoring G6PD activity prevents the dysregulation of mitochondrial function and oxidative stress experienced by these cells (79). This indicates the importance of the presence of G6PD in adult cardiomyocytes. Of note, this seems to be at odds with the high activity of G6PD also seen in proliferative cancer cells. Considering that differentiated cells seem to have almost opposite metabolic profiles compared to proliferating cells, further research needs to be done looking at the role of G6PD in cardiomyocyte development and differentiation.

1.2.2.1.2 Glucose oxidation

Differentiated cells, such as cardiomyocytes, require more ATP to sustain specialized functions such as contraction (80). As such, there is a transition from having high rates of glycolysis, to increased mitochondrial oxidative phosphorylation (Figure 1.2). This is supported by increases in TCA cycle and ETC enzymes/subunits which allows for greater ATP production (8,47). This shift is necessary for differentiation, as blocking the ETC leads to an impaired ability of ESCs to differentiate (81). Further, when key enzymes of glycolysis and the PPP are inhibited, myogenic differentiation is stimulated (82).

A crucial step in glucose oxidation is the initial mitochondrial uptake of pyruvate derived from glycolysis by the mitochondrial pyruvate carrier (MPC) complex, which transfers

pyruvate into the mitochondria to undergo further metabolism. MPC is found in low levels in intestinal stem cells, and in high amounts when these cells are differentiated (83). When glucose oxidation is blocked through the of deletion of MPC, there is an increase in stem cell number and proliferation (83).

PDH is a key enzyme that converts the end product of glycolysis, pyruvate, to acetyl-CoA. This is integral to the production of ATP, and couples the process of glycolysis and glucose oxidation. The phosphorylation of PDH inactivates this enzyme and leads to a reduction of pyruvate to acetyl-CoA, ultimately uncoupling glycolysis and glucose oxidation (84). Under these inactivated conditions is when the Warburg effect is high, such as in rapidly proliferating cells. Therefore, it would be reasonable to expect that the phosphorylated (inactive) form of PDH would predominate over the unphosphorylated (active) form PDH in rapidly proliferating cells when the Warburg effect is present and reliance on glycolysis uncoupled from glucose oxidation is high.

If PDH is disrupted with RNAi there is an increase in intestinal stem cells (ISCs) proliferation (83). This indicates the significant role that glucose oxidation plays in the regulation of stem cell fate, as inhibiting glucose oxidation through the inhibition of MPC or PDH leads to an increased stem-like state with increased proliferation.

The switch from glycolysis to mitochondrial oxidative phosphorylation as a source of ATP production in the maturing cell would be expected to be accompanied by an increase in

glucose oxidation. Curiously, however, during the initial maturation of cardiomyocytes, there is not a substantial increase in glucose oxidation, but rather an increased oxidation of other energy substrates, such as fatty acids (3). Glucose oxidation in the newborn heart does not typically increase until weaning (3). What is responsible for this delayed maturation of glucose oxidation is not clear, although competition between glucose oxidation and fatty acid oxidation as a source of TCA acetyl CoA may contribute to these low rates of glucose oxidation.

1.2.2.2 Fatty acid oxidation

Mitochondrial fatty acid oxidation plays a vital role in cardiomyocyte maturation. A dramatic increase in fatty acid oxidation occurs in the maturing heart following birth (3). Interestingly, a decrease in fatty acid oxidation is seen in the stressed heart, such as seen with congenital heart defects, that maintains a more fetal metabolic and contractile phenotype (5,85). In the transition from the fetal to newborn period, there are significant changes in energy metabolism (3). Fatty acid oxidation is low in the fetal heart as a result of the low levels of fatty acids present (20). In the newborn period, there is a shift in the metabolic profile to sustain the cellular growth that occurs during this period (86,87). This includes a shift towards increased fatty acid oxidation, which produces the majority of ATP in the newborn and supports the increased requirement for ATP from the rapidly growing and beating heart (3,88) (Figure 1.2). This is similar to the adult heart in which the majority of ATP produced is obtained from mitochondrial oxidative phosphorylation, with 60-90% of acetyl-CoA being produced from fatty acid oxidation and 10-40% being derived from the oxidation of pyruvate (27,89). Of the fatty acids that enters adult

cardiomyocytes, 70-90% are converted to acylcarnitine for oxidation via carnitine palmitoyl transferase 1 (CPT-1), and the other 10-30% enter the intracardiac triacylglycerol pool (90). Fatty acid oxidation is transcriptionally regulated by the PGC-1α/PPARα pathway (91,92). PPARα forms heterodimers with retinoid X receptor (RXR), which regulates the expression of genes involved in fatty acid activation (93), uptake (93–95), and oxidation (93,96,97). PGC-1α also transcriptionally coactivates PPARβ/δ, although there is a high degree redundancy with PPARα in terms of its regulation of fatty acid oxidation (98). This is consistent with increased levels of PGC-1α, and PPARα/β expression in the postnatal heart (28,32,99). Mitochondrial fatty acid uptake is necessary for fatty acid oxidation, and this uptake is mediated by CPT-1 (100). CPT1 is regulated through the inhibitory effects of malonyl-CoA, which is a key regulator of cardiac fatty acid oxidation (100,101). Malonyl-CoA levels are also a key regulator of fatty acid oxidation in the newborn period, with levels decreasing rapidly in the days after birth (102,103). Reduced levels of malonyl-CoA occur due to both a decrease in synthesis and an increase in degradation (102,104). Malonyl-CoA synthesis is catalyzed by acetyl-CoA carboxylase (ACC), an enzyme which is phosphorylated and subsequently inactivated after birth by AMPK (105–107). AMPK also acts as an activator of PGC-1α, which also leads to an increase in fatty acid oxidation (108). Malonyl-CoA is also reduced due to its degradation through decarboxylation by malonyl-CoA decarboxylase (MCD) (104,109). MCD expression is high in the neonatal heart which, along with the inhibition of ACC, leads to a decrease in malonyl-CoA and an increase in fatty acid oxidation (110,111).

Evidence suggests that hiPSC-CMs do not display adult cardiomyocyte metabolism, but rather maintain more fetal cardiomyocyte characteristics (112–114). However, incubating hiPSC-CMS with fatty acid increases maturation, as seen through improvements in morphology, protein expression, and metabolism (particularly through an increase in fatty acid oxidation) (115,116). During the maturation of hiPSC-CMs, PGC-1α is a major upstream regulator, which is a known transcriptional regulator of fatty acid oxidation (35). Additionally, treatment of hESC derived cardiomyocyte (hESC-CMs) with retinoic acid upregulates fatty acid oxidation, through the activation of retinoic acid receptor/RXR and PPAR/ RXR heterodimers (117). This increase in fatty acid oxidation is further evidenced by an overexpression of PDK4, which inhibits PDH activity, and an increased expression of PGC-1α, which leads to an increase in ATP production through fatty acid oxidation (117).

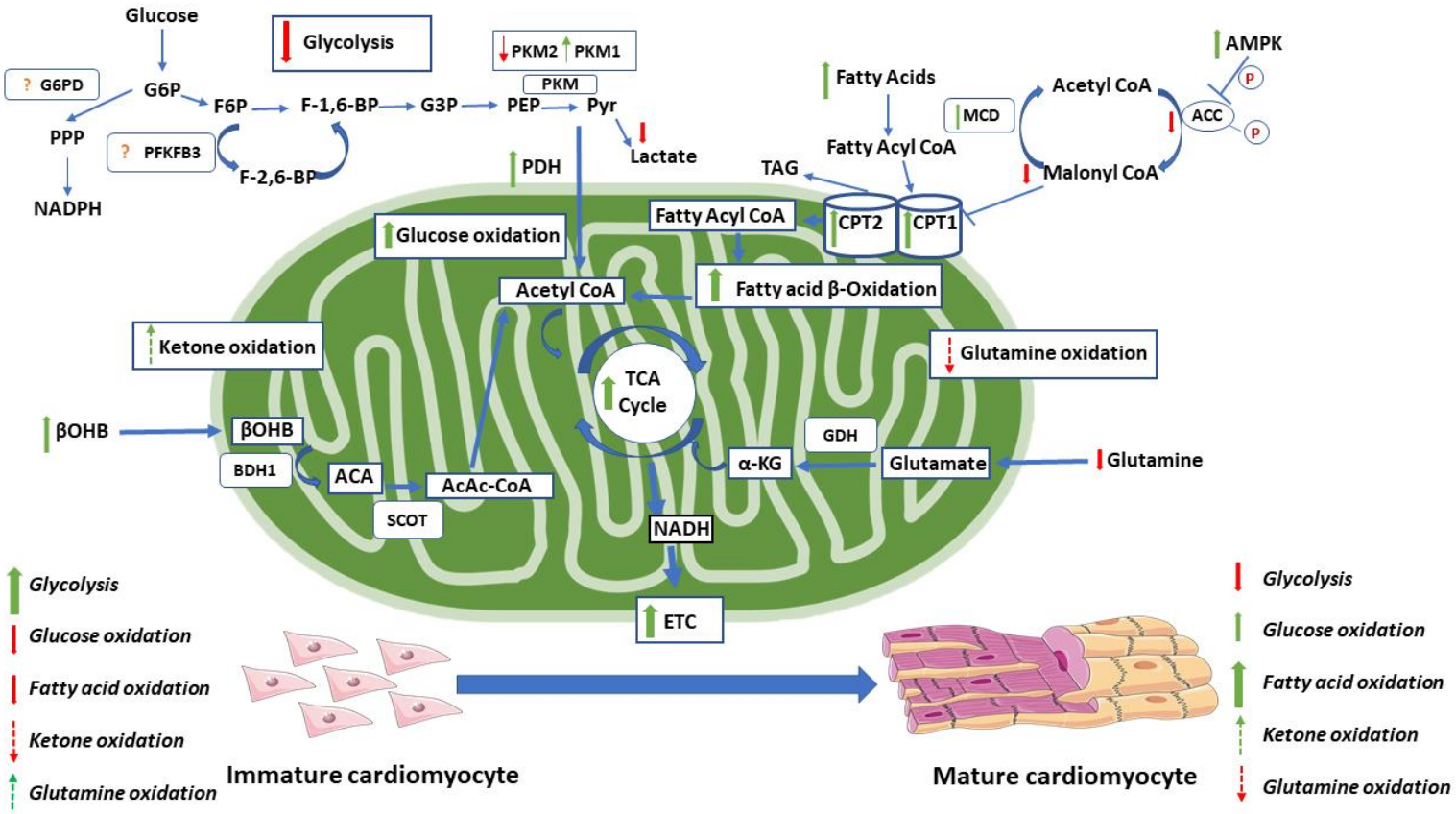

Figure 1.2. **Changes in energy metabolism during the maturation of the cardiomyocyte.** During the maturation of the cardiomyocyte there are significant changes in energy metabolism. This includes increase in oxidative metabolism, with moderate increases in glucose oxidation and dramatic increases in fatty acid oxidation. During this switch, there is also a decrease in glycolytic rates. Red arrows indicate decreases seen with maturation. Green arrows indicate increases seen with maturation. Dashed red arrows indicate proposes decreases seen with maturation (not definitely known). Dashed green arrows indicate proposed increases seen with maturation (not definitely known). The exact changes in the glycolytic regulation through PFKFB3 and G6PD within the maturing cardiomyocyte is not clear and requires further investigation. Acetoacetate (ACA). Acetoacetyl CoA (AcAc-CoA). Acetyl-CoA carboxylase (ACC). AMP-activated protein kinase (AMPK). ß-hydroxybutyrate dehydrogenase 1(BDH1). ß-hydroxybutyrate (BOHB). Carnitine palmitoyl transferase (CPT1). Electron transport chain (ETC). Fructose-1,6- bisphosphate (F-1,6-BP). Fructose-2,6-bisphosphate (F-2,6-BP). Fructose-6-phosphate (F6P). Glucose-3-phosphate (G3P). Glucose-6-phosphate (G6P). Glucose-6-phosphate dehydrogenase (G6PD). Glutamate dehydrogenase (GDH). Malonyl CoA decarboxylase (MCD). Nicotinamide dinucleotide phosphate hydrogen (NADPH). Nicotinamide dinucleotide hydrogen (NADH). Pyruvate dehydrogenase (PDH). Phosphoenolpyruvate (PEP). 6-phosphofructo-2-kinase/Fructose-2,6-bisphosphate (PFKFB3). Pyruvate kinase isoform M1/2 (PKM 1/2). Pentose phosphate pathway (PPP). Pyruvate (Pyr). Succinyl-CoA:3-oxo-acid CoA-transferase (SCOT). Tricarboxylic acid (TCA). Triacylglycerol (TAG). Adapted from Persad and Lopaschuk (1).

1.2.2.3 Ketone oxidation

Ketones bodies are small lipid-derived molecules that can serve as a circulating energy source for many tissues in the body (118,119). The majority of ketone body production occurs in the liver. Fatty acids are first metabolized in the mitochondria to form acetyl-CoA through fatty acid β-oxidation. Acetyl-CoA then undergoes a process in which ketone bodies, such as β-hydroxybutyrate (BOHB), the most abundant circulating ketone body is produced. To utilize BOHB in peripheral tissues, such as the heart, β-hydroxybutyrate dehydrogenase 1 (BDH1) facilitates a reverse process within the mitochondria in order to convert BOHB to acetyl-CoA to enter the TCA cycle (Figure 1.2 and Figure 1.3). Under condition of prolonged fasting, the ketogenic diet (low carbohydrate and high fat diet), and intense exercise, ketone production can increase (118,120).

The role of ketone oxidation in the regulation of cell fate has not been extensively studied. However, emerging evidence suggests a key role for ketones in the regulation of cell fate, such as in cancer (121,122). The increased presence of ketone bodies in the immediate postnatal period also lends to a potential role it may have in regulating cardiomyocyte fate. Ketogenic diets (KD) use a high fat and low carbohydrate diet to increase levels of circulating ketone bodies, the main ketone in humans being BOHB. BOHB has been shown to have an anti-tumor affect in tumor models, through the regulation of the immune system (121). The KD has also been shown to decrease tumor proliferation by decreasing rates of glycolysis (122). A potential mechanism for this is through the inactivation of the insulin/IGF-1 dependent phosphatidylinositol 3-kinase PI3K/Akt/mTOR pathway and the activation of AMPK (123). It should also be noted that the KD leads to increased

mitochondrial enzymes and protein content, as well as increased fatty acid oxidation (124–126). Studies on neurodegenerative disorders have found that treatment with KD leads to a PGC-1α regulated increase in mitochondrial biogenesis (127). This provides evidence that the KD can manipulate the mitochondria, the regulation of which plays an influential role in determining cell fate. Additionally, in the immediate newborn period, there is an increase in circulating ketones which provides an additional metabolic substrate during this time of cellular development (128).

1.2.2.3.1 Cell signaling properties of BOHB

BOHB is not only a fuel source for the heart, but also has cell signaling properties (Figure 1.3). One signaling pathway involves the endogenous inhibition of histone deacetylases (HDACs) (118). HDACs alter gene expression through the regulation of chromatin structure. This typically leads to transcriptional repression, but there is also evidence that HDACs can activate certain genes (129). HDACs are also capable of deacetylating lysine residues on non-histone proteins (118). As BOHB acts as an endogenous inhibitor of HDACs, it can influence gene expression through chromatin remodification (120).

HDACs comprise an enzyme family consisting of four subclasses, conserved from bacteria to humans (130). Class I HDACs (HDAC1, HDAC2, and HDAC3) function as global repressors of transcription (129). HDAC2 is a Class I HDAC that is crucial in embryonic development, particularly contributing to the normal development and morphogenesis of the heart (131). This is exhibited by the uncontrolled proliferation of ventricular cardiomyocytes observed in HDAC2-null mice (131). Global deletion of

HDAC2 has also been demonstrated to result in perinatal lethality with severe cardiac defects (131).

HDAC2 knockout and knockdown studies in animals and cell cultures are known to increase differentiation and reduce proliferation of cancerous cells (132). HDAC2 knockdown is associated with upregulation of cyclin dependent kinase inhibitors, p21 and p27, which are important enzymes in the regulation of the cell cycle (132). BOHB specifically seems to inhibit HDAC2 by increasing histone p21 gene expression (133). In hypertrophied cardiomyocytes, gene expression and metabolism are similar to fetal cells, as seen by an increased reliance on glycolytic metabolism (46,134). HDAC2 plays a role in the regulation of many fetal cardiac isoforms in cardiomyocytes, as seen in cardiac hypertrophy studies (135). The inhibition of HDAC2 may prevent this shift towards a Warburg like metabolic state seen in hypertrophied cardiomyocytes (135). Lysyl residue acetylation by histone acetyltransferases is a post-translational modification that has been found to play a role in this shift in cardiac energy metabolism (136). Fukushima et al. showed that the hyperacetylation of the fatty acid oxidation enzyme long-chain acyl-CoA dehydrogenase (LCAD) that occurs in cardiomyocyte maturation positively correlates with its activity, as well as fatty acid oxidation rates (136). As such the inhibition of HDAC2 may also regulate the metabolic maturation of cardiomyocyte. BOHB may play a role in the maturation of cardiomyocytes through its regulation of HDAC2. Given the significant changes that occur in the postnatal period and the evidence regarding the KDs effect on diseased states through regulation of metabolism, ketones and their oxidation may play

a role in the regulation of cell fate (Figure 1.3). Given the combined body of evidence, the involvement of ketones in cell maturation warrants further study

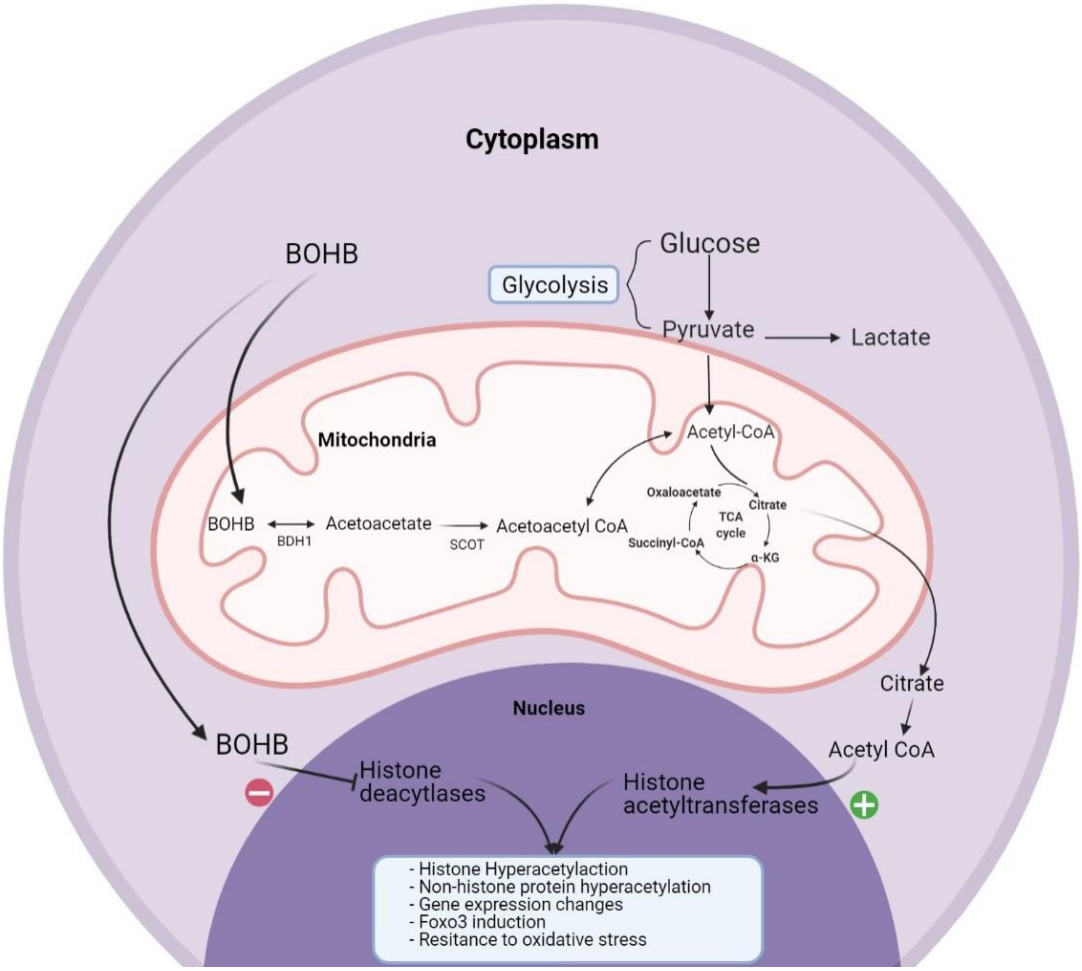

Figure 1.3. **Ketone oxidation and HDAC2 cell signaling pathways for BOHB.** Under normal cellular condition there are two potential pathways that BOHB follow. One is that it can go through the ketone oxidation, in which it is converted to acetyl-CoA and goes through the TCA cycle to produced ATP for the cell. The other is the cell signaling pathway in which BOHB is an endogenous inhibitor of histone deacetylases, generally leading to repressed gene expression and histone and non-histone hyperacetylation. β-

Hydroxybutyrate dehydrogenase 1 (BDH1). Coenzyme A (CoA). Forkhead box O3 (Foxo3). α-ketoglutarate (α-KG). The tricarboxylic acid cycle (TCA cycle). Succinyl-CoA:3-oxo-acid CoA-transferase (SCOT).

1.3 Pathological cardiac maturation

In the newborn period there are dramatic changes in cardiac energy metabolism, where decreases in cardiomyocyte proliferation is associated with an increased reliance of the heart on mitochondrial oxidative metabolism and a decrease in glycolytic rates uncoupled from glucose oxidation (the Warburg effect) (3,4,15). Specifically, fatty acid oxidation increases in the heart following birth and becomes the primary source of ATP production (3,15). Cardiac hypertrophy, which occurs secondary to congenital heart defects (CHD), can delay the normal maturation of energy metabolism in the heart (46,85,136). Cardiac hypertrophy can occur as an adaptive response to the increased mechanical load on the heart. However, if the hypertrophic response is sustained, cardiomyocytes die by apoptosis and eventually heart failure occurs (137). CHD presents in about 1% of children born in Alberta, and about 1 out of 3 of CHD newborns require corrective heart surgery shortly after birth (138). Cardiac hypertrophy can adversely affect the ability of the heart to withstand ischemic stress during surgery, which we hypothesize occurs partly through alterations in how energy demand needs are met in the cardiac tissue (85). However, little is known as to how cardiac hypertrophy alters cardiac energy metabolism in the newborn with CHD. We have previously shown that the delay in the normal maturation of fatty acid oxidation in the hypertrophied newborn heart is accompanied by low glucose oxidation rates, leading to an “energy starved” heart (46,136,138).

There is evidence that disruptions in energy metabolism during cardiomyocyte maturation may contribute to the development of heart failure secondary to congenital heart disease (46). As previously mentioned, congenital heart disease can lead to the development of hypertrophy in the neonatal heart, reverting the metabolic profile of the newborn heart to a more fetal-like metabolic state in which there is increased rates of glycolysis and reduced fatty acid oxidation, effectively hindering the ability of the newborn heart to respond to stress and efficiently circulate blood throughout the body (46).

One potential cause for this delayed maturation of fatty acid oxidation is that neonatal cardiac hypertrophy inhibits the increase in myocardial acetylation of LCAD (46). Additionally, it has been established that HDAC inhibitors (which effectively increase myocardial protein acetylation) effectively blunt cardiac hypertrophic responses both *in vitro* and *in vivo* (131). This contributed further evidence toward HDAC signaling playing a key role in the maturation of cardiac energy metabolism. Given that ketones, such as BOHB, are endogenous inhibitors of HDAC2 and are reported to increase in the newborn period (128), exploring the impact of ketones of on cardiac metabolic maturation is prudent.

1.4 H9c2 cell model

There are many difficulties associated with using primary cardiomyocytes to study cardiomyocyte maturation, which includes the fact they do not proliferate, they are fragile and the inability to maintain them in culture for prolonged periods of time; importantly, this

method also requires the sacrifice of a high number of animals in order to obtain adequate results. As such, the use of H9c2 cell allows for several advantages when exploring the molecular mechanisms of cardiomyocyte maturation. H9c2 cells are a subclone isolated from the ventricle of embryonic BDIX rat hearts (139). While theses cells are not fully differentiated to adult cardiomyocytes and do not have the capacity to contract, they do maintain several similarities to primary cardiomyocytes, including G-signalling protein expression, membrane morphology, and electrophysiological properties (137). Notably, the addition of all-trans retinoic acid (RA) to a low (1%) serum media allows for the differentiation of H9c2 cells such that they exhibit a more adult cardiomyocyte phenotype, such as cell fusion and multinucleation, by preventing myogenic transdifferentiation (24,140). Despite their inability to beat, studies have shown that H9c2 cells respond similarly to various stimuli, including hypertrophic responses, when compared to primary neonatal cardiomyocytes (137). Importantly several of these studies, including Watkins et al., (137) are done in cells that have not being differentiated. Given that adult heart tissues primarily consists differentiated cardiomyocytes without the ability to proliferate, and as discussed above proliferative capacity has a dramatic influence on energy metabolism, this was an important consideration for this project. As such, having a cell line which we are able to study the metabolic transition from a proliferative state to a differentiated non-proliferative state was crucial to create a model potentially comparable to cardiomyocytes during fetal to newborn period.

The presence of increased cardiac markers allows for the confirmation of the cardiomyocyte-like phenotype in differentiated H9c2 cells. With the maturation of

cardiomyocytes, there is increase in the expression of genes related to calcium transporters, as cytosolic calcium is used to drive the contraction of the heart (27). RA-induced differentiation leads to an increased expression of proteins related to increased calcium transport, mitochondrial biogenesis and cardiac specific markers such as Cardiac troponin T, PGC-1α and SERCA2 (24).

Given that the RA differentiation protocol for H9c2 cells yields a heterogeneous cell population (24), it is therefore not possible to determine the "efficiency" of RA-induced differentiation. Rather, the differentiation of myoblasts represents an ongoing process or maturation rather than a discrete transition from one phenotype to another. However, the analysis of markers of cardiomyocyte maturation confirms a clear increase in overall cardiomyocyte differentiation in cell lysates assessed (24). This indicates that RA-differentiated cells mimic the phenotype of mature cardiomyocytes and can be effectively used as a model for terminally differentiated ventricular cardiomyocytes in cell culture studies.

1.5 Rationale for the present study

Gaining an understanding of energy metabolism in the developing cardiomyocyte has many important implications in cardiovascular research. Given the extreme changes in normal energy metabolic maturation seen in CHDs and determining how to allow for proper maturation is pertinent. Additionally, since mature cardiomyocytes can no longer proliferate, a large effort has been made to regenerate cardiomyocytes in damaged or diseased myocardium (141). The preservation of high rates of glycolysis can effectively

maintain a cardiomyocyte precursor cell's ability to proliferate, which creates the possibility for the implantation of cardiac progenitor cells as a therapeutic strategy in regenerative medicine. However, successful implantation of cardiomyocytes would require the cells to transition towards a differentiated/adult cardiomyocyte phenotype, including alterations in energy metabolism (15). Unfortunately, this transition is not yet well-enough understood for this putative therapy to be feasible. Therefore, further research is required to better understand potential stimulations for maturing cardiomyocytes. In addition, studies often ignore the upregulation of circulating ketone bodies observed in the newborn period (128) and how that may influence this metabolic transition that is necessary for proper cardiac maturation.

1.6 Research question and objectives

Our research question is to determine the effects of ketones, specifically BOHB, on the maturation of cardiomyocytes in the H9c2 cell culture model, and whether the effects of ketones is elucidated through metabolic changes induced by the Warburg effect, or through cell signaling properties, such as the inhibition of HDAC2. Through the comparison of proliferating H9c2 cells ± BOHB with differentiated cells ± BOHB we aim to determine how metabolism of H9c2 cell are influenced by maturation and how ketones affect this process. Using small interfering ribonucleic acid (siRNA) to knockdown BDH1 we aim to determine whether or not changes due to ketones are a result of metabolic, specifically ketone oxidation, dysregulation. Finally, using the siRNA knockdown of HDAC2 we aim to verify whether or not cell signaling properties of BOHB could be regulating changes observed in proliferating H9c2 cells treated with ketones.

1.7 Hypothesis

We hypothesize that ketones will promote cardiomyocyte maturation through decreases in glycolysis, and the subsequent decrease of the Warburg effect, and/or due to an inhibition of HDAC2 signalling.

Chapter 2: Materials & Methods

2.1 Cell culture

H9c2 rat embryonic ventricular myoblast cells (ATCC) were used in all studies described and cultured according to the vendor instructions. Cells were used from a passage of 9-12. Cells were cultured and treated in T-25 cell culture flasks and incubated at 37°C, 5% CO_2, and 95% humidity in a HERAcell 150i CO_2 incubator. Cells were maintained in high-glucose Dulbecco's Modified Eagle Medium (DMEM; Sigma-Aldrich/Glibco) (10 ml), completed with 10% fetal bovine serum (FBS; Sigma-Aldrich), penicillin (100 U/ml), and streptomycin (100 µg/ml) (Sigma-Aldrich). Cells were cultured to 70-80% before passaging with trypsin (Glibco).

2.1.1 Proliferating cells

Proliferating cells were cultured in complete DMEM until they reached 80-90% confluency (usually about 3-5 days after cells were passaged). During this time, the cell culture media was changed every 24-72 hours. BOHB (β-Hydroxybutyrate; Sigma-Aldrich) was dissolved in double distilled water (ddH_2O), sterilized via filtration through a 2µM filter, and stored at 4°C. To study the effects of ketones in proliferating H9c2 cells, two groups were used in this study: 1) absence of 1mM BOHB, and 2) presence of 1mM BOHB.

2.1.2 Differentiating cells

H9c2 cells were differentiated to obtain a more mature cardiomyocyte phenotype. Once proliferating cells reached 60% confluence, they were washed with sterile DMEM without additives before being treated with differentiating media containing 1% FBS, penicillin (100 U/ml), streptomycin (100 µg/ml), and RA (1 µM) (Arcos Organic) for 7-days (24,140). RA was prepared in dimethyl sulfoxide (DMSO; Sigma-Aldrich). RA is light sensitive and has low stability (142), therefore the addition RA to the differentiation media was done daily in the dark, media was changed daily, and flasks were wrapped in aluminum foil and stored in a dark incubator. To study the effects of ketones in differentiating H9c2 cells, two groups were used in this study: 1) absence of 1mM BOHB, and 2) presence of 1mM BOHB.

2.2 Cell counting

Cells were photographed at various time points using a EVOS Core AMG light microscopy at a magnification of 10X, and aperture of 4/10 PH (used for phase observations at 4x and 10x). The number of cells were counted in the center 2.5mm^2 of the flask using a handheld cell counter. Cells were then counted on PowerPoint images using a handheld counter. Differences in cell numbers at different time points were used to observe changes in cellular proliferation.

2.3 Metabolic measurements

2.3.1 Time course

Time courses for glycolysis, fatty acid oxidation, glucose oxidation, and ketone oxidation were completed to determine time points at which metabolic rates in the H9c2 cells were linear in order to standardize the comparison of these metabolic rates. Metabolic measurements were performed as specified in sections 2.3.2 through 2.3.3.1. For glycolysis linearity was determined over a three-hour times point. One ml of buffer was extracted every 30 minutes (Figure 2.1A) and calculated to reflect the metabolic rate of the total flask. For oxidative rates (glucose, ketones, and palmitate) separate flasks were incubated for 1 hour, 2 hours or 3 hours (Figure 2.1B, C, D). Based on the time course data, incubation time for official experiments were chosen as 1 hour for glycolytic rates, and 3 hours for oxidative metabolic rates.

A

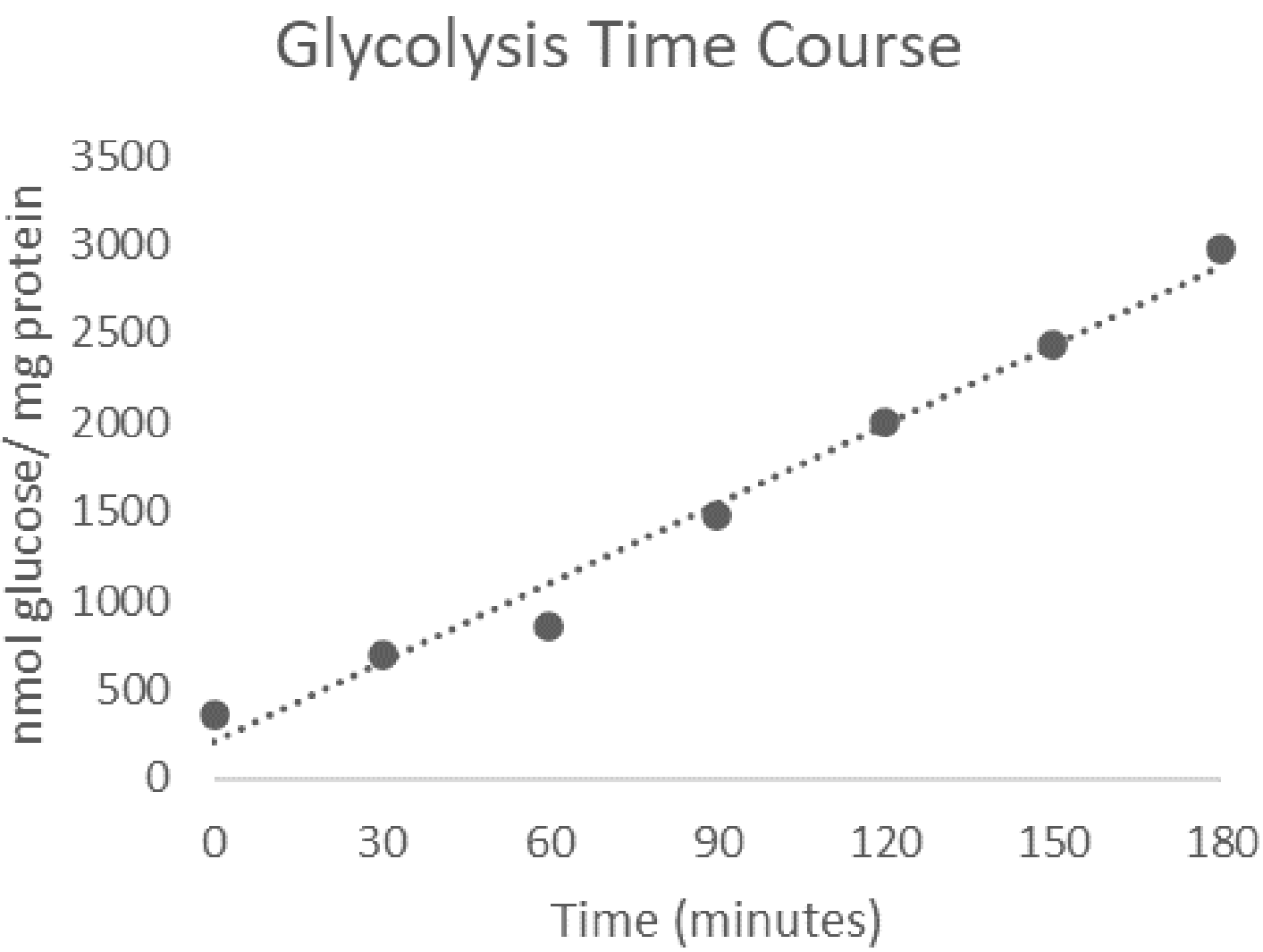
Glycolysis Time Course
nmol glucose/ mg protein
3500
3000
2500
2000
1500
1000
500
0
0
30
60
90
120
150
180
Time (minutes)

B

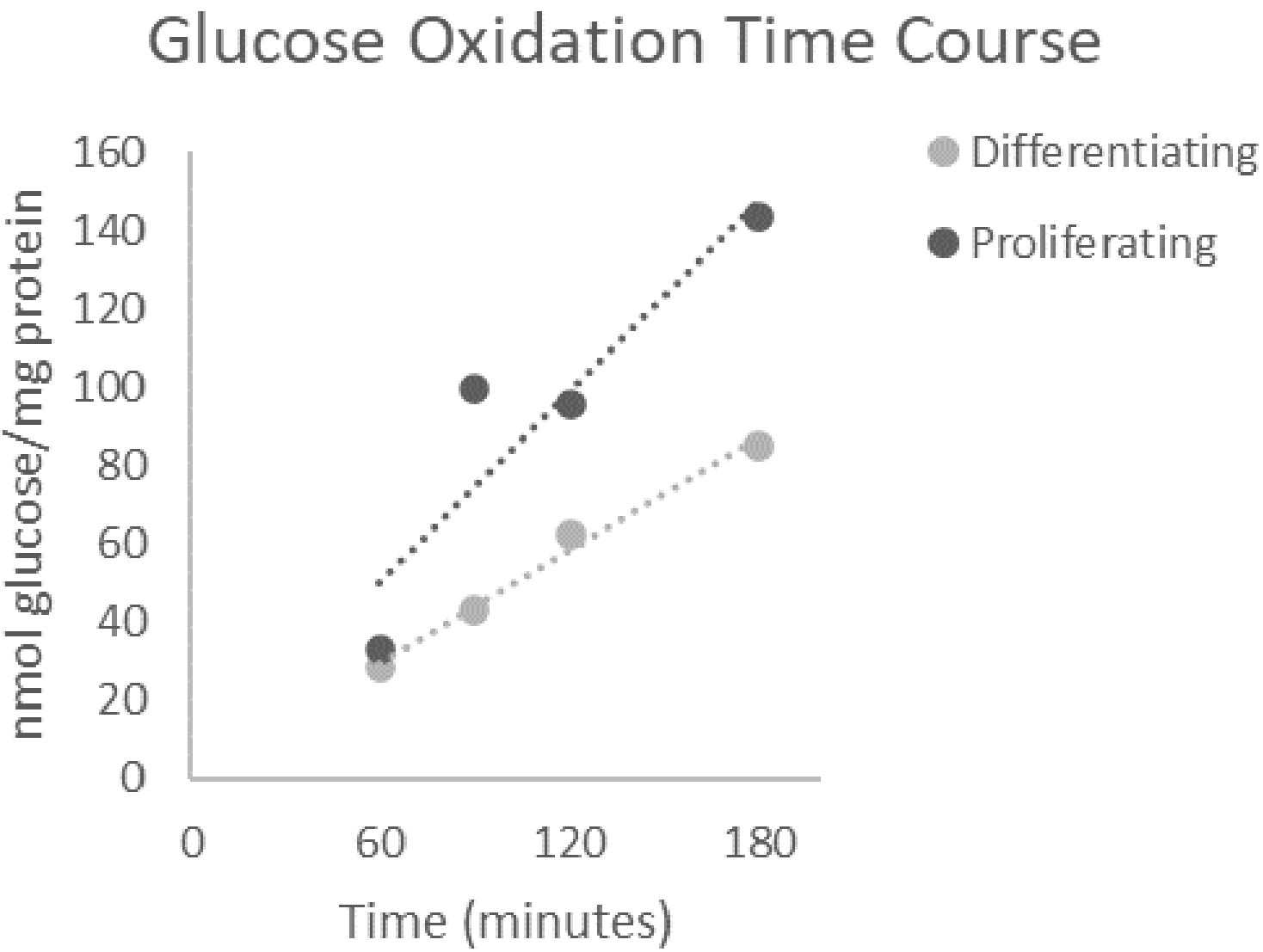
Glucose Oxidation Time Course
nmol glucose/mg protein
160
140
120
100
80
60
40
20
0
0
60
120
180
Time (minutes)
Differentiating
Proliferating

c

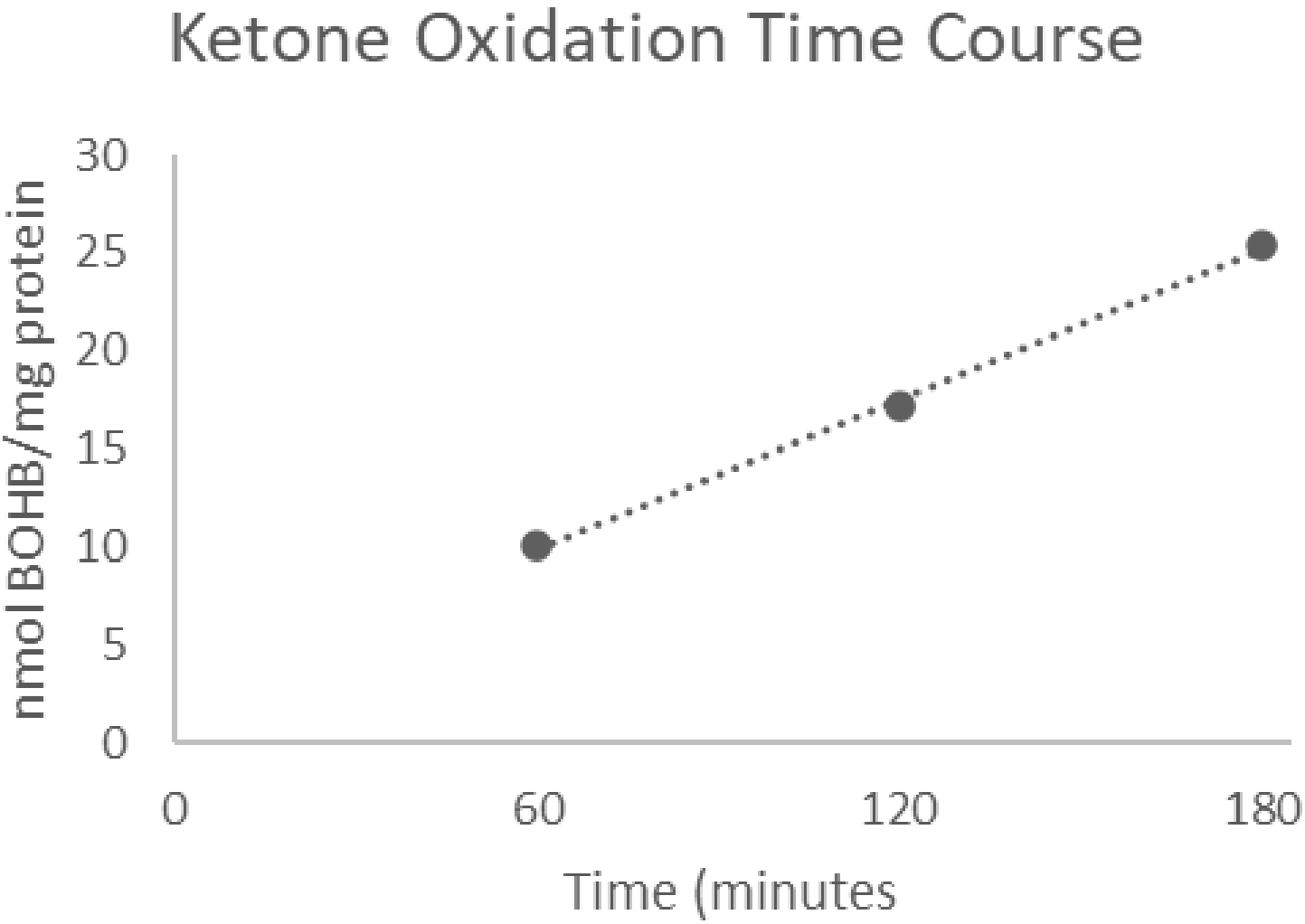
Ketone Oxidation Time Course
nmol BOHB/mg protein
30
25
20
15
10
5
0
0
60
120
180
Time (minutes

D

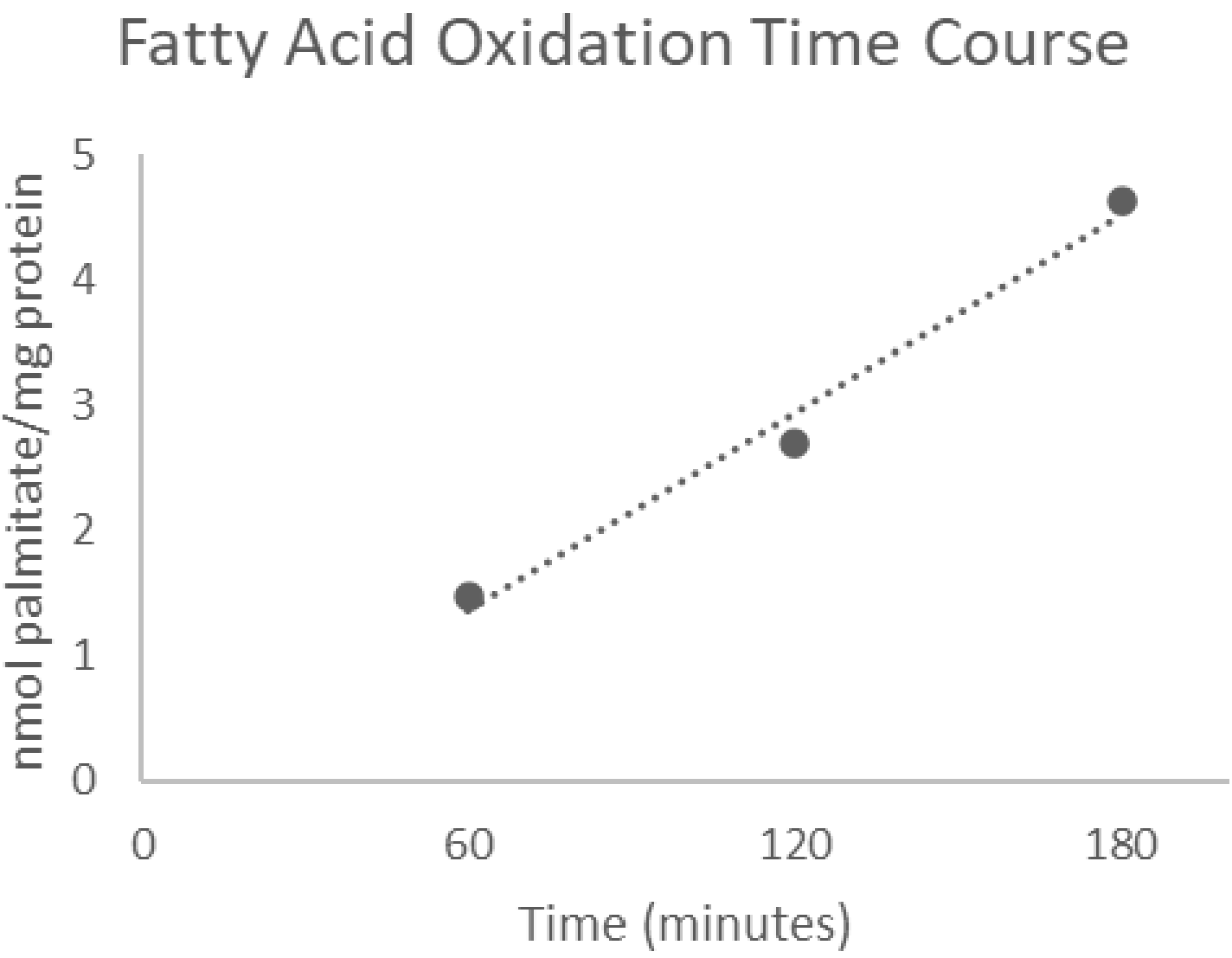

Figure 2.1. **Preliminary time course of metabolic measurements in H9c2 cells**: Glycolysis (**A**), glucose oxidation (**B**), ketone oxidation (**C**), palmitate oxidation (**D**).

2.3.2 Perfusion buffer

Perfusion buffer was made with 1X Krebs Henseleit buffer (25 mM $NaHCO_3$, 4.7 mM KCl, 118.5 mM NaCl, 1.2 mM $MgSO_4$, 1.2 mM KH_2PO_4, 2.5 mM $CaCl_2$) containing palmitate (0.8 mM; Sigma-Aldrich) bound to 4% fatty acid free bovine serum albumin (BSA; Equitech-Bio, Inc.), D-(+)-glucose (5 mM; Sigma-Aldrich), D+βHOB (0.6 mM; Sigma-Aldrich), and insulin (100 µU/ml; HumulinR). To directly measure metabolism, D-[5-^{3}H(N)] glucose (Perkin Elmer), D-[^{14}C-(U)]-glucose (Perkin Elmer), [3-^{14}C]-BOHB (ARC), or [1-^{14}C]-palmitic acid (Perkin Elmer) in the buffer were radiolabelled to specifically measure either glycolysis, glucose oxidation, ketone oxidation, or palmitate oxidation, respectively. Only one substrate, respectively, was labeled for each specific experiment. For all metabolic measurements, the buffer was filtered and oxygenated using the oxygenator system of a Langendorff perfusion apparatus before the buffer was added to each flask.

2.3.3 Perfusion protocol

Cell culture media was aspirated, and cells were washed twice with one times phosphate-buffered saline (PBS). 6 ml of the cell perfusion buffer, prepared as described above (section 2.3.2), was then added to each flask and the air inside the flask was saturated with carbogen (95% O_2, 5% CO_2) for 20 seconds before the flasks were tightly closed to create a closed system with minimal gas exchange.

For the measurement of palmitate, glucose, and ketone oxidation, an apparatus containing a hyamine trap was attached to each flask and in order to allow the collection

of the CO_2 released from the cells. The hyamine trap contained a GF/B glass microfiber filter (Whatman) soaked with 100 µL hyamine hydroxide 10x (Perkin Elmer). Connections between the apparatus and flask were further sealed with parafilm to prevent CO_2 leakage. Flasks were then placed in a 37°C incubator (Labnet 211DS) for a three-hour time period before flasks were injected with 5 ml of 9 M sulfuric acid (H_2SO_4). Sealed flasks were then left in the 37°C incubator overnight to ensure maximal release of CO_2. The injection of H_2SO_4 liberated CO_2 from the cells into the gaseous phase, which was then trapped by hyamine soaked microfiber glass filter the hyamine trap apparatus. The filter paper was then transferred to scintillation vials, 4 ml of EcoLite (+) ^{TM} (MP Biomedicals) was added and vials were then counted in a scintillation counter measuring ^{14}C beta light emission.

For the measurement of glycolysis, flasks were sealed using non-vented closed caps. Flasks were placed in the 37°C incubator for 2 hours, with samples of the perfusion buffer extracted at the 1-hour and 2-hour time point. A water extraction assay (143) involving the evaporation and condensation of water was used to determine the amount of tritiated water release from the cells at the two time points.

2.3.3.1 Water extraction assay

Once samples were extracted, 200 µL non-metabolized perfusion buffer, 200 µL metabolized perfusion buffer form each flask, and 200 µL radiolabelled ^3H_2O (Perkin Elmer) were aliquoted in triplicate to capless Eppendorf tubes located in scintillation vials

containing 500 µL of ddH_2O. Caution was used to ensure no radiolabelled perfusion buffer came into contact with the scintillation tubes. 200 µL of unmetabolized buffer and radiolabelled H_2O were also aliquoted in triplicate to empty scintillation vials and stored in the dark until the other samples undergoing the water extraction assay protocol were complete. Scintillation vials for water extraction were then tightly sealed before being placed in a 50°C incubator for 24 hours so that the water from the samples would vaporize. Vials were then transferred to a 4°C fridge overnight so that aforementioned vapour would condense into the scintillation vial. Capless tubes were then carefully removed, and any remaining water droplets on the outside of the tubes were collected into the respective scintillation tubes. 4 ml of EcoLite (+) ^{TM} was then added to all of the prepared scintillation tubes, as well as into three empty scintillation tubes (blanks), before being counted in a scintillation counter to measure ^3H beta light emission.

2.3.3.2 Metabolic rate calculation

Disintegration per minute (DPM) were used to calculate metabolic rates. For glycolytic measurements, DPM for samples were extrapolated to represent the entire flask's content. Rates were then calculated based on the concentration of each respective substrate before being normalized per hour and by total protein concentration per flask. For oxidative rates (glucose, ketones, palmitate) three representative flasks were lysed and protein concentration was averaged before normalizing rates. For glycolysis, each metabolic rate was normalized to the protein concentration of the respective flasks.

2.3.4 Glucose uptake

The uptake of glucose was determined by measuring radioactive beta emission DPMs of 50 µl aliquots of cell lysate. Since extraneous radiolabeled perfusate was extensively washed before harvesting (see section 2.4), these counts were representative of the internal glucose taken up by the cell. This was then calculated to reflect nmol glucose per mg protein and added to the nmol glucose per mg protein values from the glycolytic rate. Together, the sum of these two values are presented as the total amount of glucose that was taken up by the cell.

2.3.5 Palmitate uptake

First, we started by quantifying triacylglycerol levels using a colorimetric serum triacylglycerol quantification kit (Cell Biolabs, Inc.) in the cells to determine if triacylglycerol levels changed between treatment groups as described by the supplier. These values were then normalized to mg protein and multiplied by three to determine the amount of palmitate within the cells. We then incubated cells with [1-^{14}C]-palmitic acid for three hours in order to determine the amount of palmitate accumulated in the cell during metabolic the incubation period. The difference between the palmitate in the cells incubated with radioactive palmitate vs the non-incubated cells were calculated to determine to accumulation. This was then added to the amount of exogenous palmitate metabolized to determine the total amount of palmitate taken up into the cells.

2.3.6 ATP production/contribution calculation

Using the steady-state metabolic rates, ATP production was calculated. Values used to calculate the relative ATP production of each substrate metabolized were 2 ATP/mol of glucose metabolized by glycolysis (144) and 29 ATP/mol of glucose oxidized (144), 105 ATP/mol of palmitate oxidized (144), and 21.25 ATP/mol of BOHB oxidized (145). We were then able to use these values to calculate the percent contribution of each metabolic pathway to total ATP production.

2.4 Cell harvesting

Either cell culture medium or perfusion buffer was aspirated from the flasks or 6-well plates, depending on the experiment, and they were subsequently rinsed one time (twice if cells were previously in radiolabelled perfusion buffer in order to wash away external radioactive contamination) with room temperature PBS and once with cold PBS (1-3 ml). 100 µL of RIPA lysis buffer (containing a cocktail of protease inhibitor (1:1000; Sigma-Aldrich), phosphatase inhibitors (PPI) IV (1:200; MEMD Millipore Corp.) and PPI II (1:200; Sigma-Aldrich) was added to each flask or well before being placed on ice. The surface of the flasks/plates were then scraped continuously for 2 minutes with a cell scraper before the cell lysate was collected. Cell lysates were homogenized by pipetting the lysate up and down continuously for a 1-minute period using a 200 µL pipette. Once homogenized, cell lysates were collected in Eppendorf tubes and centrifuged for 15 minutes at 7385 rpm (4°C) to ensure mitochondrial elements remained in the supernatant. The supernatant was then collected in pre-weighed tubes and weighed with the supernatant before being stored at -80°C. Difference between empty Eppendorf weight and weight with the supernatant was used to determine total µL of lysate per flask.

2.5 Protein assays

The concentration of proteins in H9c2 cell lysates obtained was determined using the Bradford Method for protein quantification (146). Once determined, the protein concentrations for individual cell lysates were used to create samples of standardized protein concentrations for protein analysis by sodium-dodecyl sulfate polyacrylamide gel electrophoresis (SDS-PAGE) and Western blotting. Protein concentrations were also used to determine the amount of total protein per flask, which was then used to normalize the metabolic data.

2.6 Western blotting

Samples for Western blotting were prepared from homogenized cell lysates in a buffer containing 5% SDS, 0.1% bromophenol blue, Tris buffer, and 16% β-mercaptoethanol (loading buffer).15-20 µg of the denatured protein samples were separated in 8-12% acrylamide gels using SDS-PAGE and transferred to polyvinylidene difluoride (PVDF) microporous membranes as previously described (147). After blocking in 5% non-fat milk for one hour to prevent non-specific binding (148), membranes were probed at 4°C overnight (with exception of α-tubulin, which was incubated at room-temperature for 1 hour) with primary antibodies as listed in Table 1. Membranes were incubated with the appropriate secondary antibodies for 1 hour at room temperature. Relevant bands were visualized with enhanced chemiluminescence and quantified with Image J® software. A-

tubulin was used as a loading control for all proteins analysed, and phosphorylated proteins were compared to the total respective non-phosphorylated protein present.

Table 1. **List of antibodies used to probe for proteins during western blot analysis.** Specifies antibody dilution, company, molecular weight, catalogue number and clonality.

Antibody	Dilution	Company	Molecular Weight (kDa)	Catalogue #	Clonality
BDH1	1:5000-1:2000	Novus Pharmaceuticals	37	NBP1-88673	Polyclonal
HDAC2	1:250	Cell signaling	60	2540S	Polyclonal
SERCA2a	1:250	Invitrogen	110	MA3-910	Monoclonal
Cardiac Troponin T	1:1000	R&D Systems	42	MAB18742	Monoclonal
PGC-1α	1:500	Santa Cruz	90	sc-13067	Polyclonal
PPARα	1:500	Santa Cruz	55	sc-9000	Polyclonal
PKM2	1:1000	Cell Signaling Technology	60	4053S	Monoclonal
G6PD	1:1000	Cell Signaling Technology	58	12263S	Monoclonal
PFKFB3	1:1000	ABNova	60	H00005209-M08	Monoclonal
PDH	1:500	Cell Signaling Technology	43	2784S	Polyclonal
p-PDH	1:1000	Cell Signaling Technology	43	31866S	Polyclonal
Akt	1:1000	Cell Signaling Technology	60	9272S	Polyclonal
p-Akt	1:500	Cell Signaling Technology	60	9271S	Polyclonal
IDH	1:1000	Cell Signaling Technology	45	8137	Monoclonal
LCAD	1:1000	Abcam	47	Ab129711	Polyclonal
CPT1a	1:1000	Sigma-Aldrich	86	SAB2108104	Polyclonal
CPT1b	1:1000	Novus Pharmaceuticals	100	NBP2-92666	Polyclonal
ATGL	1:1000	Invitrogen	60	MA5-38135	Monoclonal
KLF7	1:1000	Santa Cruz	38	Sc-398576	Monoclonal
FOXO3a	1:1000	Abcam	71	Ab23683	Polyclonal
α-Tubulin	1:10,000	Cell Signaling Technology	50	3873S	Monoclonal

2.7 siRNA knockdowns

Prior to siRNA treatment, H9c2 cells were passaged at least 2 times post-seeding before being passaged into 6 well plates for siRNA treatment. For all siRNA knockdowns the following common products were used: scrambled negative control (Santa Cruz Biotechnology); Opti-MEM (Invitrogen); Lipofectamine (Invitrogen); Antibiotic free complete media. After siRNA incubation, cells were collected from the 6 well plates, combined per group, and split into flasks for further treatment before metabolic measurements (as described above in section 2.3) were conducted and/or cell lysate was harvested (as described above in section 2.4).

2.7.1 siRNA optimization

Before final experiments took place, studies were conducted to optimize the timing and concentration of siRNA used.

2.7.2 BDH1 knockdown

45 nM of commercial BDH1 siRNA (Invitrogen; see Table 2 for further details) and equivalent negative scramble control siRNA (see Table 2) were complexed with Lipofectamine RNAiMAX in Opti-MEM reduced-serum transfection medium, then allowed to incubate for 5 minutes at room temperature before transfection of H9c2 cells. Cells were then incubated with the siRNA complex in the 37°C cell culture incubator for 48 hours before H9c2 cells in the plate were split into flasks and incubated in the presence

or absence of 1mM BOHB (as described in section 2.1.1) for 6 days before further metabolic experiments were performed as previously described (Section 2.3).

2.7.3 HDAC2 knockdown

50 nM of commercial HDAC2 siRNA (Santa Cruz Biotechnology; see table 2 for further details) and equivalent negative scramble control siRNA were complexed with Lipofectamine RNAiMAX in Opti-MEM reduced-serum transfection medium, then allowed to incubate for 5 minutes at room temperature before transfection of H9c2 cells. Cells were incubated with the siRNA complex in the 37°C cell culture incubator for 36 hours before H9c2 cells in the plate were split into flasks and incubated in the presence or absence of 1mM BOHB for 6 days (as described in section 2.1.1) before further metabolic experiments were performed as previously described (section 2.3).

Table 2. **siRNA sequences** (sense and antisense), target transcript, assay ID and company.

Name	**Sense (5'->3')**	**Antisense (5'->3')**	**Assay ID**	**Company**
BDH1 siRNA	GCUGUCCUGGUUACAGGCUtt	AGCCUGUAACCAGGACAGtt	195881	Invitrogen
HDAC2 siRNA*	CAUGAGGGACGGUAUAGAUtt	AUCUAUACCGUCCCUCAUGtt	sc-270150A	Santa Cruz
	CCAAUGAGUUGCCAUAUAAtt	UAUAUGGCAACUCAUUGGtt	sc-270150B	
	GGAAUGUCGCUGAUCAUAAtt	UUAUGAUCAGCGACAUUCCtt	sc-270150C	
Negative Control	Was not provided by vendor	Was not provided by vendor	N/A	Santa Cruz

* HDAC2 siRNA sc-270150 from Santa Cruz is a pool of the three different siRNA duplexes listed.

2.8 Quantification and statistical analysis

Quantified data were presented as mean ± SEM. Data from different treatment groups was compared with two-way ANOVA, and metabolic contribution within groups was compared with one-way ANOVA, each followed by Tukey's test for multiple comparison. Differences in cell proliferation between control and BOHB-treated groups were compared with an unpaired t-test. $P<0.05$ were considered to be significant. All statistical analysis was performed using the GraphPad Prism9 software.

CHAPTER 3: Results

3.1 Proliferating vs differentiated cells ± ketones

3.1.1 Retinoic acid treatment differentiates H9c2 cells

To differentiate the H9c2 cells to a mature cardiomyocyte phenotype, a 7-day RA treatment was used. This treatment was successful in differentiating the cells, as was visibly apparent with the use of a light microscope to image the cells at the end stage of their incubation (80% confluence for proliferating cells and 7-days post differentiation treatment for differentiated cells) in which differentiating cells were visibly longer than proliferating cells (Figure 3.1A and 3.1B). The successful differentiation of the H9c2 cells was further examined by Western blotting for cardiac troponin T, SERCA2, and PGC-1α key markers of cardiomyocyte maturation. RA treatment increased cardiac troponin T, SERCA2, and PGC-1α indicating that the differentiation process not only morphologically altered the cell structure but molecularly altered H9c2 cells to a mature cardiomyocyte phenotype (Figure 3.1C-E).

A

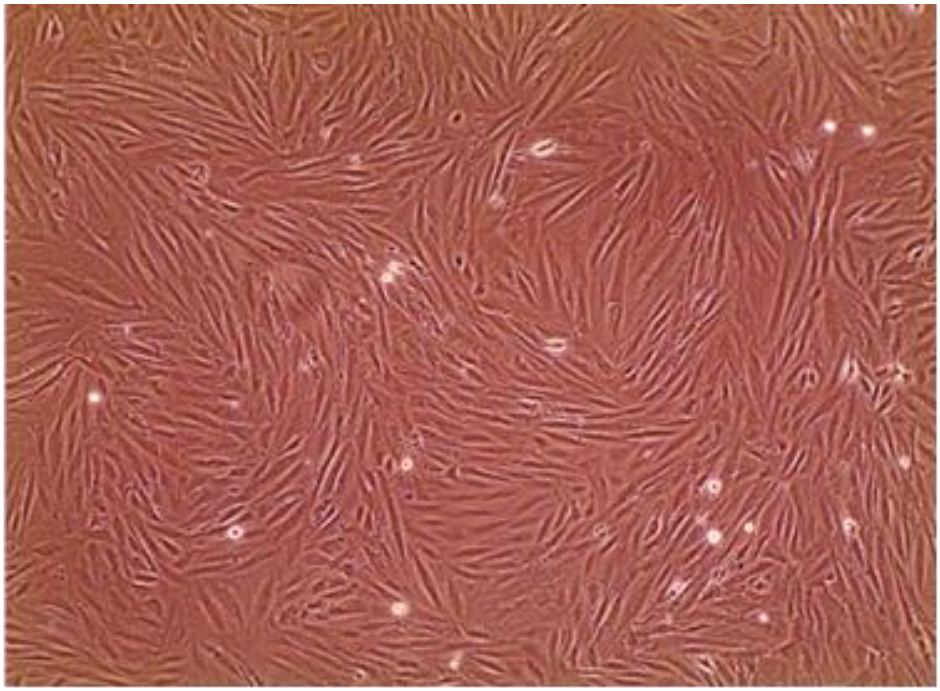

Proliferating

B

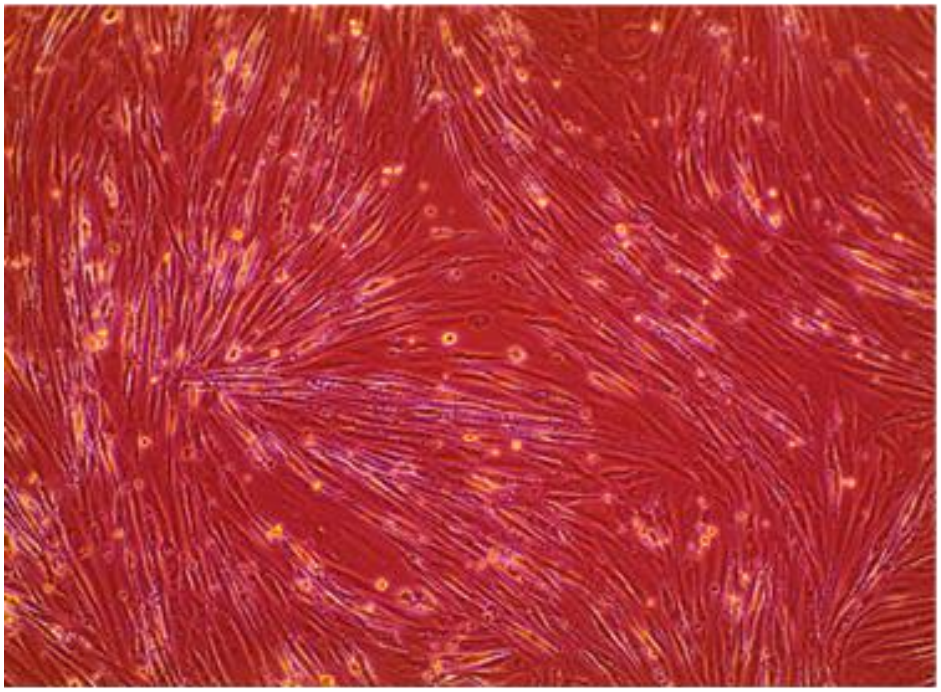

Differentiating

C

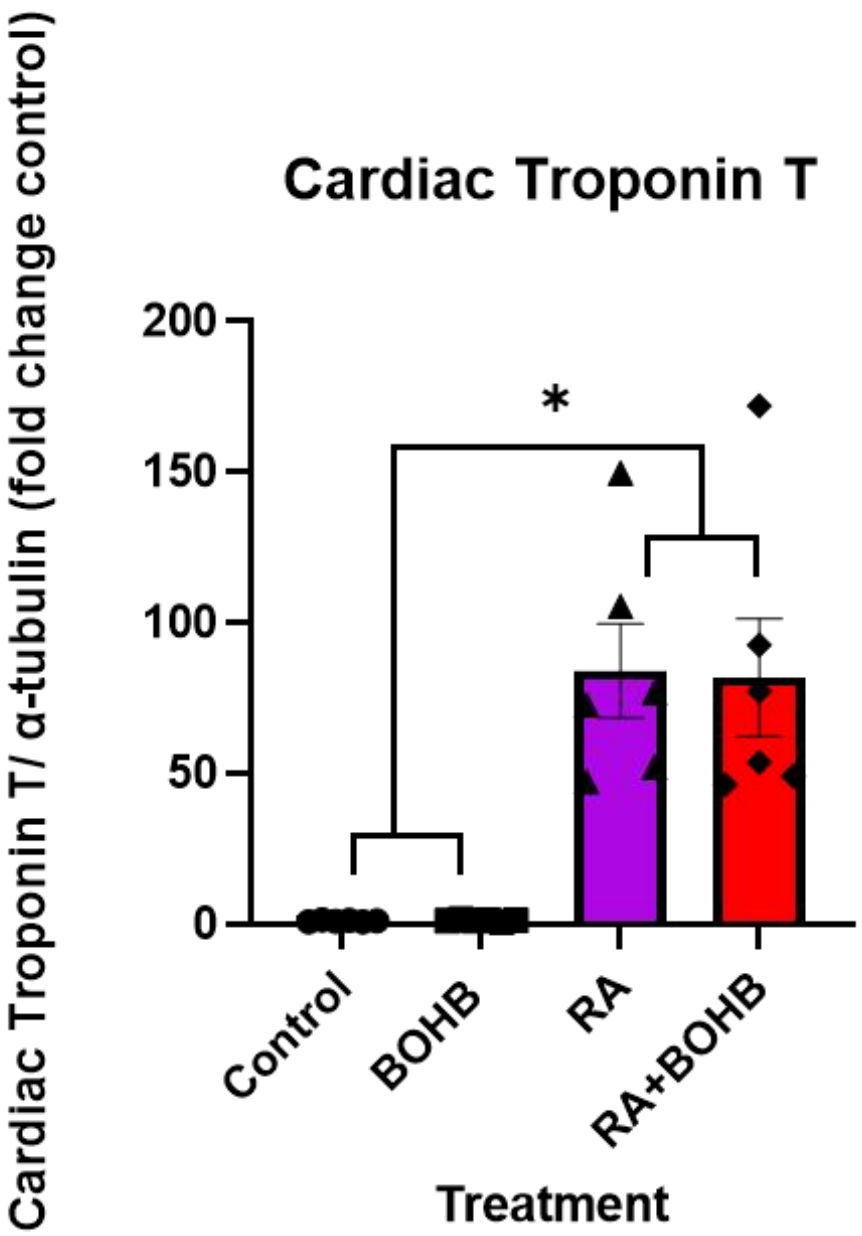
Cardiac Troponin T
Cardiac Troponin T/ α-tubulin (fold change control)
200
150
100
50
0
*
Control
BOHB
RA
RA+BOHB
Treatment

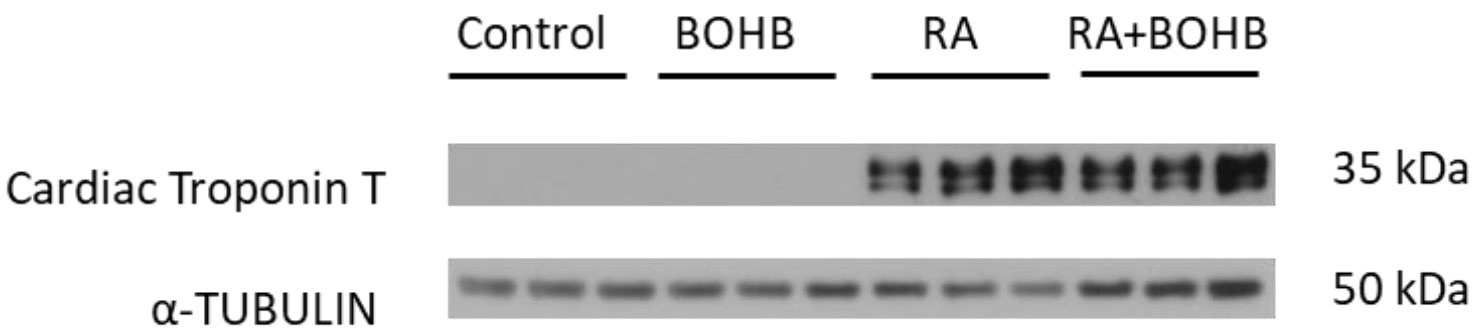
Control
BOHB
RA
RA+BOHB
Cardiac Troponin T
35 kDa
α-TUBULIN
50 kDa

D

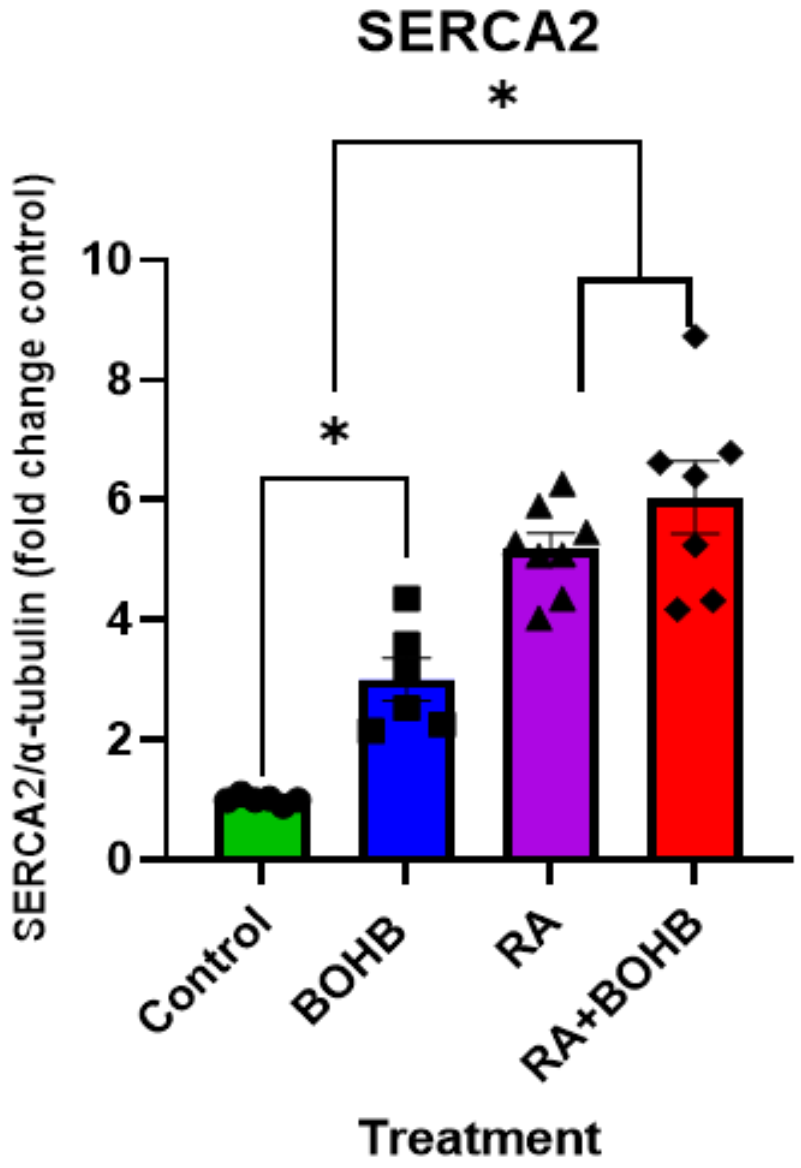
SERCA2
*
*
SERCA2/α-tubulin (fold change control)
10
8
6
4
2
0
Control
BOHB
RA
RA+BOHB
Treatment

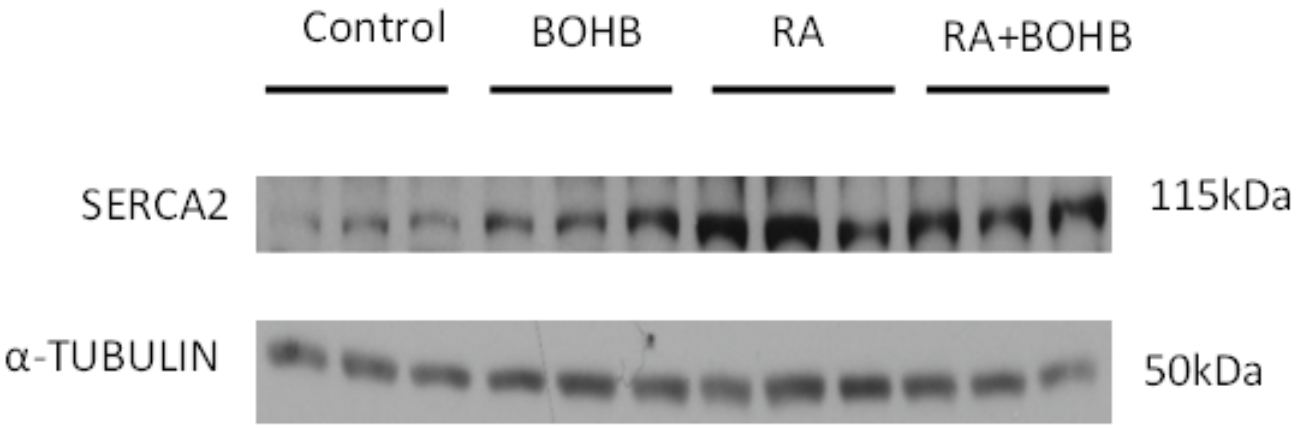
Control
BOHB
RA
RA+BOHB
SERCA2
115kDa
α-TUBULIN
50kDa

E

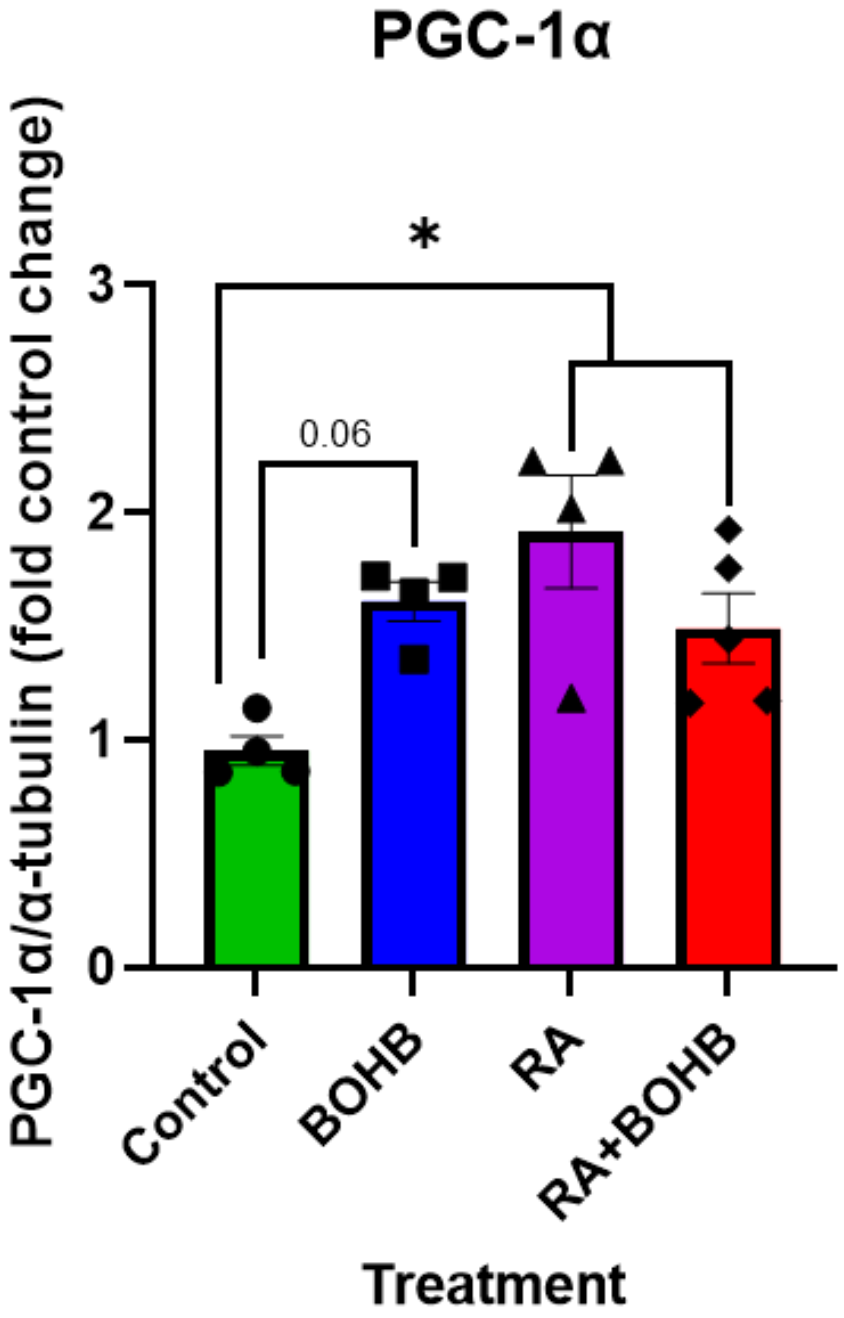
PGC-1α
PGC-1α/α-tubulin (fold control change)
*
0.06
3
2
1
0
Control
BOHB
RA
RA+BOHB
Treatment

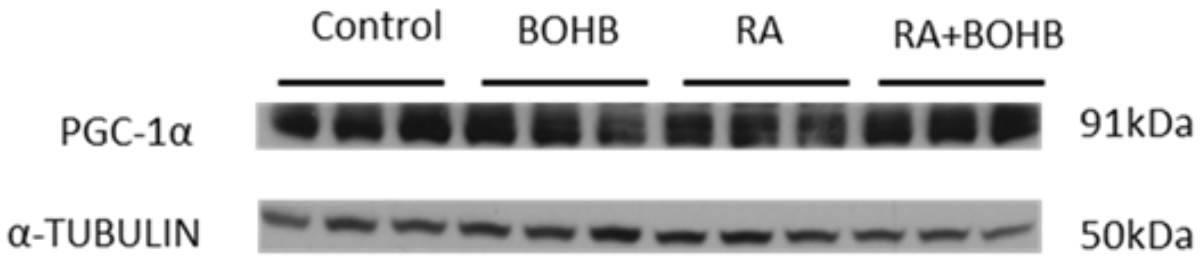
Control
BOHB
RA
RA+BOHB
PGC-1α
91kDa
α-TUBULIN
50kDa

Figure 3.1. Adding ketones to proliferating H9c2 cells leads to increases in cardiomyocyte maturation markers (**A**) and differentiating cells (**B**). Expression of cardiac troponin T (**C**), SERCA2 (**D**) and PGC-1α was also assessed ©. n= 4-6. Individual values for each group. Data are presented as a scatter plot with its mean ± SEM. Data were analyzed with Two-way ANOVA followed b Tukey's for multiple comparisons. Samples collected from separate flasks at the end of culture or metabolic incubation. *p < 0.05.

3.1.2 Ketones did not affect the proliferation rates of H9c2 cells, but did lead to maturation

To determine the effects of BOHB on cell proliferation in H9c2 cells, proliferating cells were cultured in both the presence and absence of BOHB until 80% confluent. Cells were counted on each day of growth, and the difference in cells between the last two days of growth was used as an indicator of cell proliferation. Although no statistical difference was seen between the control and BOHB treatment groups, there seemed to be a slight trend showing decreased proliferation in BOHB treated cells compared to controls (Figure 3.2A). Despite no changes in proliferation, BOHB does appear to promote maturation to a cardiomyocyte phenotype, as seen by significant increases in SERCA2 and a trended increase in PGC-1α expression (Figure 3.1D-E). It is also important to note that there were no statistically significant differences in the number of cells on the last day of incubation for any treatment (Figure 3.2B).

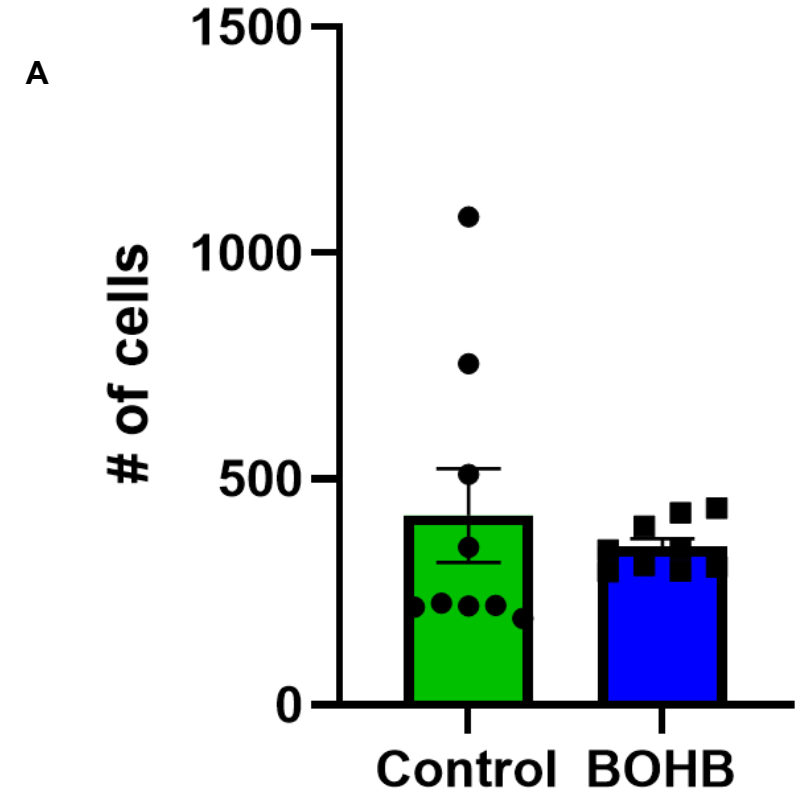
A
1500
1000
500
0
# of cells
Control
BOHB

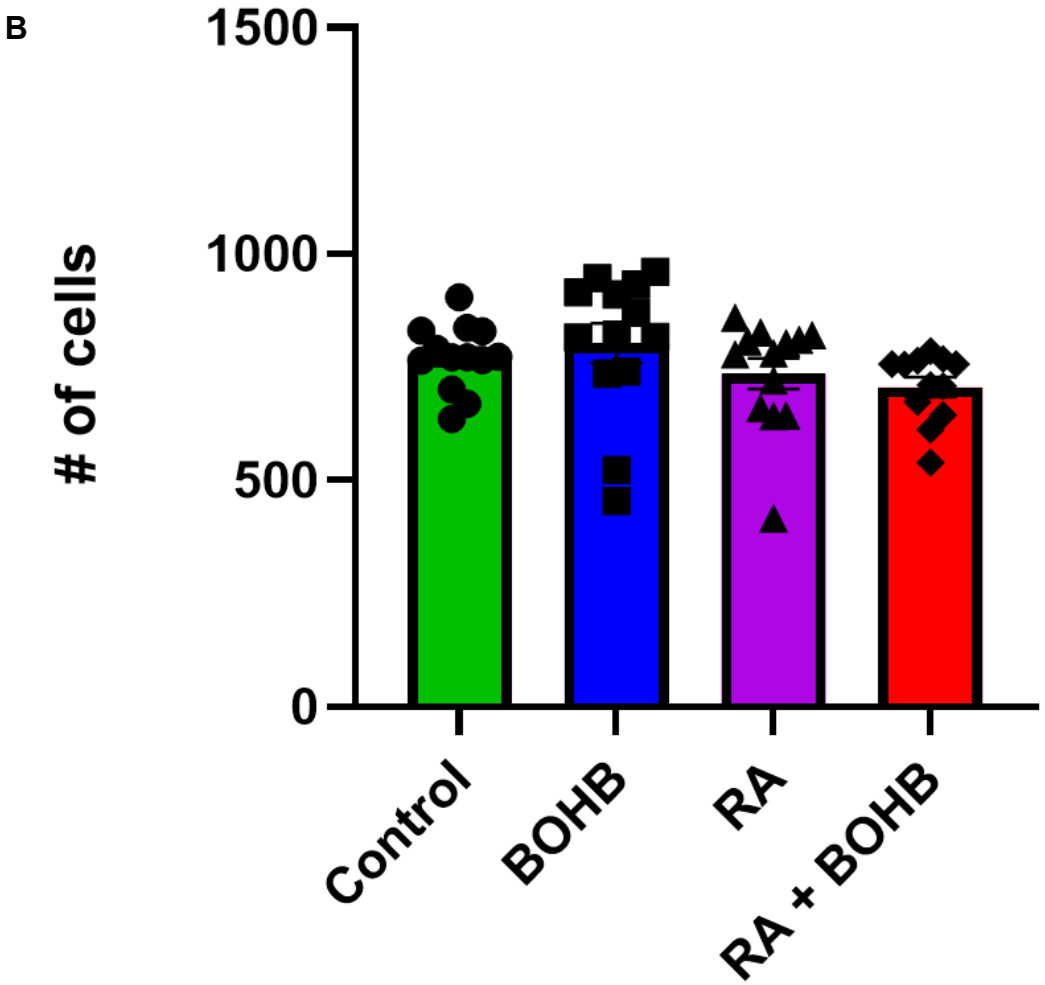
B
1500
1000
500
0
# of cells
Control
BOHB
RA
RA + BOHB

Figure 3.2. H9c2 cardiomyocytes did not change in proliferation with the addition of ketones. Cell counts between the last two days of growth were examined to investigate the difference in proliferation between control and BOHB treatment (**A**) (n=9 for each experimental group). To ensure the same amount of cells were being perfused/lysed between groups, cells were counted on the last day of growth (**B**). n=13 for control, BOHB & Ra. n= 12 for RA + BOHB. Data were analyzed with Two-way ANOVA followed by Tukey's for multiple comparisons. *$p < 0.05$.

3.1.3 Glucose metabolism in proliferating vs differentiated cells ± ketones

By directly studying glucose metabolism, I was able to determine the rates of glycolysis and glucose oxidation in proliferating and differentiated cells ± 1mM BOHB. Differentiation led to a dramatic 78% decrease in glycolysis (866.2 ± 65.06 vs 192.8 ± 51.73 nmol • mg • protein^{-1} hr^{-1}, $p < 0.05$). This was observed in the presence and absence of ketones (Figure 3.3A). Further, BOHB treatment caused a 28% decrease in glycolysis in proliferating cells (866.2 ± 65.06 vs 622.2 ± 85.07 nmol • mg protein^{-1} • hr^{-1}, $p < 0.05$) (Figure 3.3A). Glucose oxidation was decreased in differentiated cells relative to proliferating cells ($p < 0.05$), and BOHB treatment caused a decrease in glucose oxidation in differentiated cells ($p < 0.05$), but no significant change in proliferating cells (Figure 3.3B). Overall, there were no changes in glucose uptake with the addition of ketones. However, glucose uptake was substantially lower in the differentiated ± ketones cells compared to the proliferating ± ketones cells (Figure 3.3C). The phosphorylation of PDH is associated with a reduced coupling between glycolysis and glucose oxidation. The phosphorylation of PDH to total PDH protein was assessed using western blot analysis.

The differentiated cells experienced a reduced ratio of p-PDH/t-PDH, indicating increased coupling between glycolysis and glucose oxidation (Figure 3.3D). Phosphorylated to total Akt, an indicator of insulin signalling, was unchanged between treatments (Figure 3.3E). IDH, a key enzyme of the TCA cycle to produce α-ketoglutarate, was increased in differentiated ± BOHB treated cells (Figure 3.3F). Key glycolytic enzymes G6PD, PFKFB3, and PKM2 were also assessed using western blot analysis. G6PD expression was increased in the proliferating + BOHB group and the differentiated ± BOHB groups (Figure 3G). There were no differences in PFKFB3 levels between any groups (Figure 3H). PKM2 expression was upregulated in the differentiated ± BOHB groups, with no changes in the proliferating groups (Figure 3I).

A

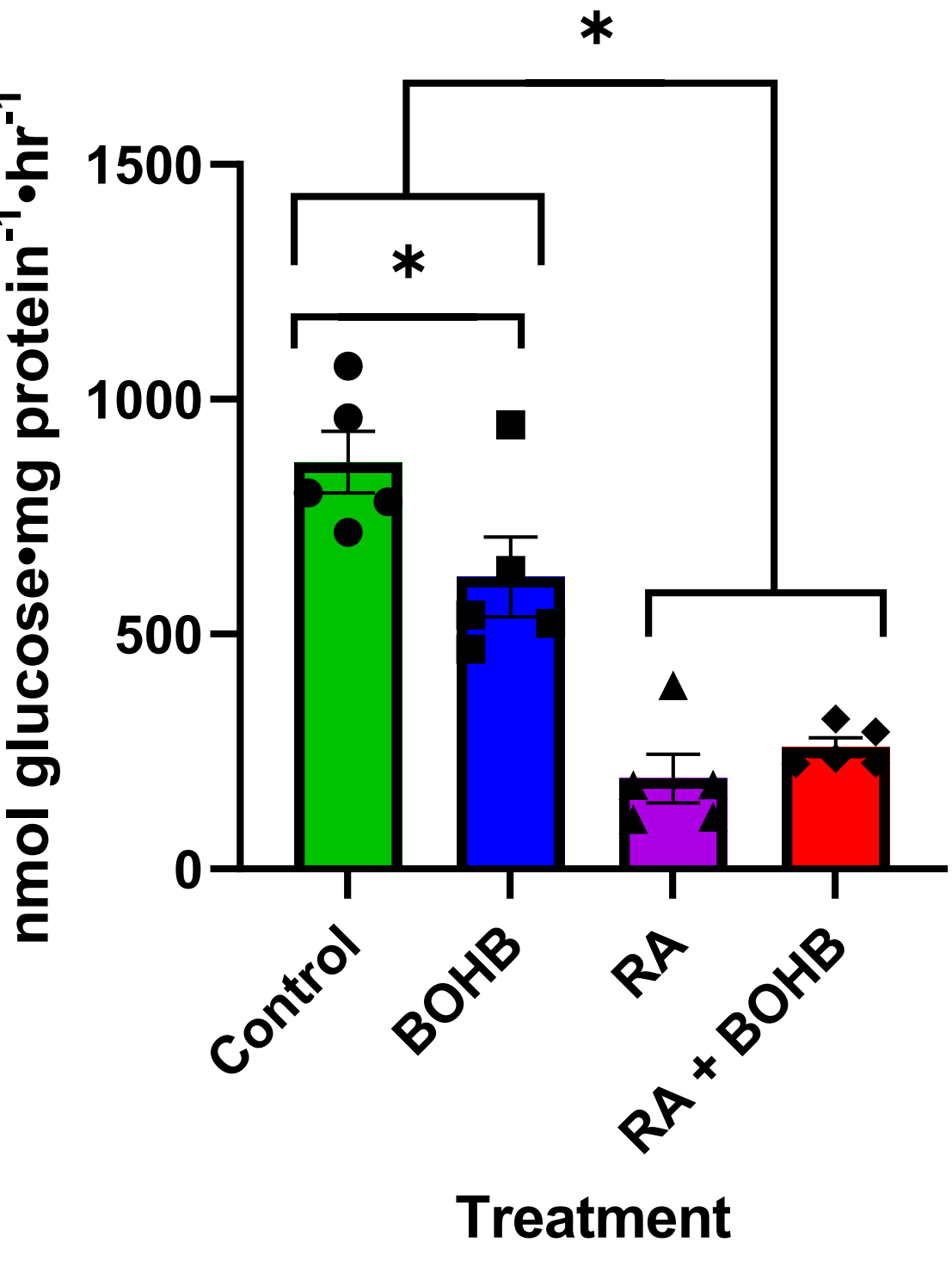
Glycolysis
*
*
1500
1000
500
0
nmol glucose•mg protein-1•hr-1
Control
BOHB
RA
RA + BOHB
Treatment

B

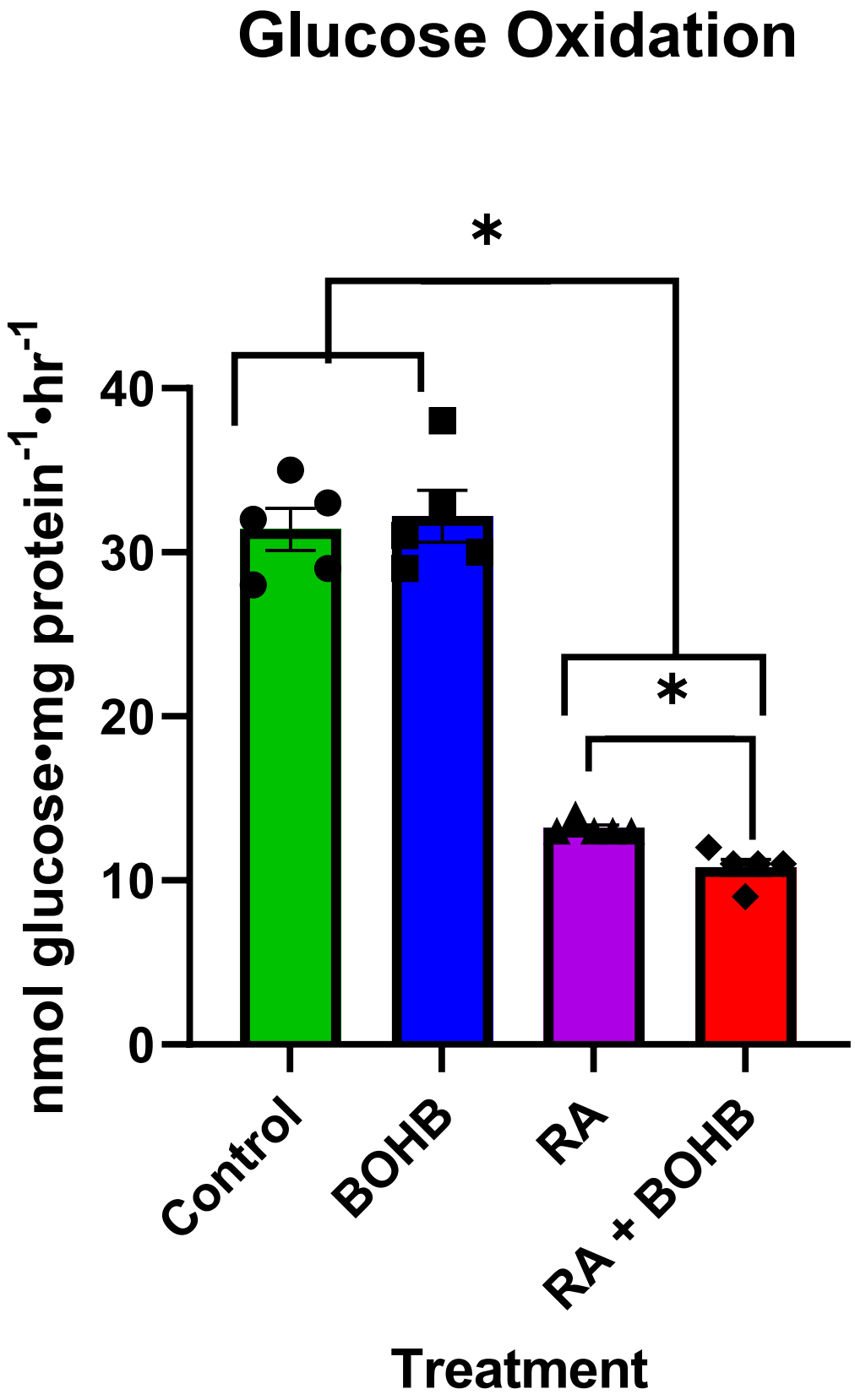
Glucose Oxidation
*
*
nmol glucose•mg protein-1•hr-1
40
30
20
10
0
Control
BOHB
RA
RA + BOHB
Treatment

c

Glucose uptake

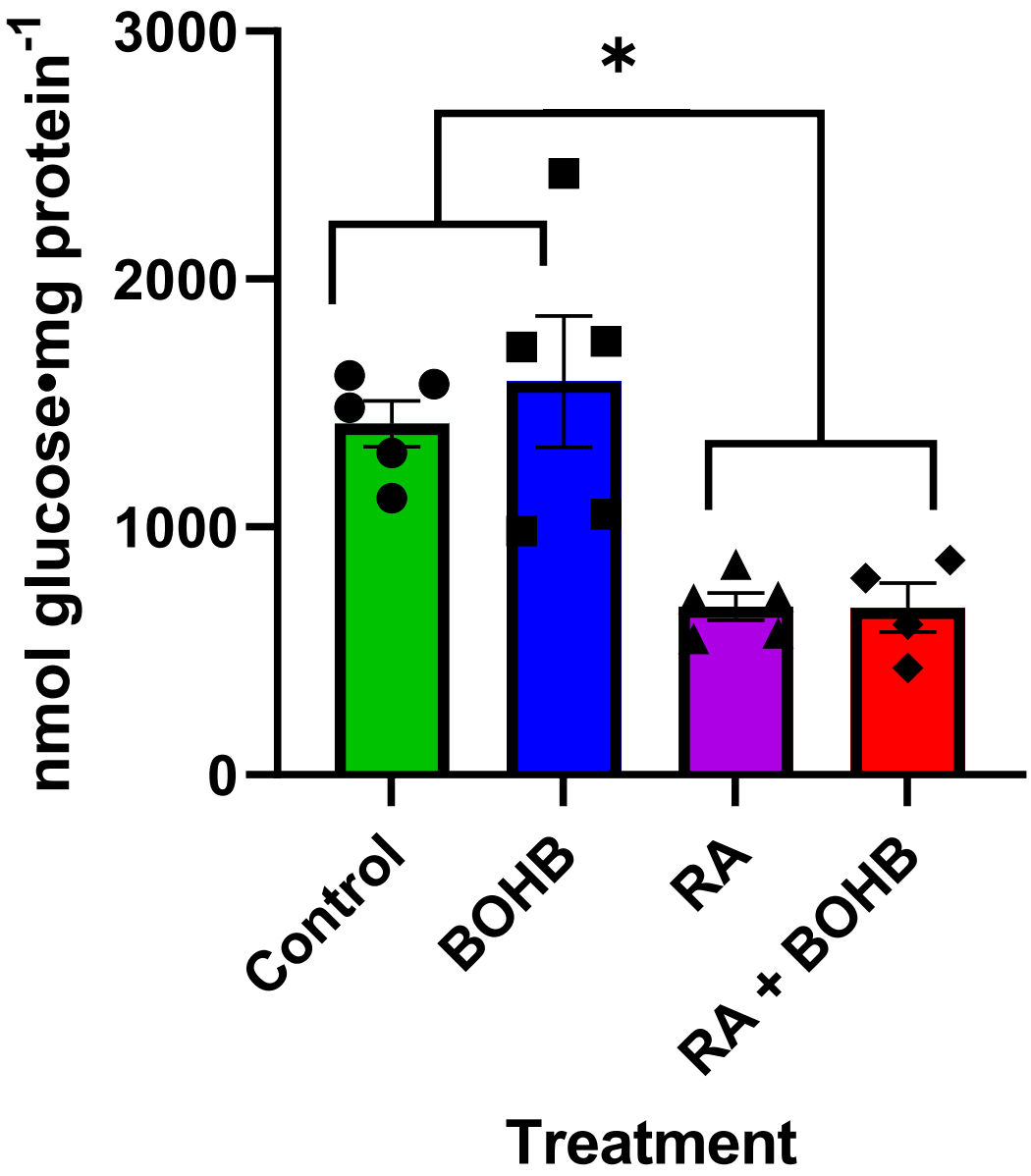

D

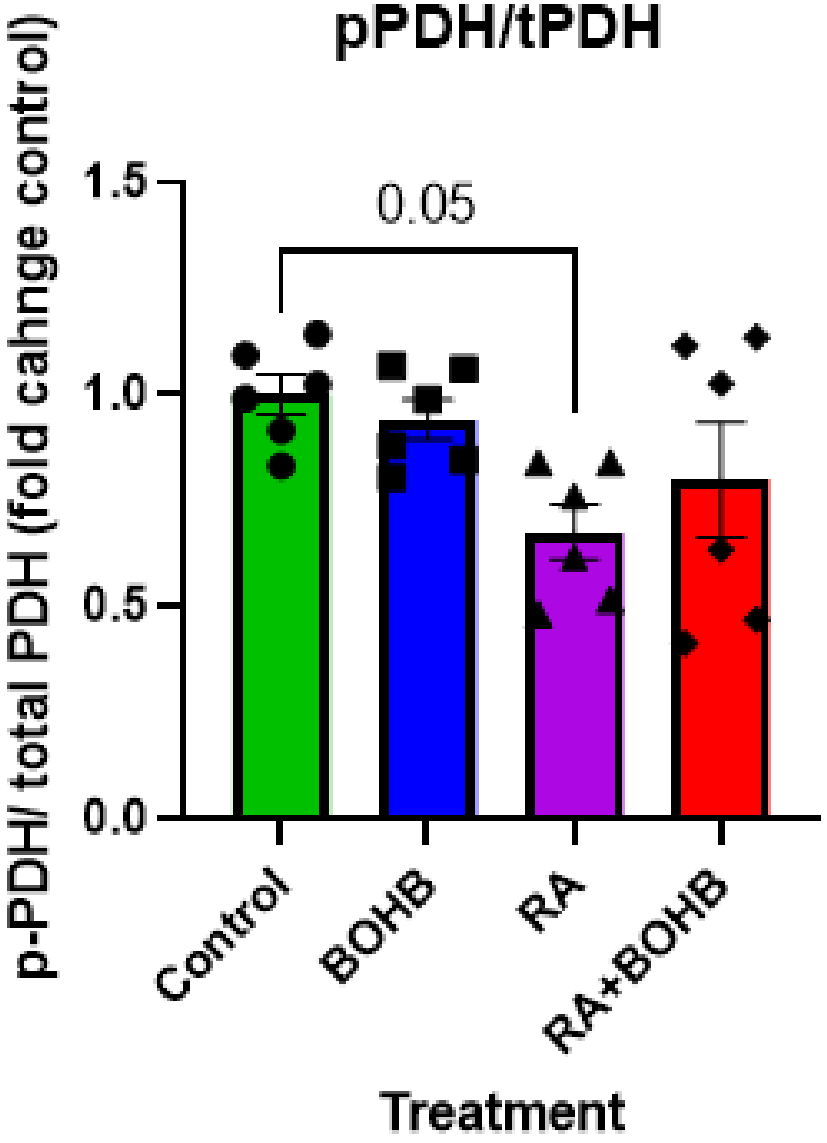
pPDH/tPDH
p-PDH/ total PDH (fold cahnge control)
1.5
1.0
0.5
0.0
0.05
Control
BOHB
RA
RA+BOHB
Treatment

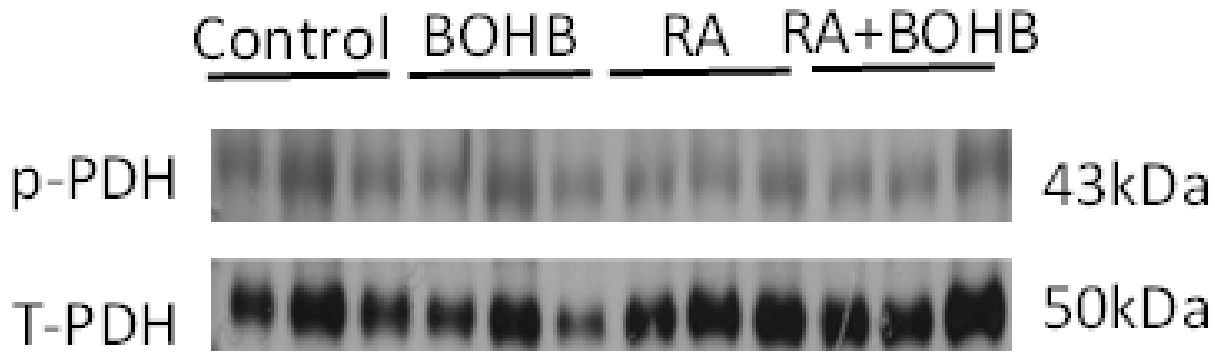
Control
BOHB
RA
RA+BOHB
p-PDH
43kDa
T-PDH
50kDa

E

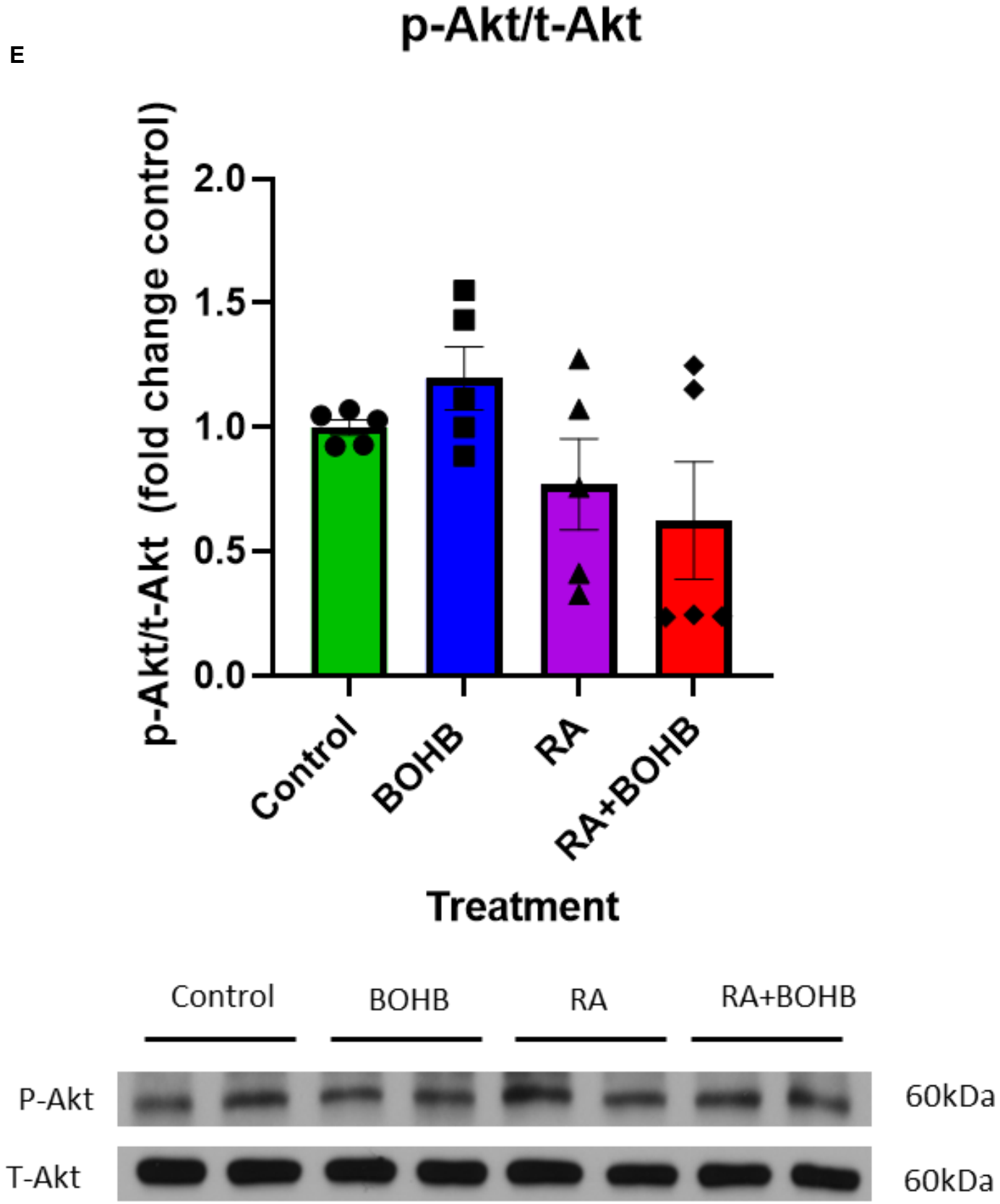
p-Akt/t-Akt
p-Akt/t-Akt (fold change control)
2.0
1.5
1.0
0.5
0.0
Control
BOHB
RA
RA+BOHB
Treatment
Control
BOHB
RA
RA+BOHB
P-Akt
60kDa
T-Akt
60kDa

F

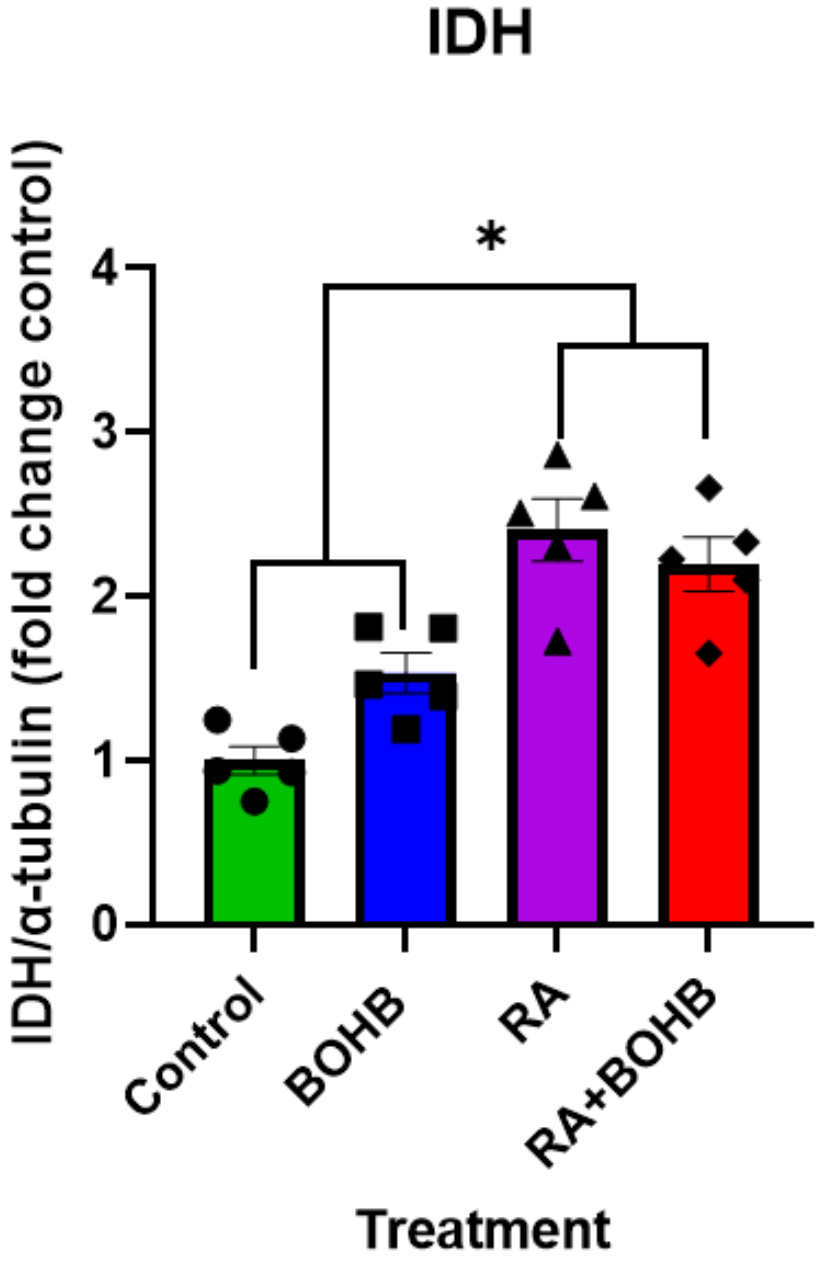
IDH
IDH/α-tubulin (fold change control)
*
4
3
2
1
0
Control
BOHB
RA
RA+BOHB
Treatment

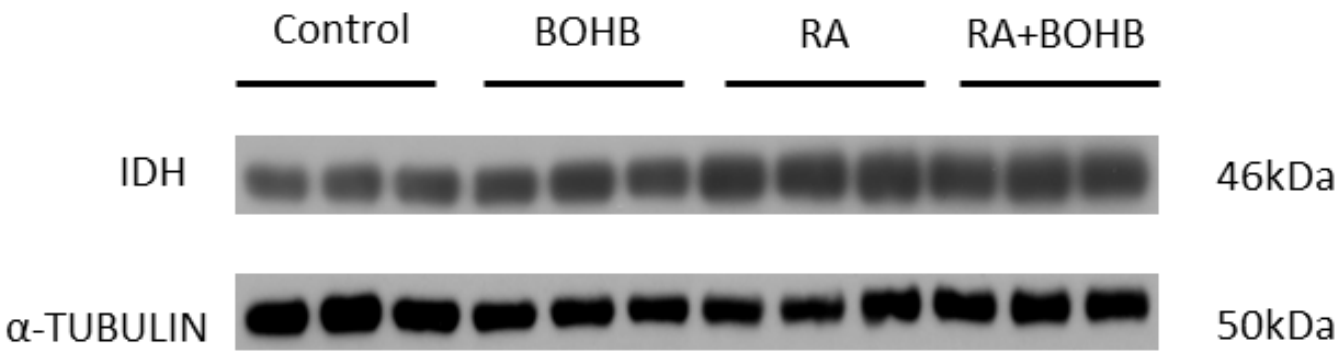
Control
BOHB
RA
RA+BOHB
IDH
46kDa
α-TUBULIN
50kDa

G

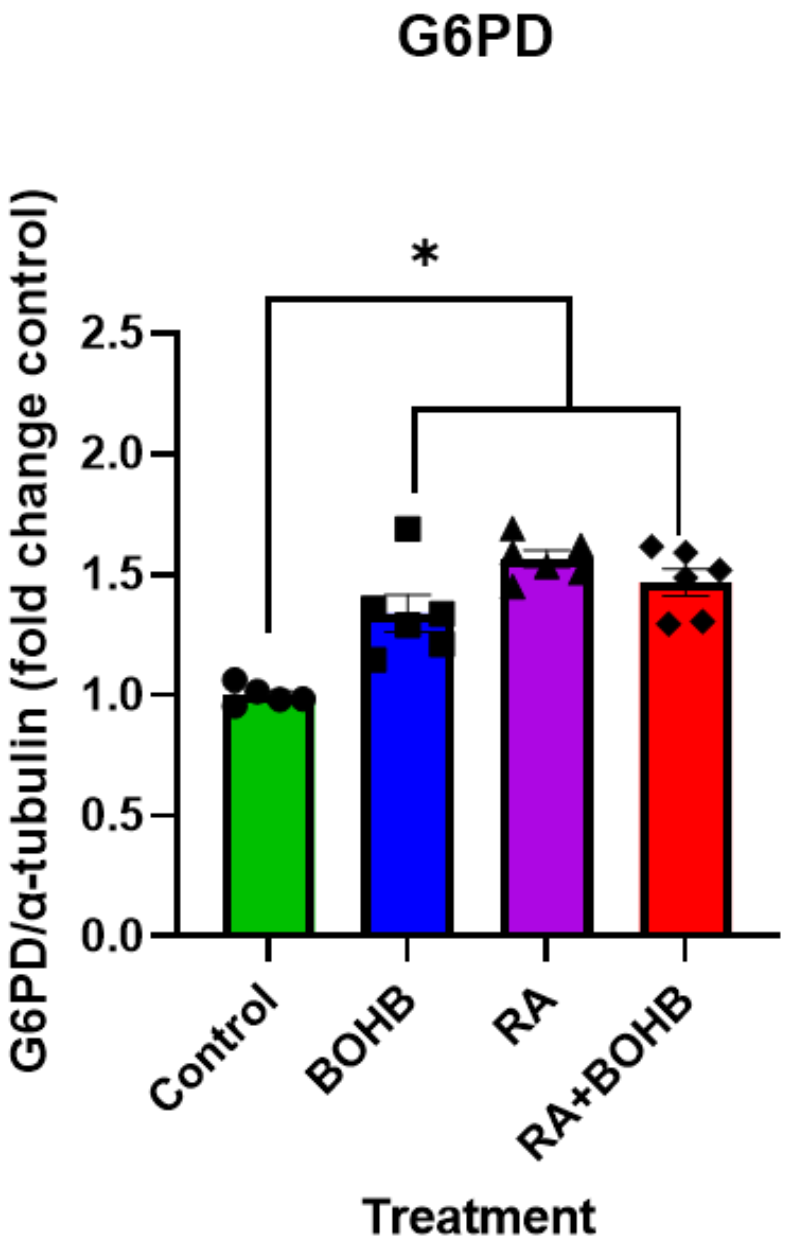
G6PD
*
G6PD/α-tubulin (fold change control)
2.5
2.0
1.5
1.0
0.5
0.0
Control
BOHB
RA
RA+BOHB
Treatment

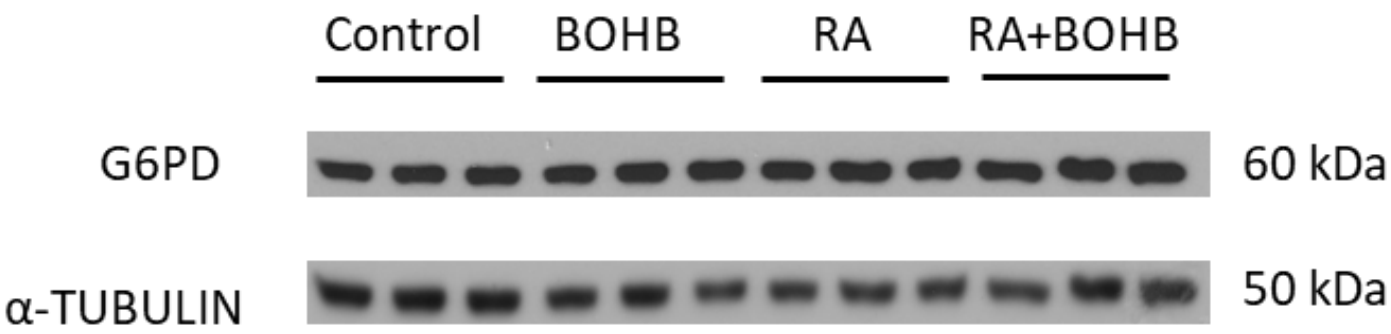
Control
BOHB
RA
RA+BOHB
G6PD
60 kDa
α-TUBULIN
50 kDa

H

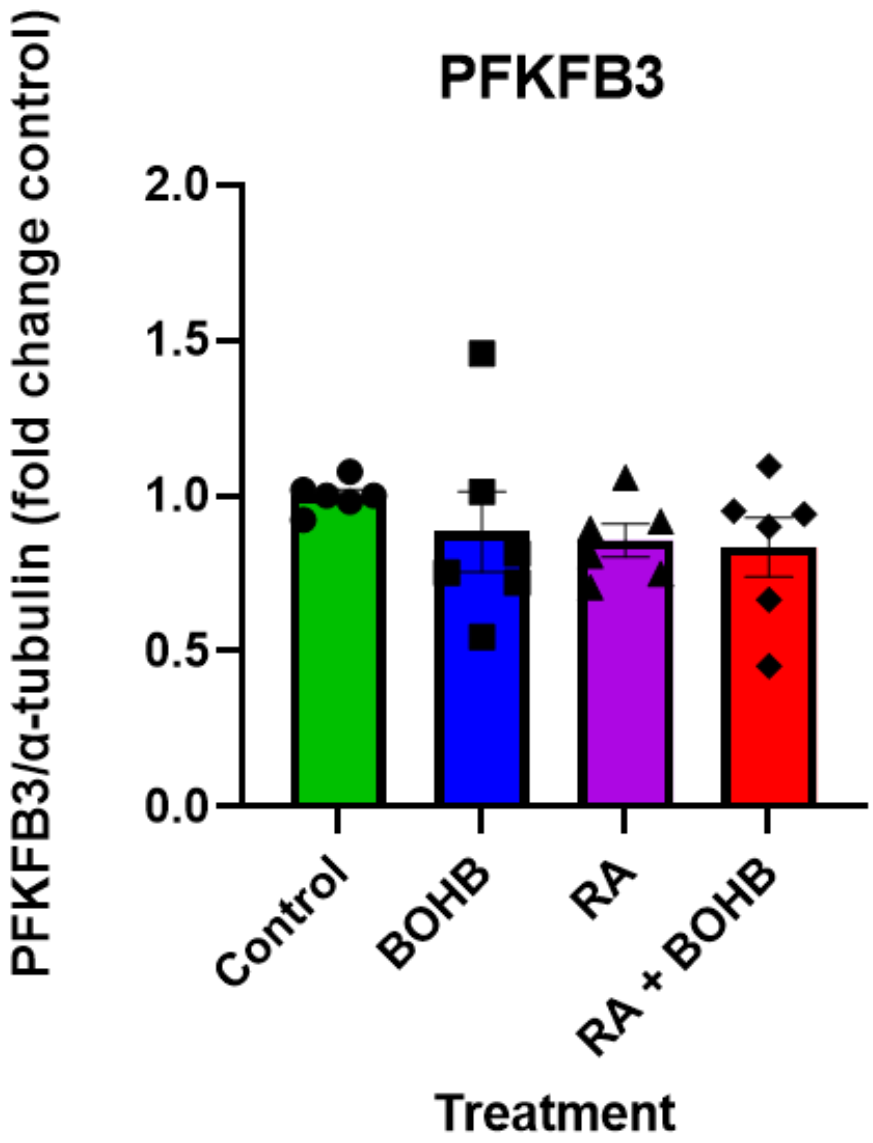
PFKFB3
PFKFB3/α-tubulin (fold change control)
2.0
1.5
1.0
0.5
0.0
Control
BOHB
RA
RA + BOHB
Treatment

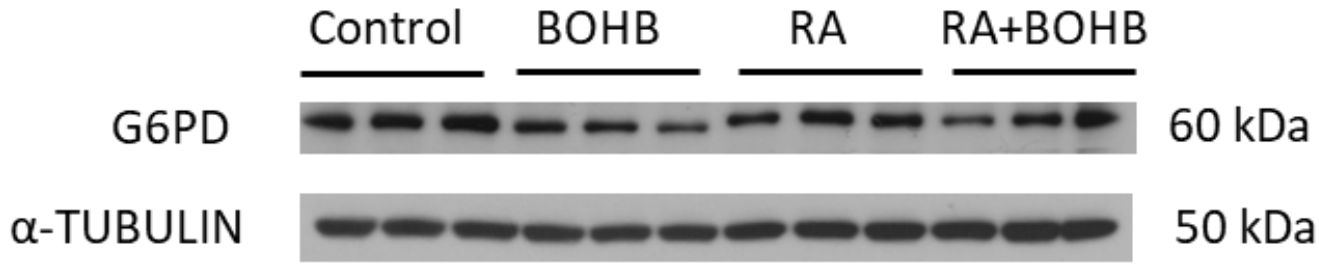
Control
BOHB
RA
RA+BOHB
G6PD
60 kDa
α-TUBULIN
50 kDa

I

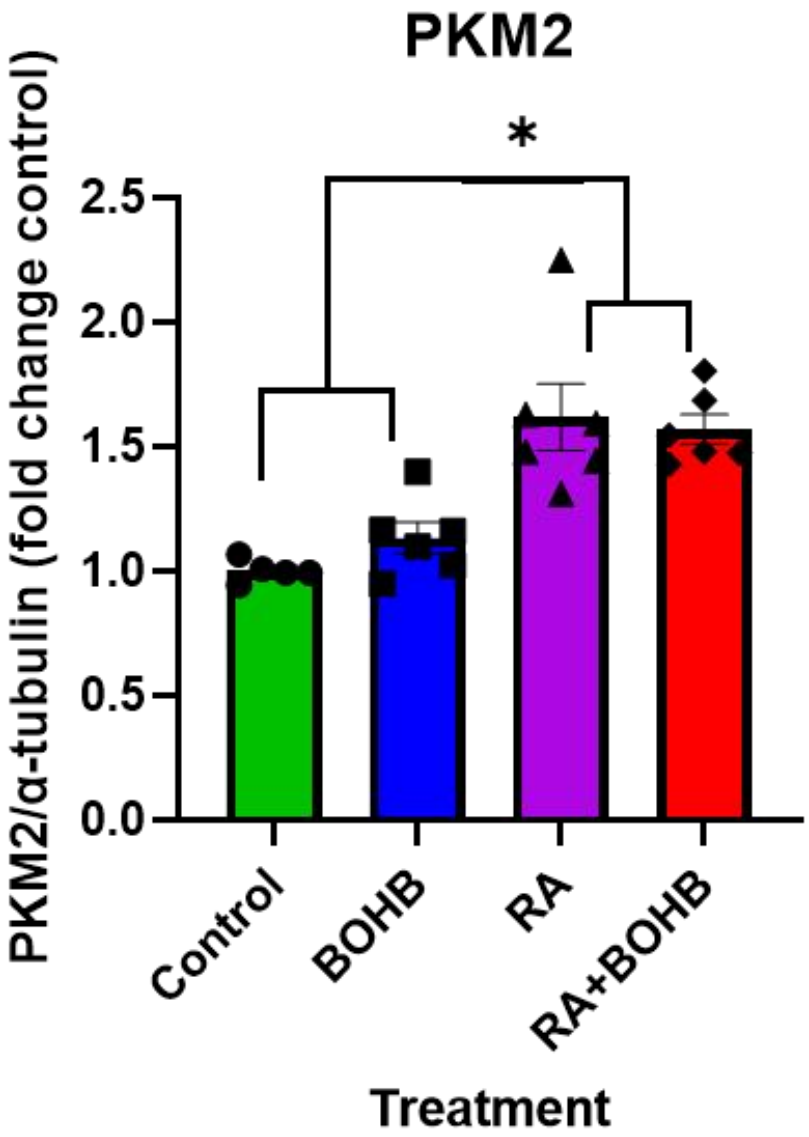
PKM2
*
PKM2/α-tubulin (fold change control)
2.5
2.0
1.5
1.0
0.5
0.0
Control
BOHB
RA
RA+BOHB
Treatment

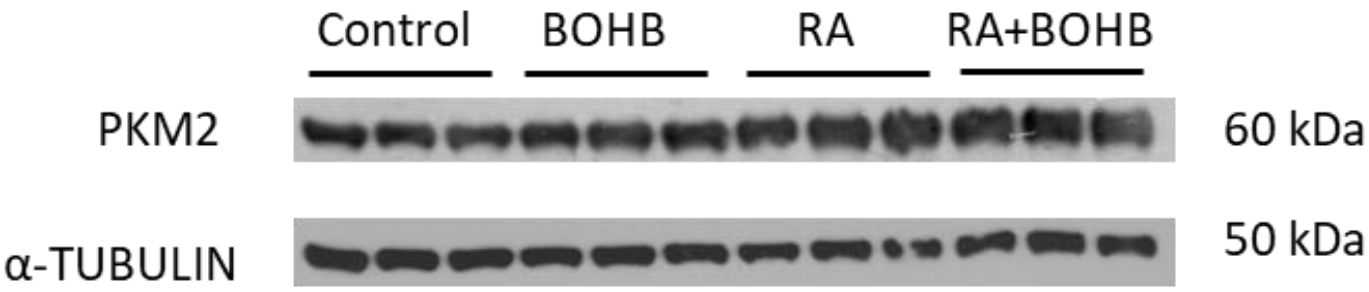
Control
BOHB
RA
RA+BOHB
PKM2
60 kDa
α-TUBULIN
50 kDa

Figure 3.3. The Warburg effect is reduced with cardiomyocyte differentiation and when ketones are added to proliferating cardiomyocytes. Glycolysis (**A**), glucose oxidation (**B**) and glucose uptake (**C**). Protein expression and quantification for proteins related to glucose metabolism: phosphorylated pyruvate dehydrogenase (PDH) over PDH (**D**), phosphorylate Akt over total A©(**E**), isocitrate dehydrogenase (IDH) (**F**), glucose 6 phosphate dehydrogenase (G6PD) (**G**), 6-phosphfructo-2-kinase/fructose-2,6-biphosphate 3 (PFKFB3) (**H**), pyruvate kinase isoform M2 (PKM2) (**I**). n= 5-6 for each experimental group. Individual values for each group are presented as a scatter plot with its mean ± SEM. Data were analyzed with Two-way ANOVA followed by Tukey's for multiple comparisons. Samples collected from separate flasks at the end of culture or metabolic incubation. *$p < 0.05$.

3.1.4 Ketone metabolism and signalling in proliferating vs differentiated cells ± ketones

Through the detection of $^{14}CO_2$ the oxidation of 3-^{14}C-BOHB was measured. There were no statistical differences in ketone oxidation between the treatments (Figure 3.4A). However, adding ketones to both proliferating and differentiated cells led to a trend toward increased ketone oxidation. BDH1 is a key enzyme in the ketone oxidation pathway. Despite no changes in ketone oxidation, BDH1 protein expression increased dramatically in differentiated H9c2 cells ± ketones (Figure 3.4B). BOHB is an endogenous inhibitor of HDAC2. Therefore, we also looked at the protein expression of HDAC2 and its downstream target forkhead box O3 (Foxo3a). HDAC2 expression was reduced in differentiated cells ± BOHB, and there seemed to be no effect due to ketones (Figure 3.4C). When looking at the downstream target Foxo3a, protein expression was reduced

in proliferating cells treated with ketones as well as in differentiated cells ± BOHB (Figure 3.4D).

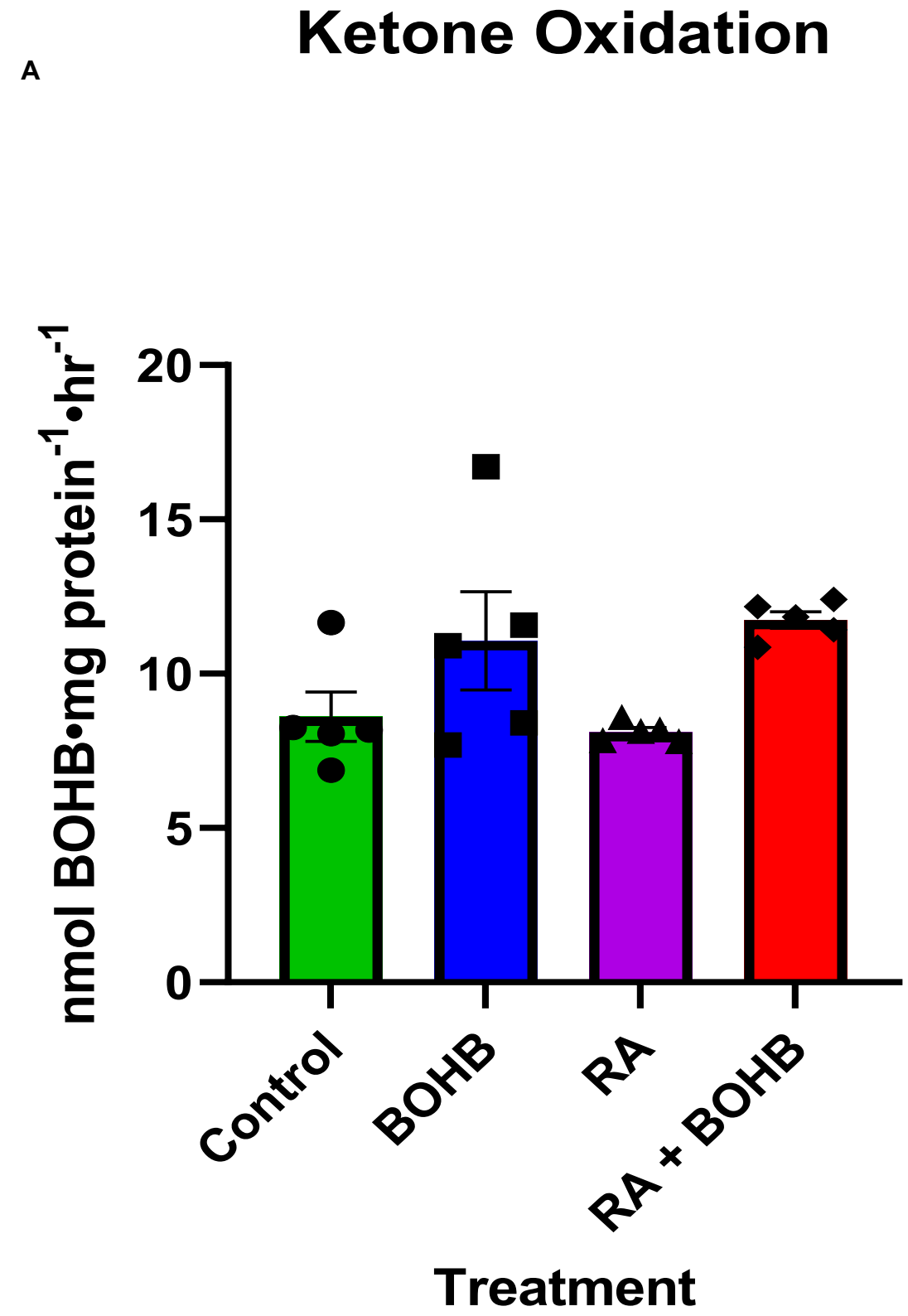

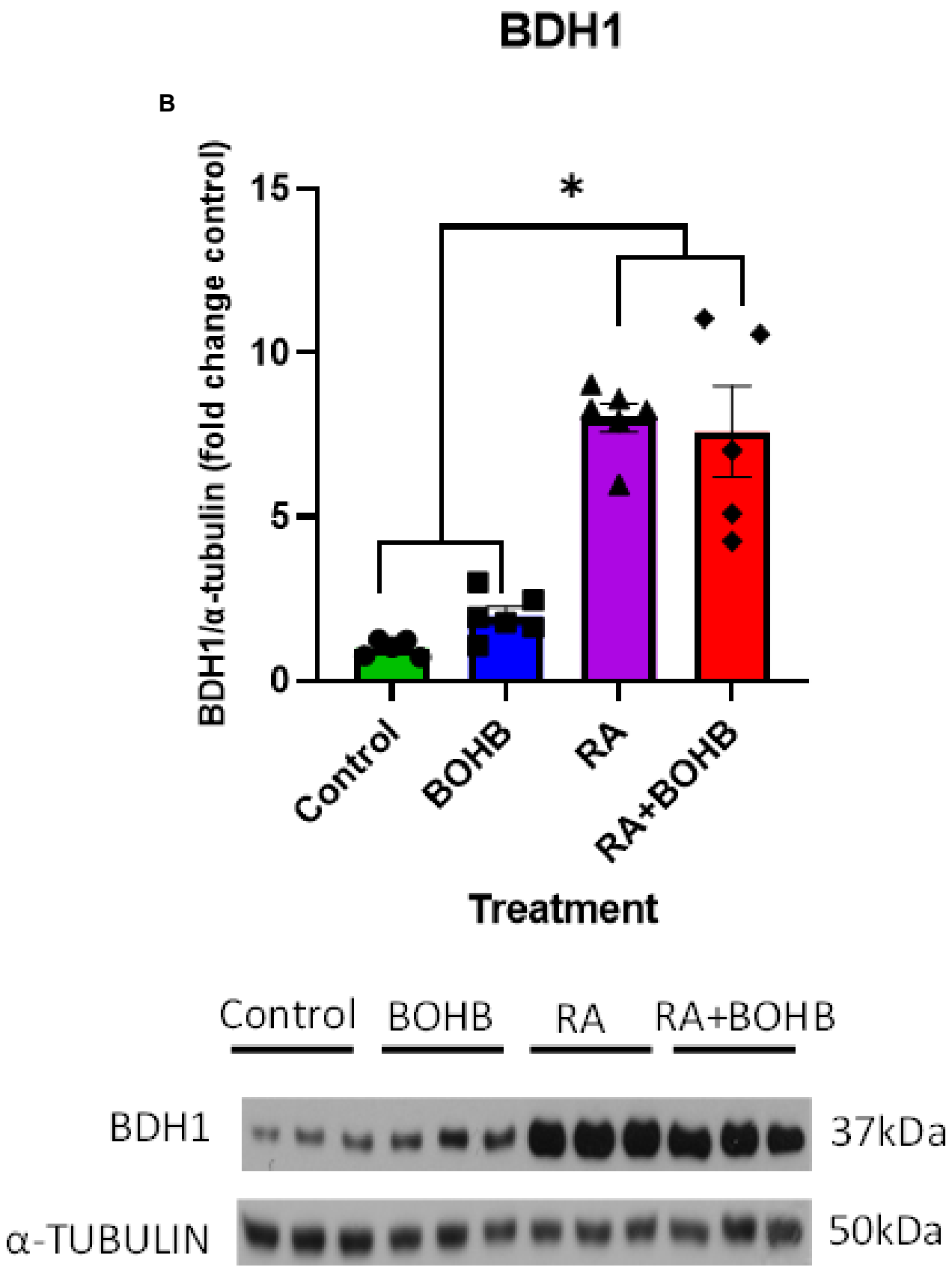
BDH1
B
BDH1/α-tubulin (fold change control)
15
10
5
0
*
Control
BOHB
RA
RA+BOHB
Treatment
Control
BOHB
RA
RA+BOHB
BDH1
37kDa
α-TUBULIN
50kDa

c

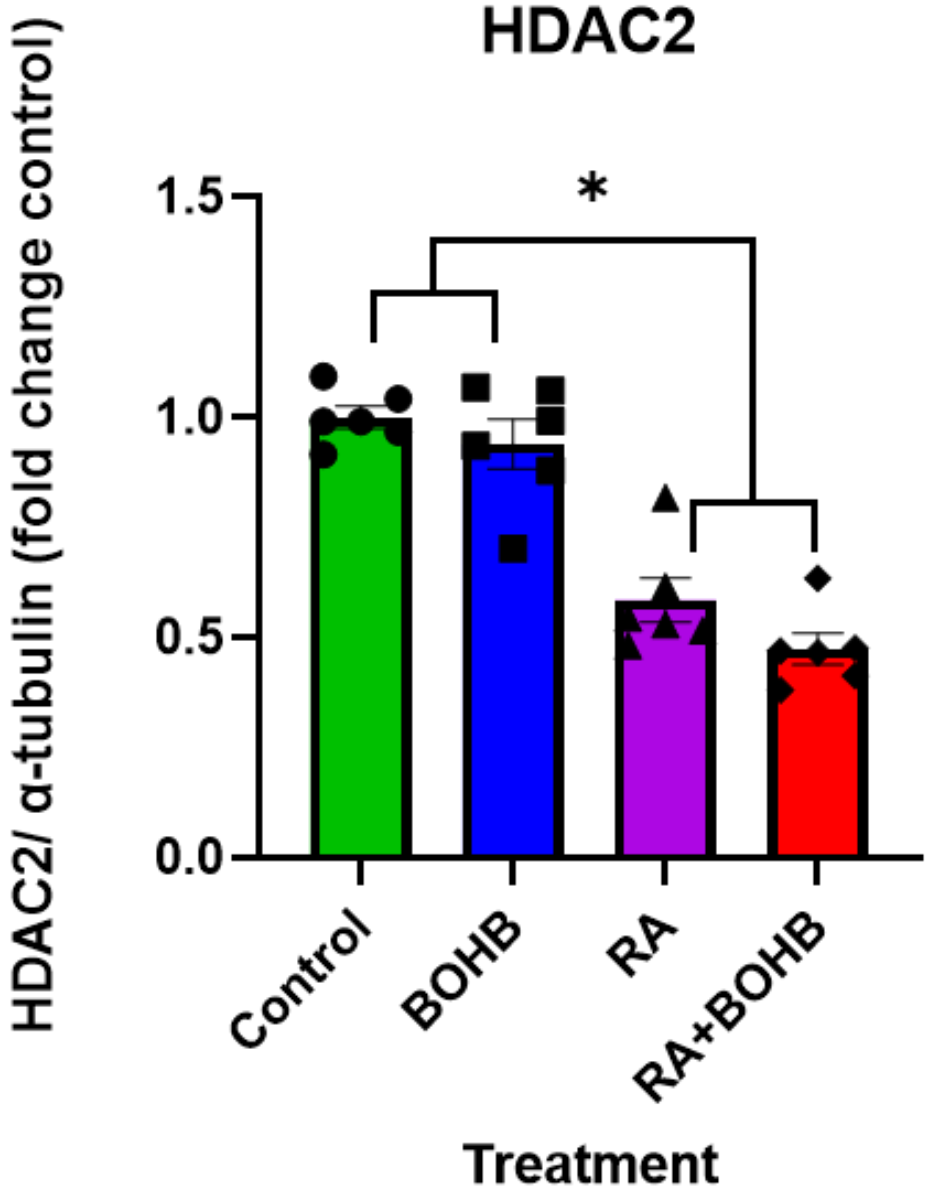
HDAC2
HDAC2/ α-tubulin (fold change control)
1.5
1.0
0.5
0.0
*
Control
BOHB
RA
RA+BOHB
Treatment

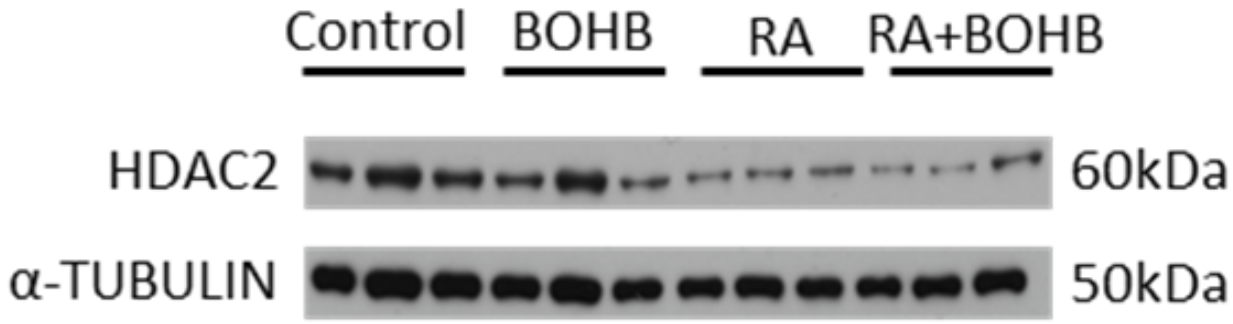
Control
BOHB
RA
RA+BOHB
HDAC2
60kDa
α-TUBULIN
50kDa

D

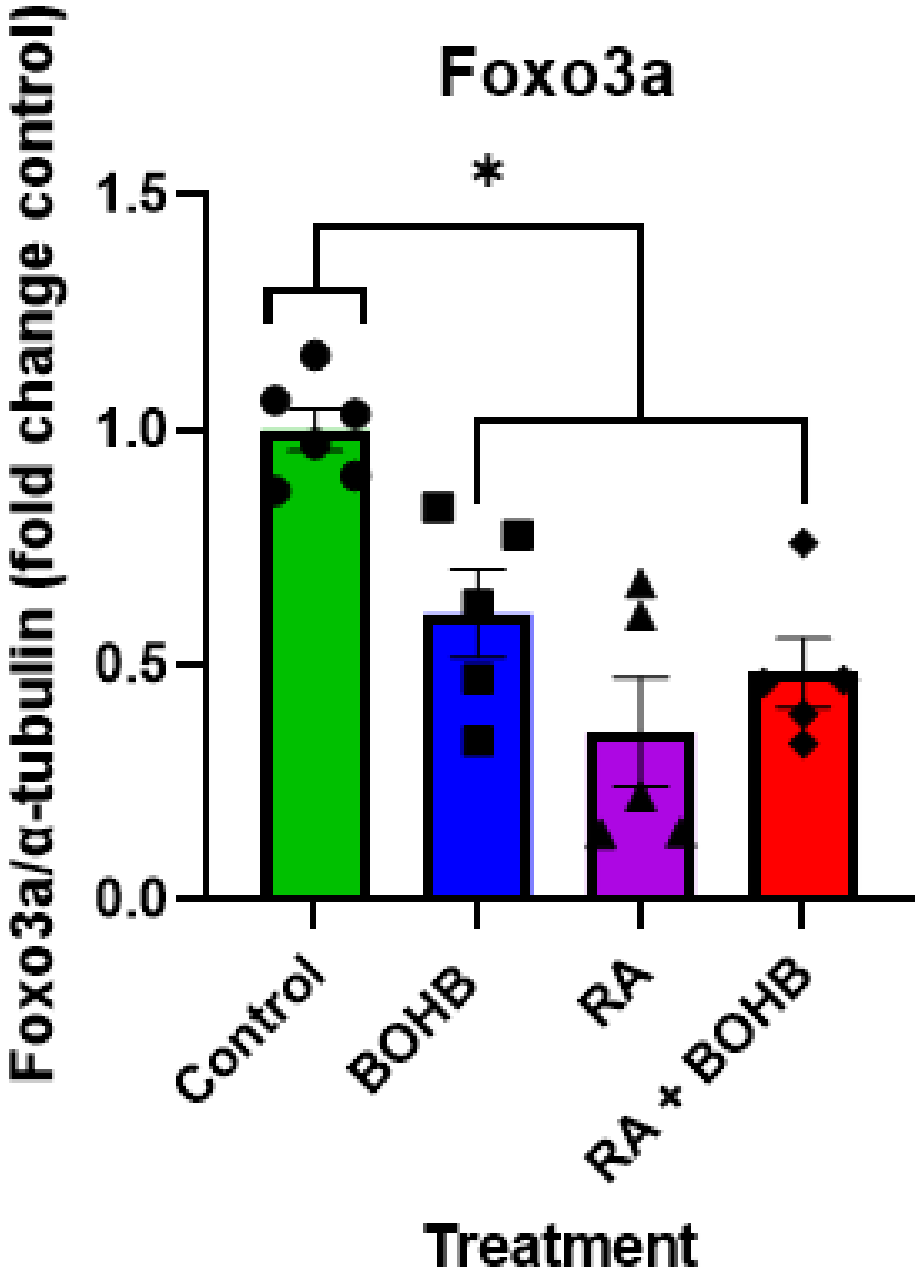
Foxo3a
*
Foxo3a/α-tubulin (fold change control)
1.5
1.0
0.5
0.0
Control
BOHB
RA
RA + BOHB
Treatment

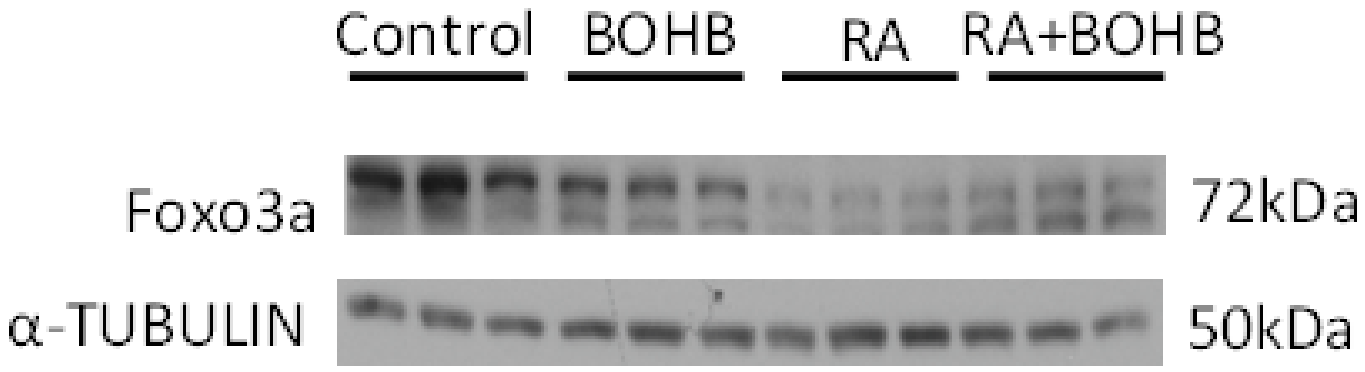
Control
BOHB
RA
RA+BOHB
Foxo3a
72kDa
α-TUBULIN
50kDa

Figure 3.4. Ketone oxidation does not change with differentiation of H9c2 cardiomyocytes. Direct measure of ketone oxidation (**A**). Protein expression and quantification for β-hydroxybutyrate dehydrogenase (BDH1) (**B**), histone deacetylase 2 (HDAC2) (**C**) and forkhead box O3 (Foxo3a) (**D**). n= 5-6. Values for each group are presented as a scatter plot with its mean ± SEM. Data were analyzed with Two-way ANOVA followed by Tukey's for multiple comparisons. Samples collected from separate flasks at the end of culture or metabolic incubation. *p < 0.05.

3.1.5 Fatty acid metabolism in proliferating vs differentiated cells ± ketones

Through the detection of $^{14}CO_2$ the oxidation of 1-^{14}C-palmitate was measured. While there were statistical differences in palmitate oxidation between proliferating ± BOHB treated cells and differentiation ± BOHB treatment (Figure 3.5A), these values were overall extremely low. Palmitate uptake into the cells was not statistically different between treatment groups (Figure 3.5B). PPARα regulates the gene expression of several genes involved in fatty acid β oxidation. PPARα protein expression was significantly upregulated in differentiated ± BOHB treated cells compared to control cells (Figure 3.5C). CPT1 enzymes exist on the outer mitochondrial membrane and transfer acyl groups from acyl-CoA to acylcarnitine, which is subsequently transported into the mitochondria. While CPT1A is more commonly expressed in hepatocytes and CPT1B is more common in cardiomyocytes, both are expressed in heart tissue. CPT1A expression increased in differentiated ± BOHB cells compared to proliferating ± BOHB cells (Figure 3.5D). However, CPT1B expression did not change between treatment groups (Figure 3.5E). LCAD is a major enzyme involved in fatty acid β-oxidation, and there were no

changes in the protein expression for this enzyme between any of the treatment groups (Figure 3.5F). ATGL facilitates the lipolysis of triacylglycerols. Compared to proliferating ± BOHB treated cells, there was an increase in ATGL expression in differentiation ± BOHB cells (Figure 3.5G).

A

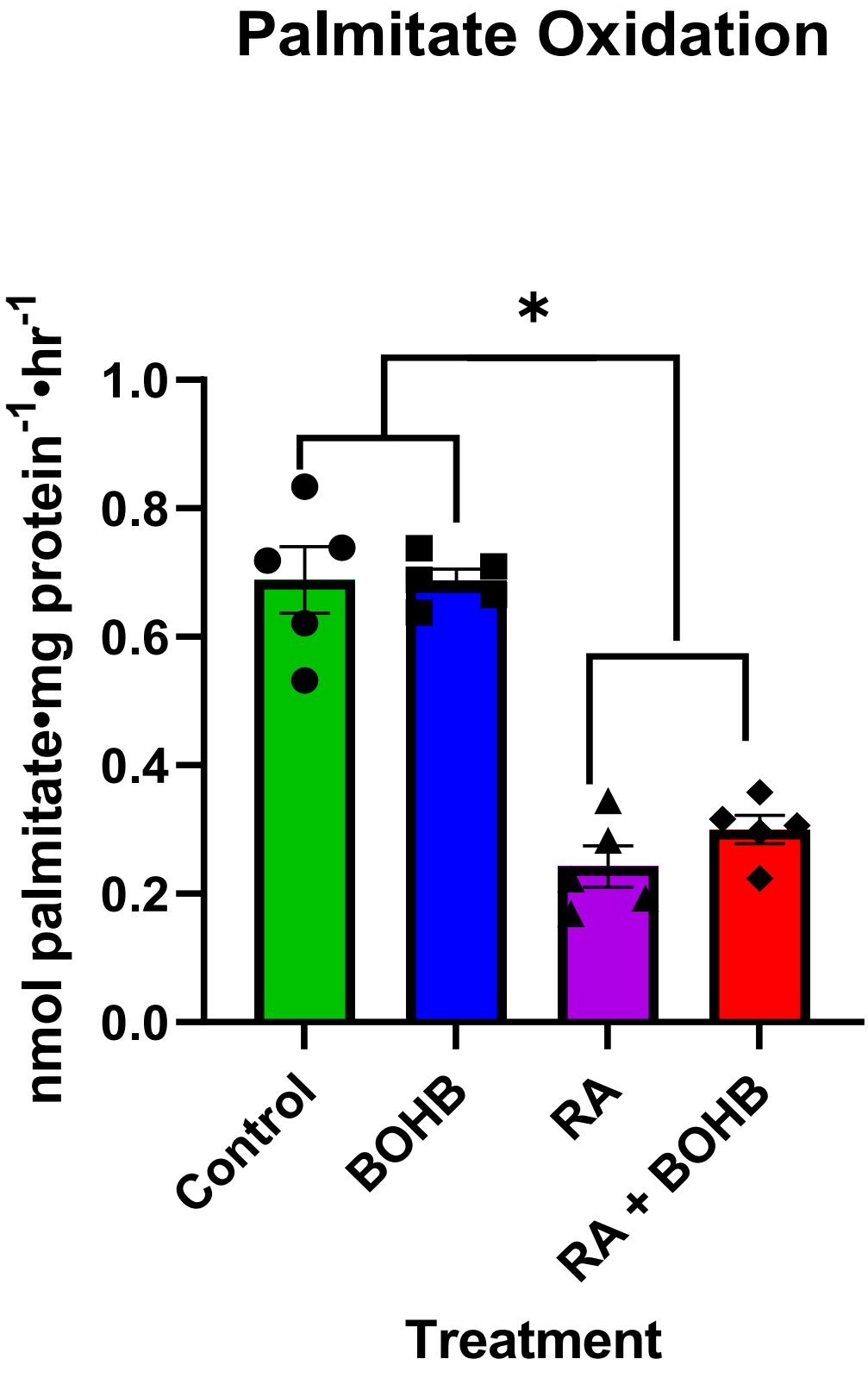

B

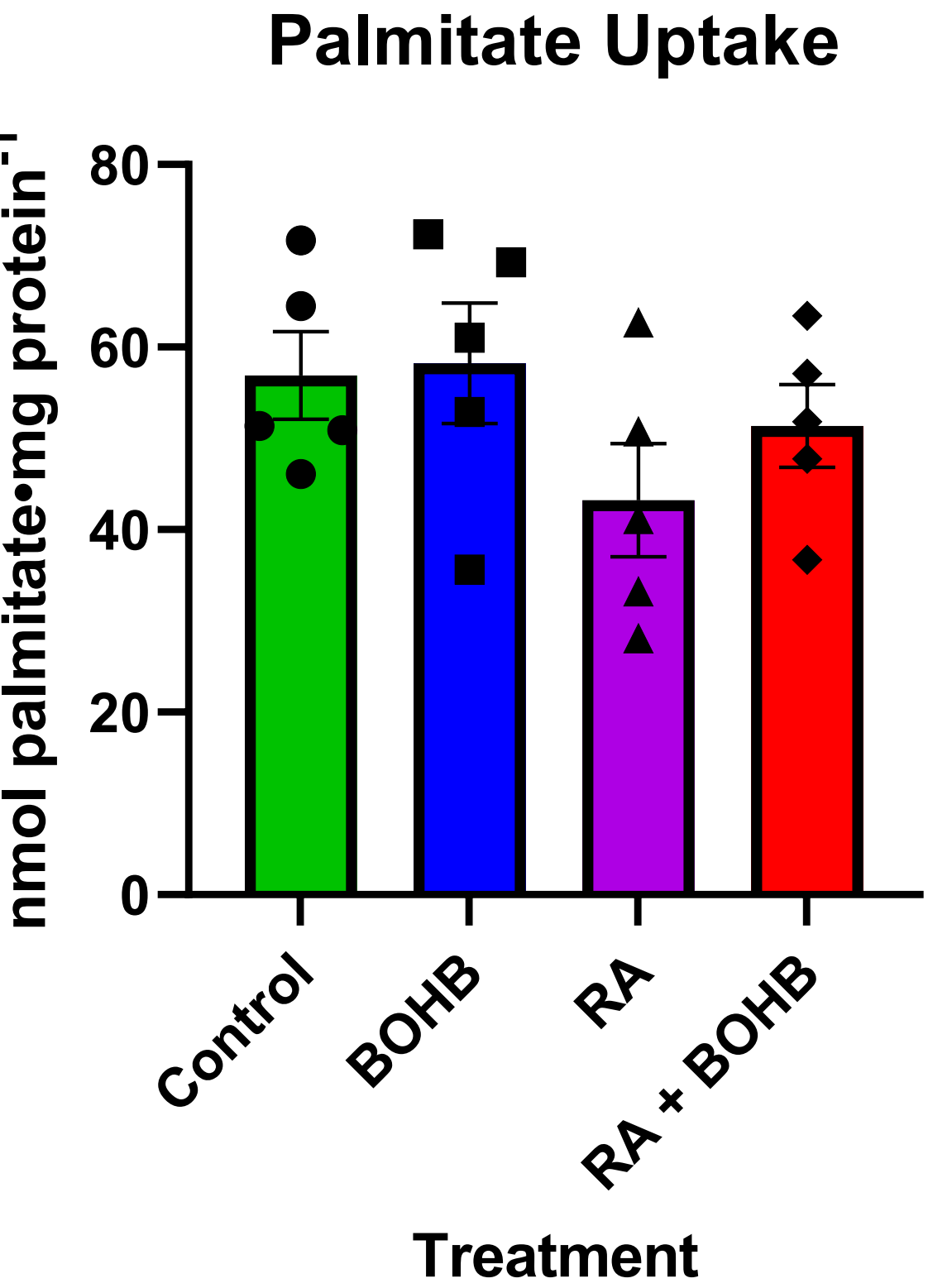
Palmitate Uptake
nmol palmitate•mg protein-1
80
60
40
20
0
Control
BOHB
RA
RA + BOHB
Treatment

c

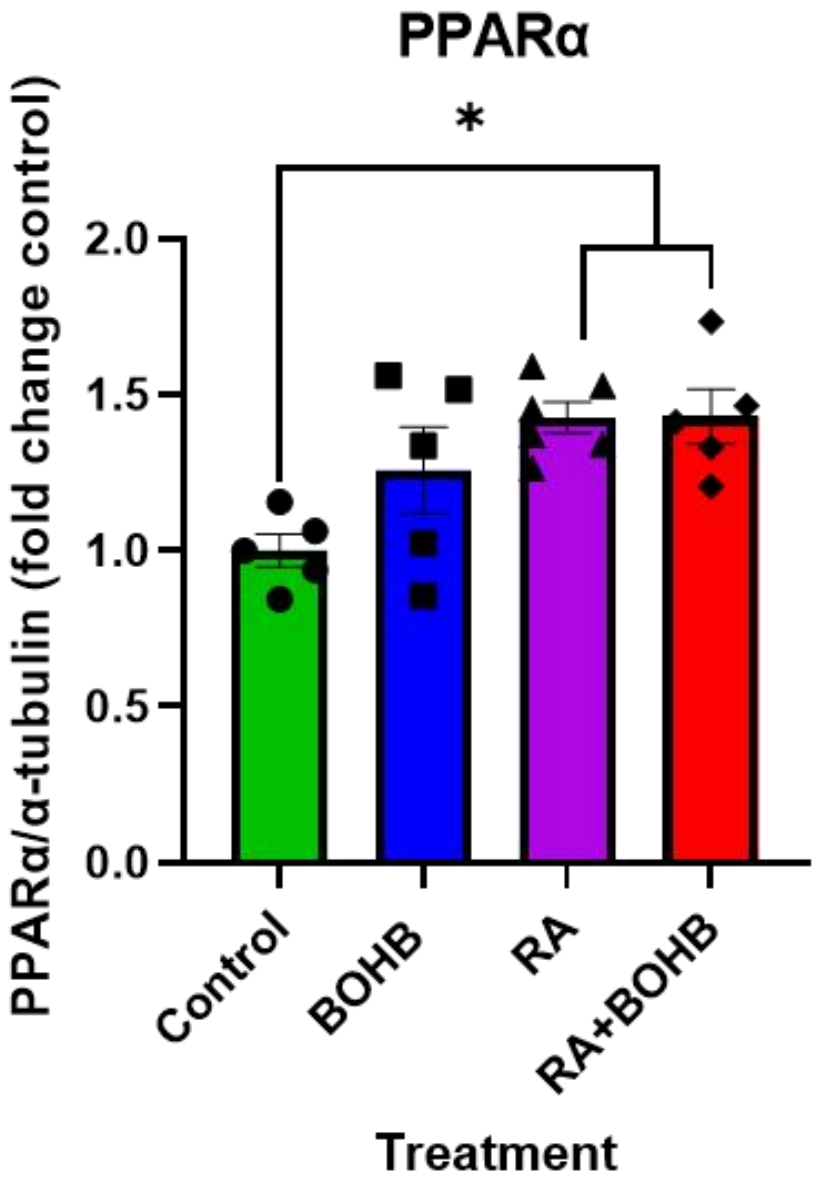
PPARα
*
PPARα/α-tubulin (fold change control)
2.0
1.5
1.0
0.5
0.0
Control
BOHB
RA
RA+BOHB
Treatment

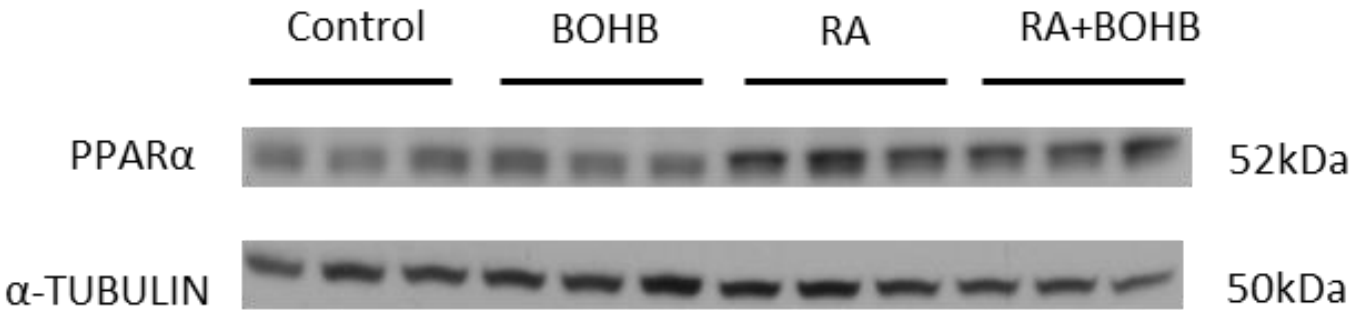
Control
BOHB
RA
RA+BOHB
PPARα
52kDa
α-TUBULIN
50kDa

D

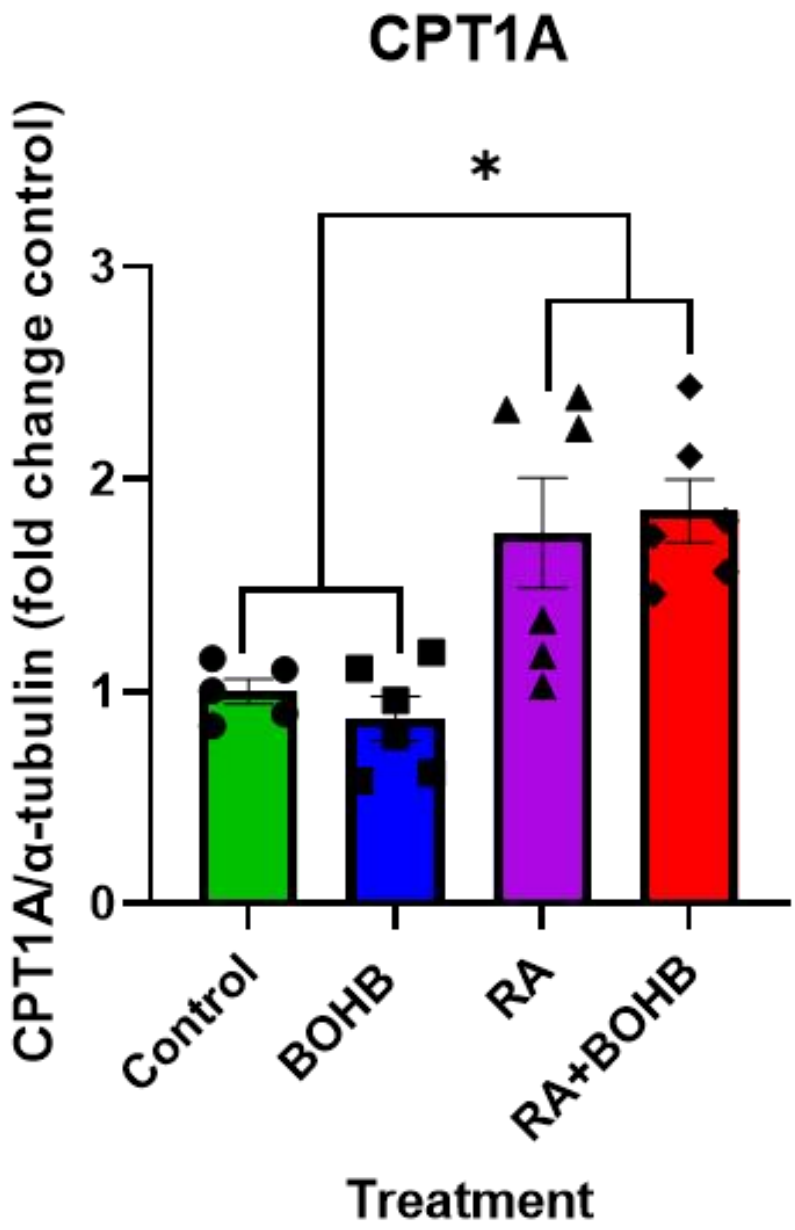
CPT1A
*
CPT1A/α-tubulin (fold change control)
3
2
1
0
Control
BOHB
RA
RA+BOHB
Treatment

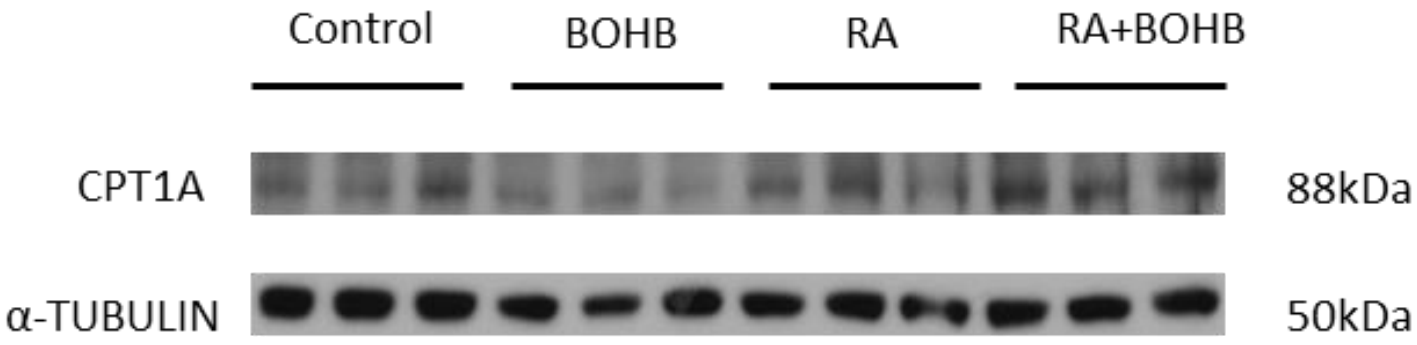
Control
BOHB
RA
RA+BOHB
CPT1A
88kDa
α-TUBULIN
50kDa

E

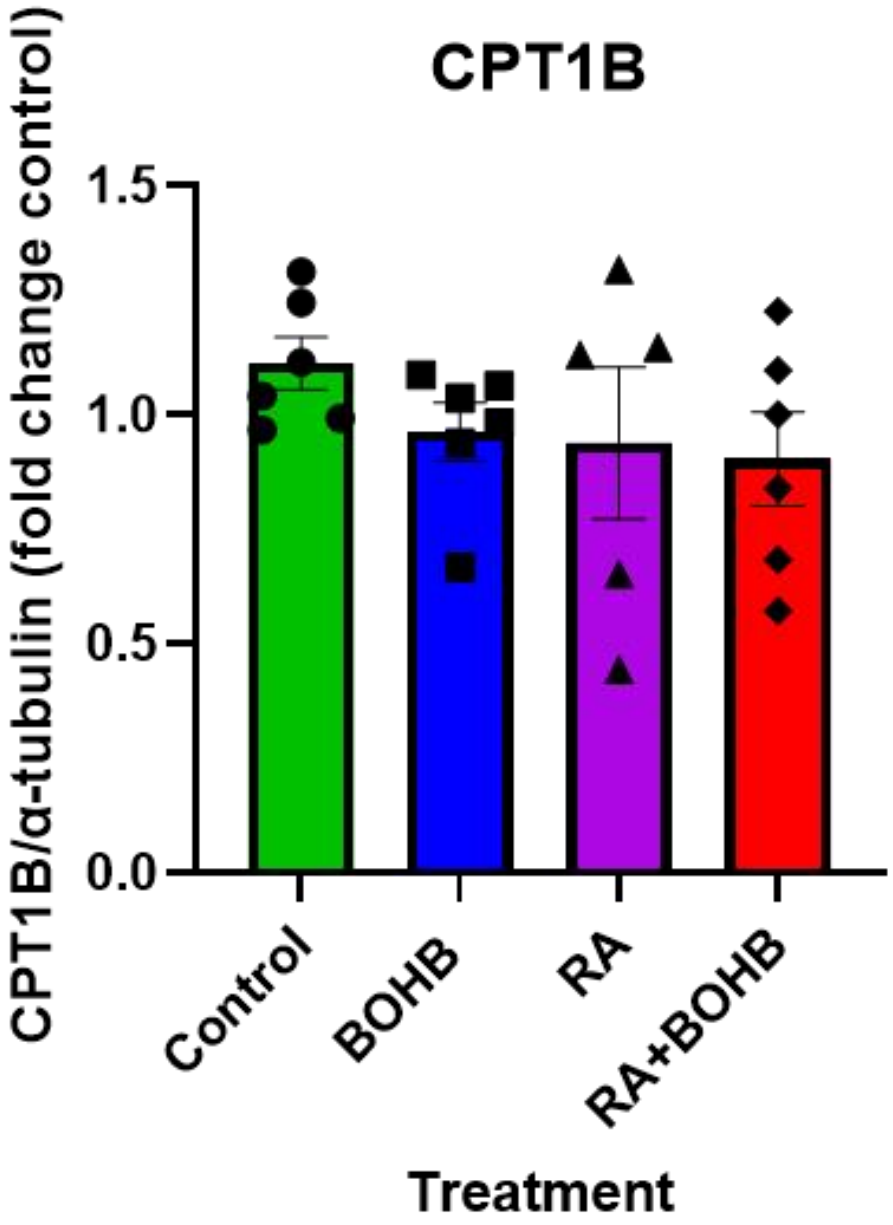
CPT1B
CPT1B/α-tubulin (fold change control)
1.5
1.0
0.5
0.0
Control
BOHB
RA
RA+BOHB
Treatment

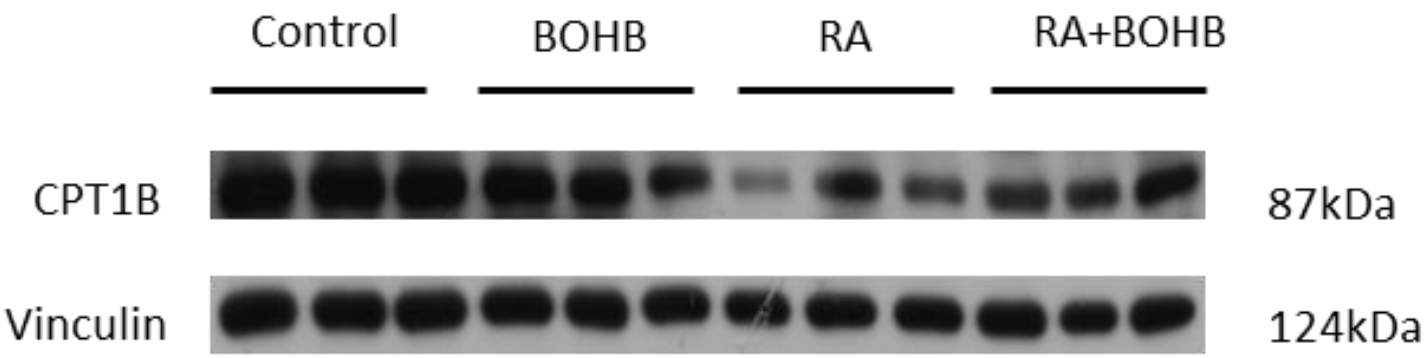
Control
BOHB
RA
RA+BOHB
CPT1B
87kDa
Vinculin
124kDa

F

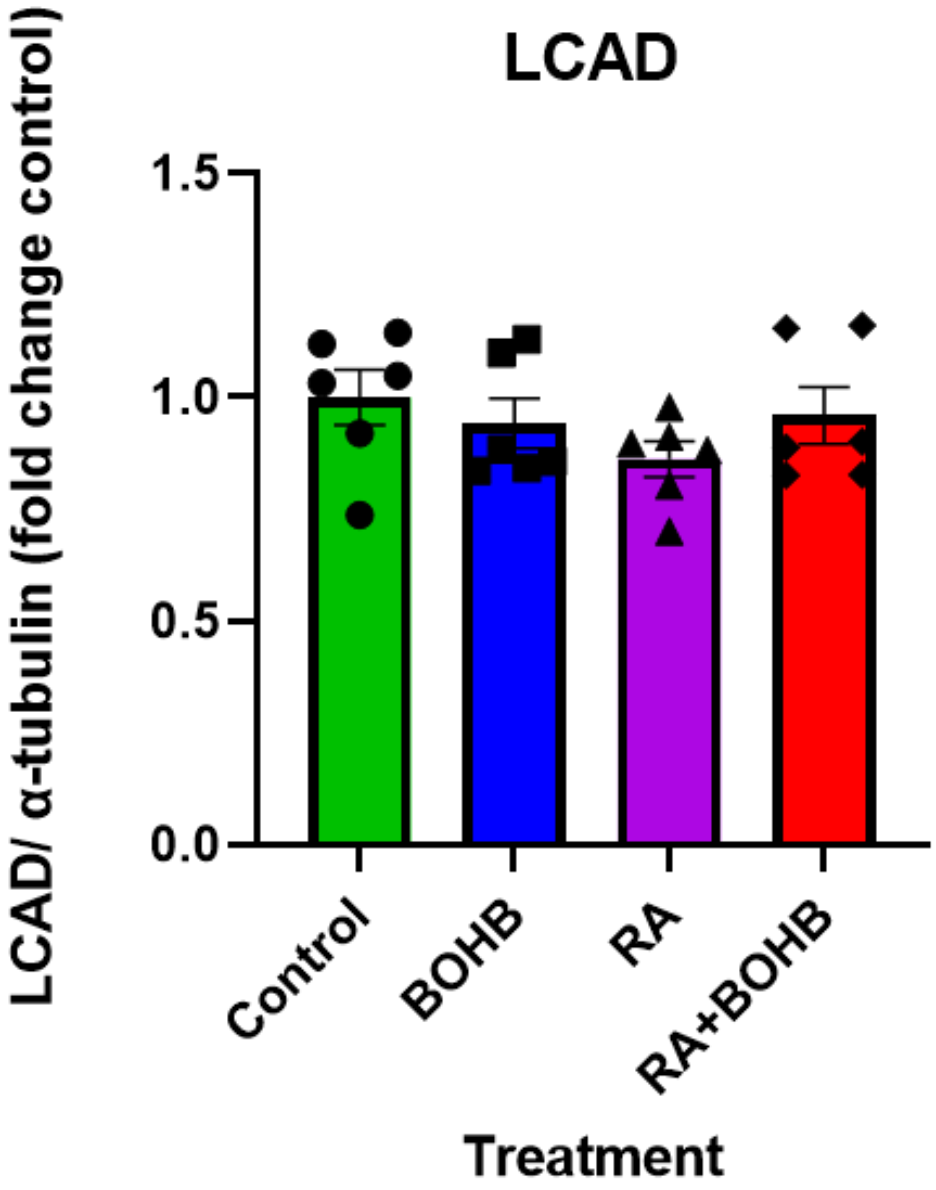
LCAD
LCAD/ α-tubulin (fold change control)
1.5
1.0
0.5
0.0
Control
BOHB
RA
RA+BOHB
Treatment

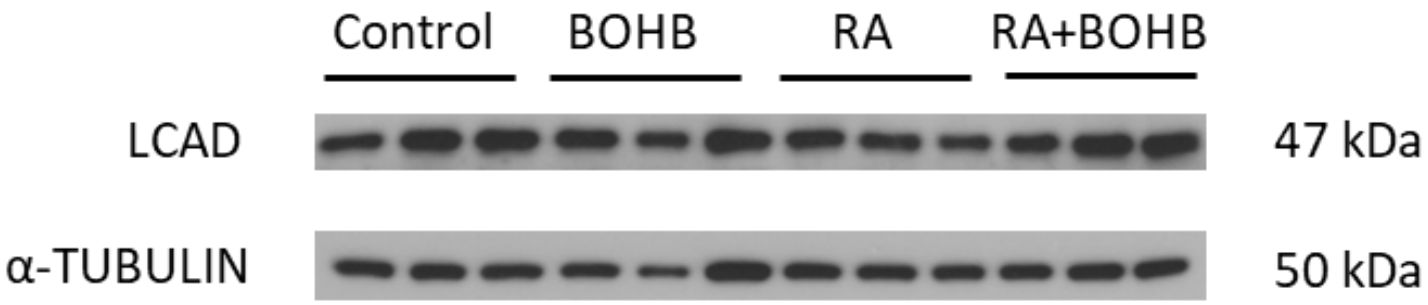
Control
BOHB
RA
RA+BOHB
LCAD
47 kDa
α-TUBULIN
50 kDa

G

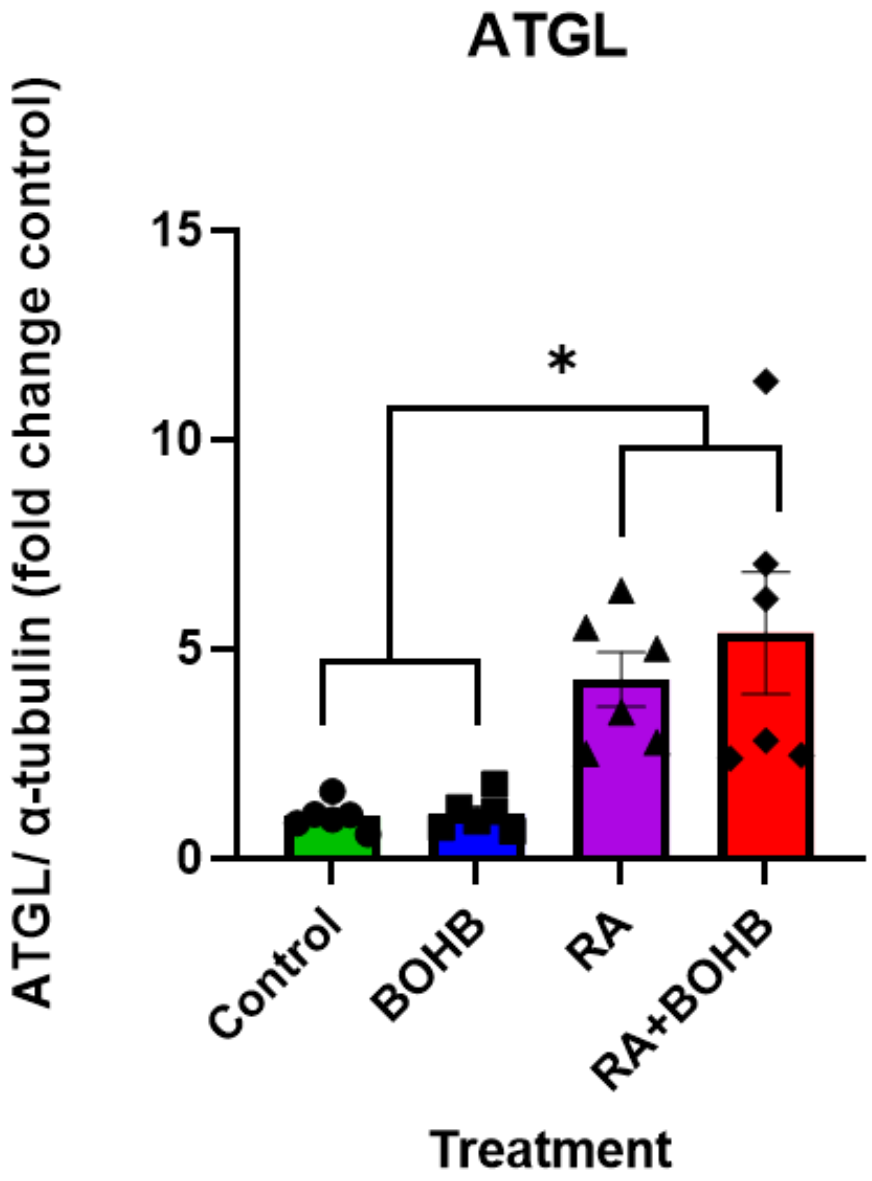
ATGL
ATGL/ α-tubulin (fold change control)
15
10
5
0
*
Control
BOHB
RA
RA+BOHB
Treatment

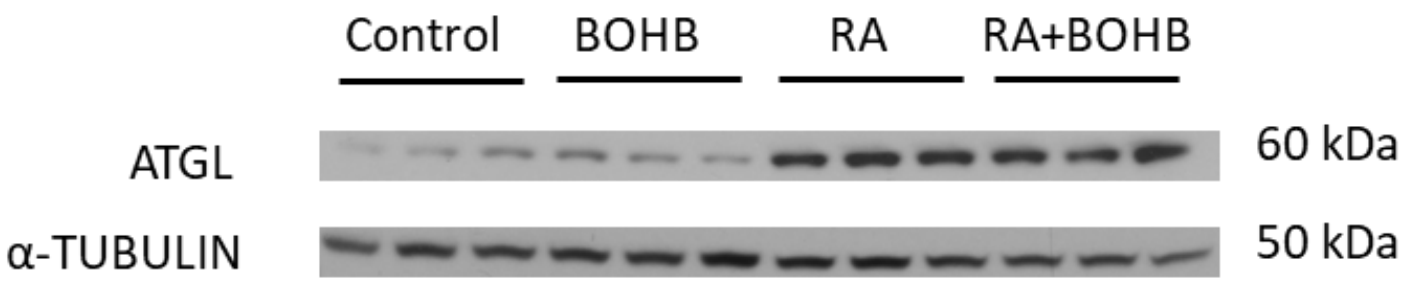
Control
BOHB
RA
RA+BOHB
ATGL
60 kDa
α-TUBULIN
50 kDa

Figure 3.5. Fatty acid oxidation does not change with the addition of ketones to H9c2 cardiomyocytes. Direct measure of palmitate oxidation (**A**) and palmitate uptake (**B**). n=5 for each experimental group. Protein expression and quantification for peroxisome proliferator-activated receptor α (PPARα) (**C**), carnitine palmitoyl transferase 1A (CPT1A) (**D**), CPT1B (**E**), long-chain acyl-CoA dehydrogenase (LCAD) (**F**), and adipose triglyceride lipase (ATGL) (**G**). n=4-6 for each experimental group. Individual values for each group are presented as a scatter plot with its mean ± SEM. Data were analyzed with Two-way ANOVA followed by Tukey's for multiple comparisons. Samples collected from separate flasks at the end of culture or metabolic incubation. *$p < 0.05$.s.

3.1.6 ATP production and % contribution of proliferating vs differentiated cells ± ketones

Compared to control cells, ATP production was dramatically lowered in differentiating cells ± BOHB. Interestingly, in proliferating cells treated with ketones, total ATP production was reduced compared to control cells (Figure 3.6A). How the different metabolic processes contribute to ATP production was different depending on the treatment group, however, palmitate oxidation provided minimal ATP and was constant between treatments (Figure 3.6B). The contribution of glycolysis was reduced in proliferating cells treated with ketones and differentiated cells ± BOHB. The contribution of ATP from ketone oxidation was increased in the differentiated ± BOHB cells despite no changes in ketone oxidation.

A

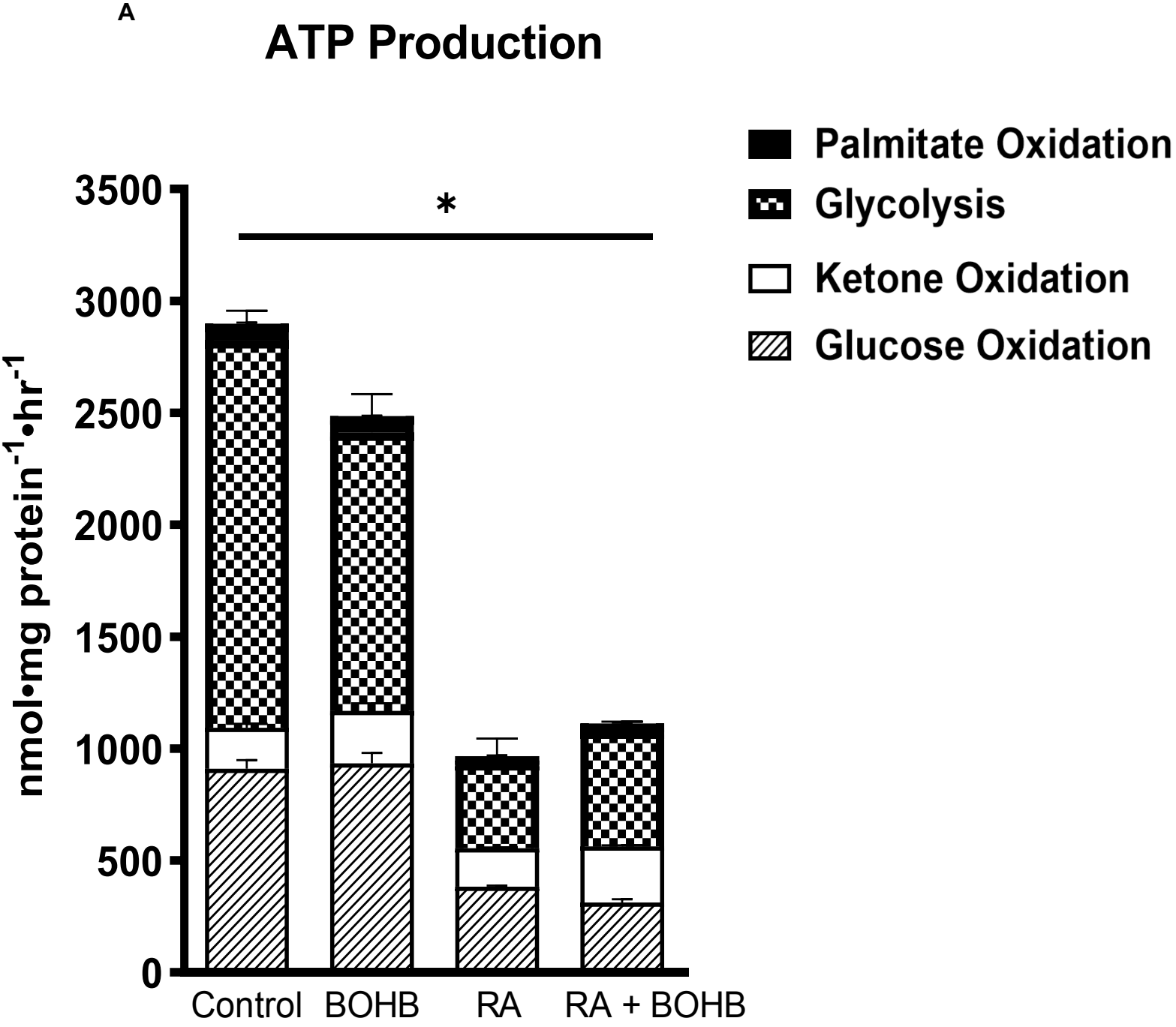
ATP Production
Palmitate Oxidation
Glycolysis
Ketone Oxidation
Glucose Oxidation
*
3500
3000
2500
2000
1500
1000
500
0
nmol•mg protein-1•hr-1
Control
BOHB
RA
RA + BOHB

B

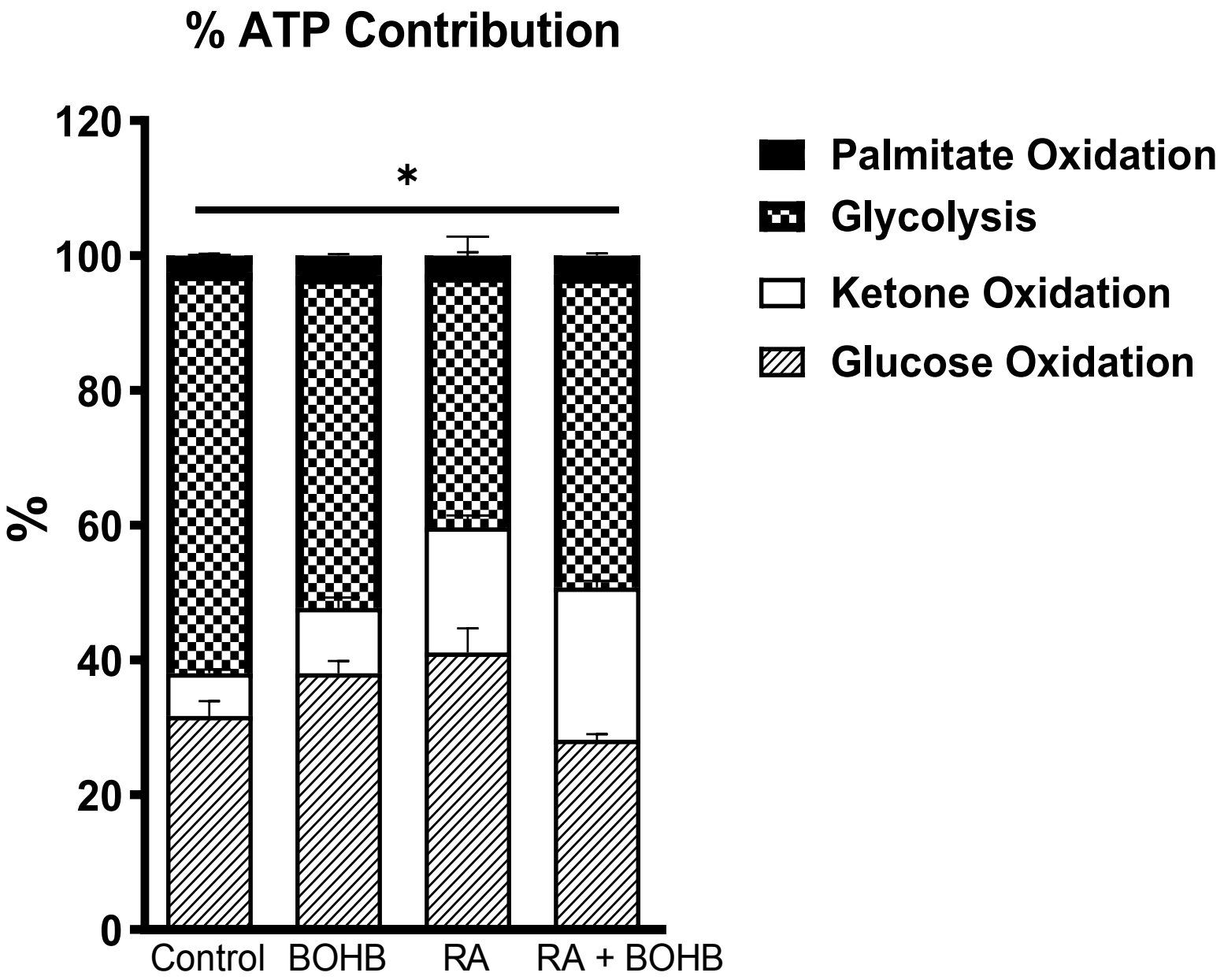
% ATP Contribution
120
100
80
60
40
20
0
%
*
Control
BOHB
RA
RA + BOHB
Palmitate Oxidation
Glycolysis
Ketone Oxidation
Glucose Oxidation

Figure 3.6. ATP production is reduced in differentiated H9c2 cardiomyocytes. Total ATP production (**A**) and the percent ATP contribution (**B**) from glycolysis decreased with RA, which was reversed with BOHB. Glucose had a similar but opposite effect. n= 5 for each experimental group. Data were analyzed with Two-way and One-way ANOVA followed by Tukey's for multiple comparisons. *p < 0.05.

3.1.7 KLF7 in proliferating vs differentiated cells ± ketones

KLFs are zinc-finger DNA binding protein class of transcriptional regulators. In this study, KLF7 expression was increased with the addition of ketones in proliferating cells. However, it remained unchanged in differentiated cells ± ketones compared to the control proliferating cells (Figure 3.7A).

A

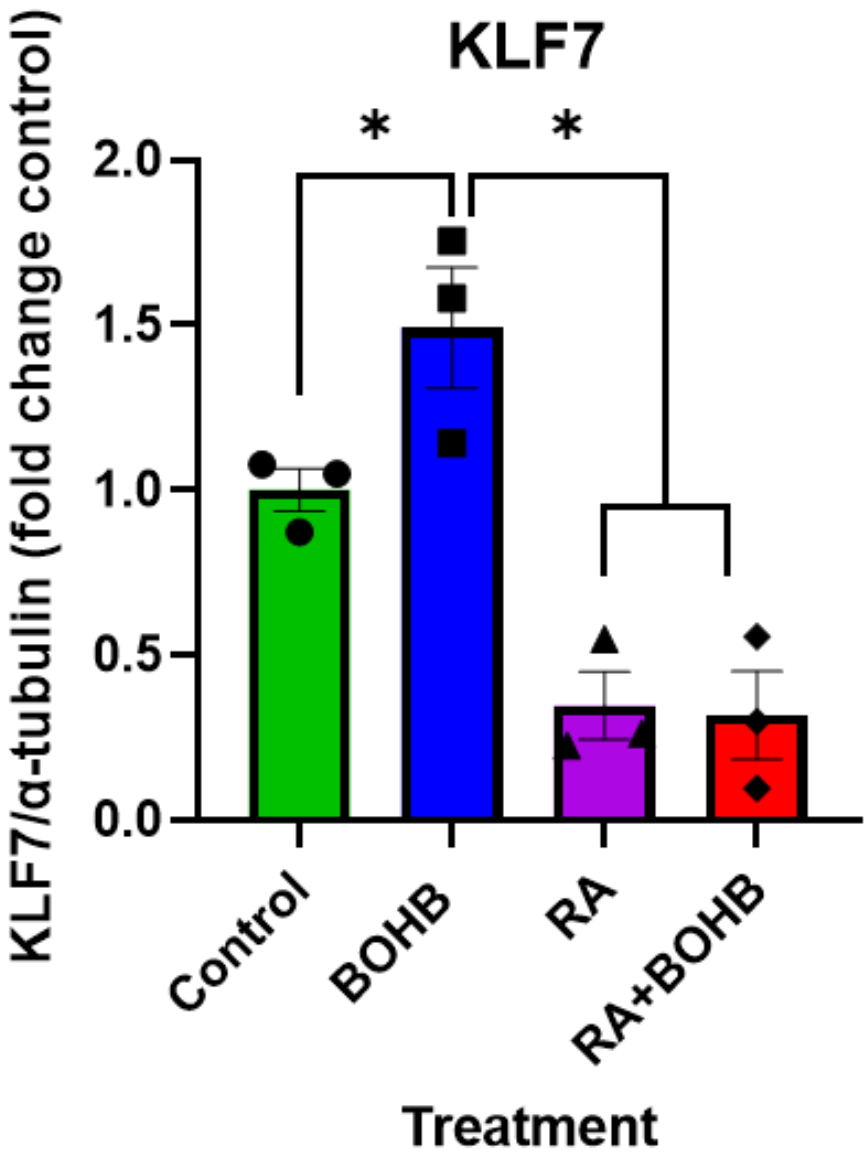
KLF7
KLF7/α-tubulin (fold change control)
2.0
1.5
1.0
0.5
0.0
*
*
Control
BOHB
RA
RA+BOHB
Treatment

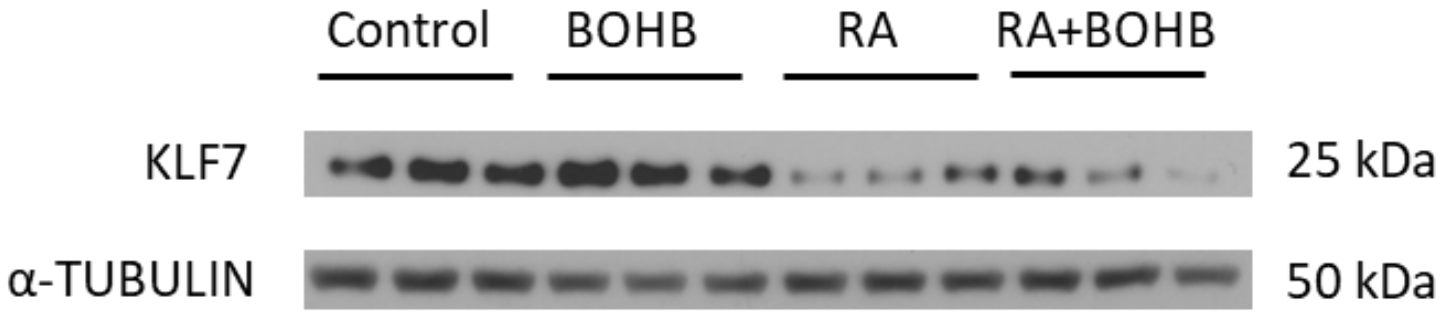
Control
BOHB
RA
RA+BOHB
KLF7
25 kDa
α-TUBULIN
50 kDa

Figure 3.7. Kruppel Like Factor 7 (KLF7) protein expression is increased with the addition of ketones to proliferating H9c2 cells. KLF7 measured with western blot analysis (**A**). n=3 for each experimental group. Individual values for each group are presented as a scatter plot with its mean ± SEM. Data were analyzed with Two-way ANOVA followed by Tukey's for multiple comparisons. Samples collected from separate flasks at the end of culture or metabolic incubation. *p < 0.05.

3.2 siRNA knockdown of BDH1 in proliferating cells ± BOHB

3.2.1 Optimization of siRNA knockdown of BDH1

To determine the optimal concentration of BDH1 siRNA to use in this series of experiments, I assessed the company's suggested concentration (15nM) as well as double (30nM) and triple (45nM) suggested concentration for a 48-hour incubation period. From this, 45nM was determined as the best concentration to induce a suitable BDH1 knockdown (Figure 3.8A).

A

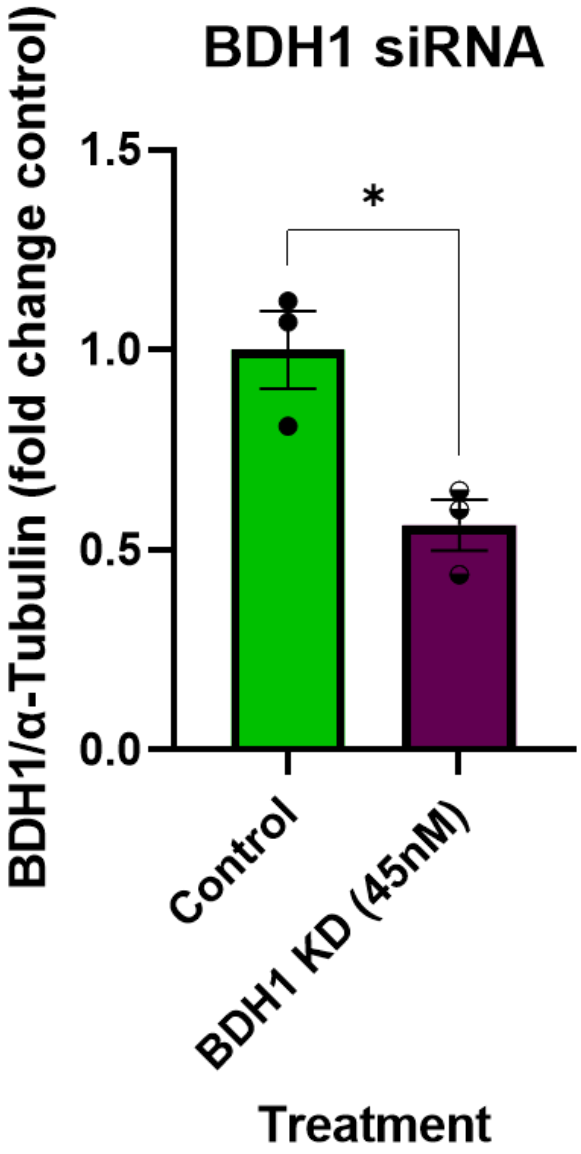
BDH1 siRNA
BDH1/α-Tubulin (fold change control)
1.5
1.0
0.5
0.0
*
Control
BDH1 KD (45nM)
Treatment

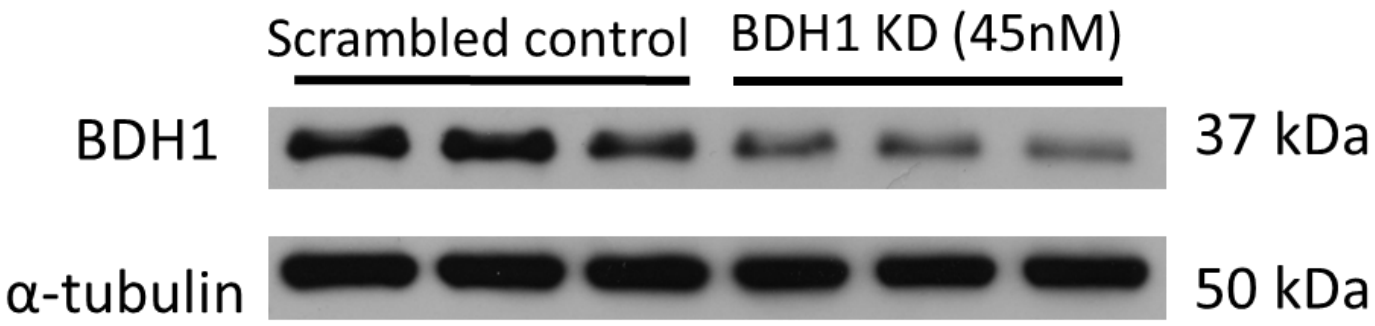
Scrambled control
BDH1 KD (45nM)
BDH1
37 kDa
α-tubulin
50 kDa

Figure 3.8. Optimization of BDH1 siRNA knockdown to determine the best concentration of siRNA. BDH1 enzyme expression (**A**). n=3 for each experimental group. Individual values for each group are presented as a scatter plot with its mean ± SEM. Data were analyzed with a paired t-test. Samples collected from separate flasks at the end of culture or metabolic incubation. *p < 0.05.

3.2.2 BDH1 Knockdown in proliferating cells ± ketones

BDH1 expression was markedly reduced in proliferating cells treated with BDH1 siRNA in the presence and absence of ketones. In order to further validate the BDH1 knockdown, an increase sample number is required, and obtaining these results are currently in progress.

A

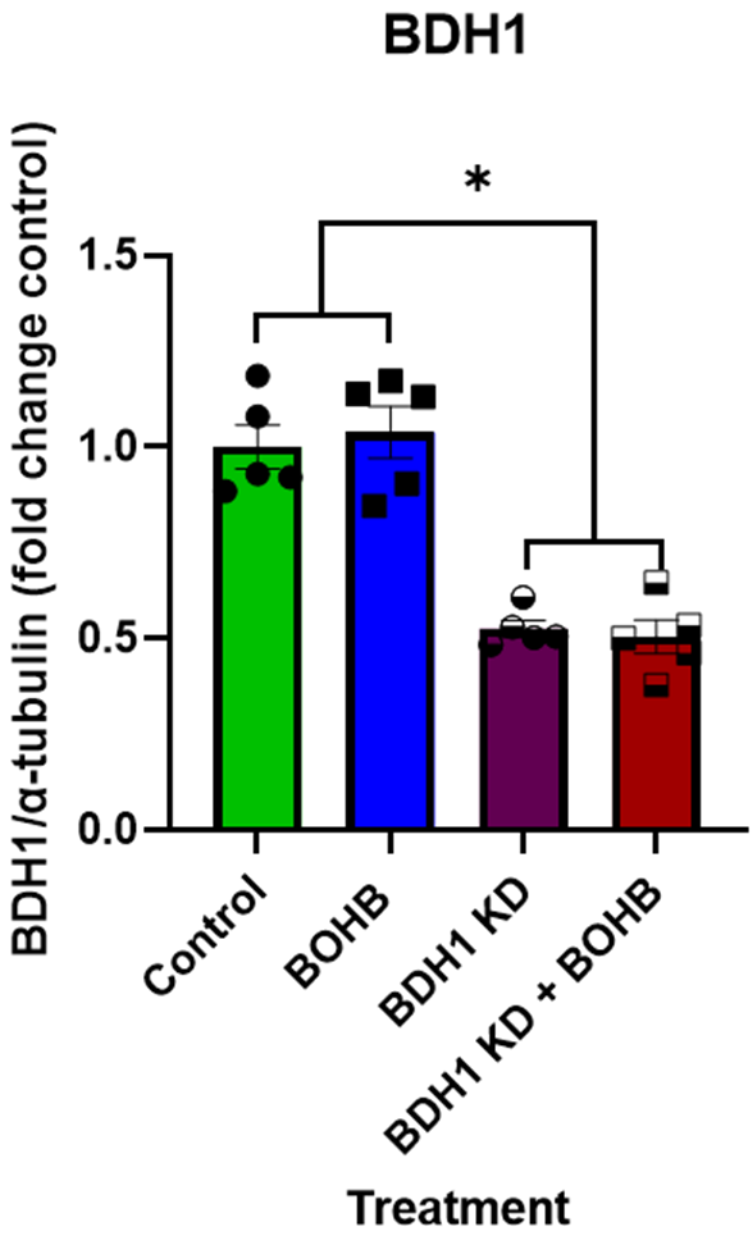
BDH1
*
BDH1/α-tubulin (fold change control)
1.5
1.0
0.5
0.0
Control
BOHB
BDH1 KD
BDH1 KD + BOHB
Treatment

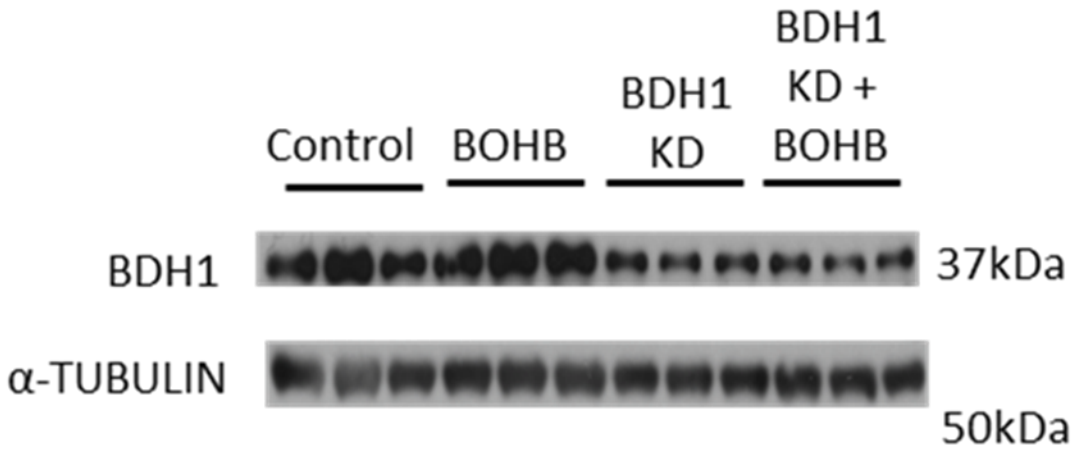
Control
BOHB
BDH1 KD
BDH1 KD + BOHB
BDH1
37kDa
α-TUBULIN
50kDa

Figure 3.9. BDH1 was knocked down with siRNA treatment of proliferating H9c2 cells ± ketones. BDH1 protein expression (**A**). n=5 for each experimental group. Individual values for each group are presented as a scatter plot with its mean ± SEM. Data were analyzed with Two-way and One-way ANOVA followed by Tukey's for multiple comparisons. Samples collected from separate flasks at the end of culture or metabolic incubation. *$p < 0.05$.

3.2.3 Metabolic measurements of BDH1 knockdown in proliferating H9c2 cells ± BOHB

In line with previous experiments (Figure 3.3A), there was a reduction in glycolysis in proliferating cells treated with ketones (Figure 3.10A). Interestingly, this was not changed when BDH1 was knocked down in these cells and treated with ketones. Glucose oxidation was significantly unchanged between treatment groups. However, trends toward increased rates in the presence of ketones were seen in both control and BDH1 siRNA-treated cells (Figure 3.10B). As expected with the knockdown of BDH1, a key enzyme facilitating ketone oxidation, there was a marked reduction in ketone oxidative rates when cells were treated with BDH1 siRNA both in the presence and absence of ketones (Figure 3.10C). The addition of ketones in the scrambled control siRNA-treated cells led to an upregulation of ketone oxidation. Unlike the previous experiments described in section 3.2, fatty acid oxidation rates were not measured as the previous rates observed were negligible and did not substantially contribute to the production of ATP.

A

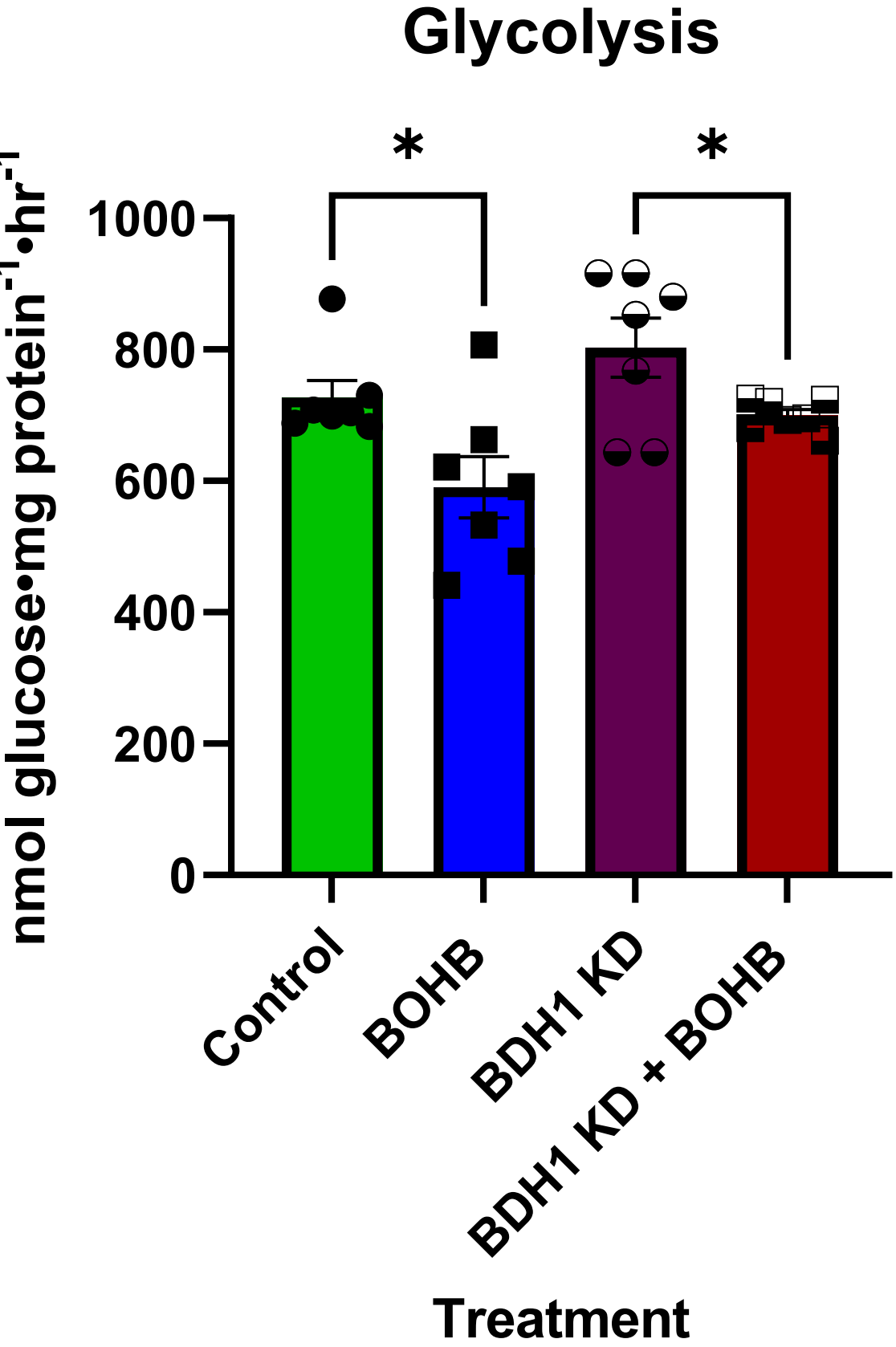
Glycolysis
*
*
nmol glucose•mg protein-1•hr-1
1000
800
600
400
200
0
Control
BOHB
BDH1 KD
BDH1 KD + BOHB
Treatment

B

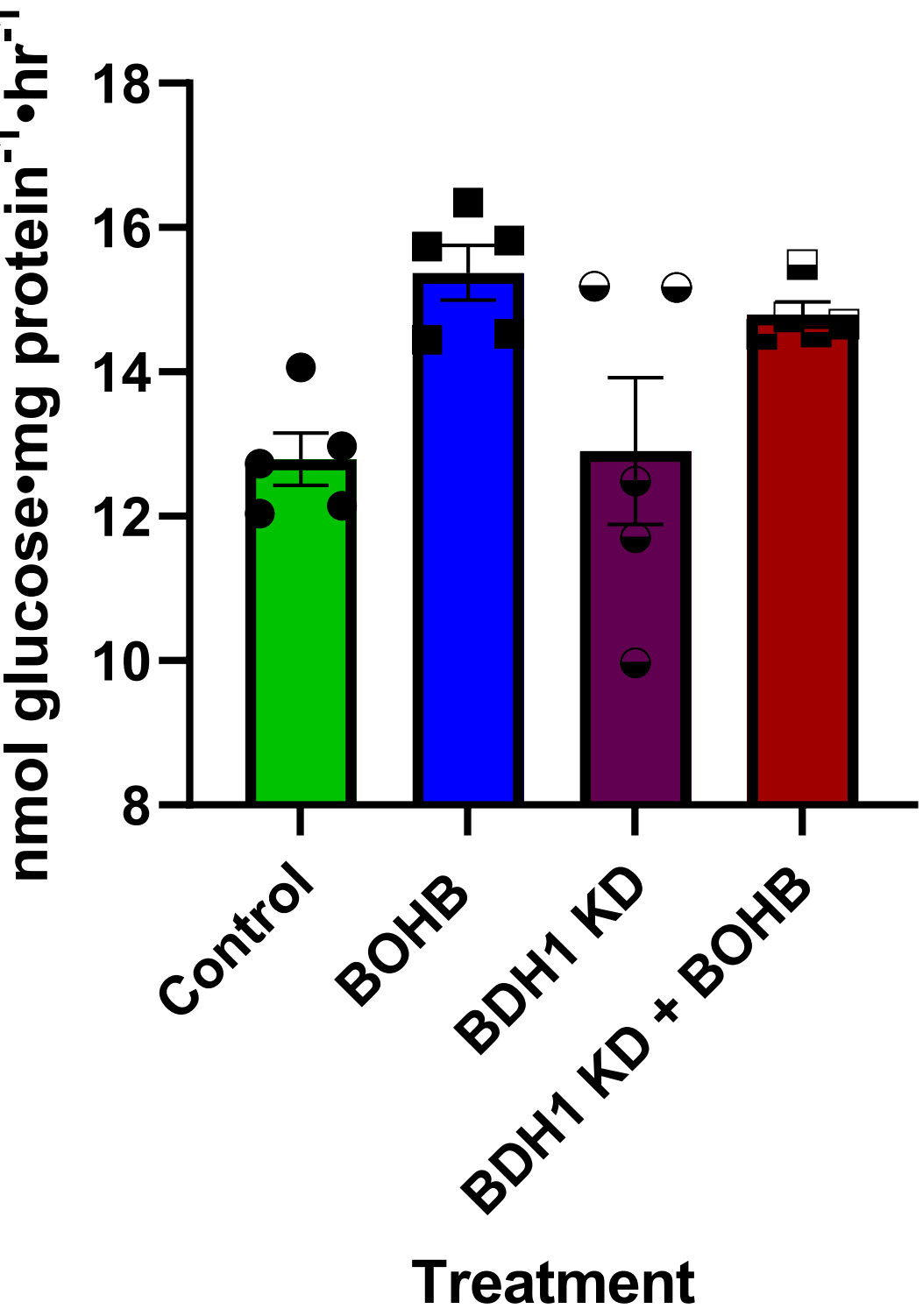
Glucose Oxidation
nmol glucose•mg protein-1•hr-1
18
16
14
12
10
8
Control
BOHB
BDH1 KD
BDH1 KD + BOHB
Treatment

c

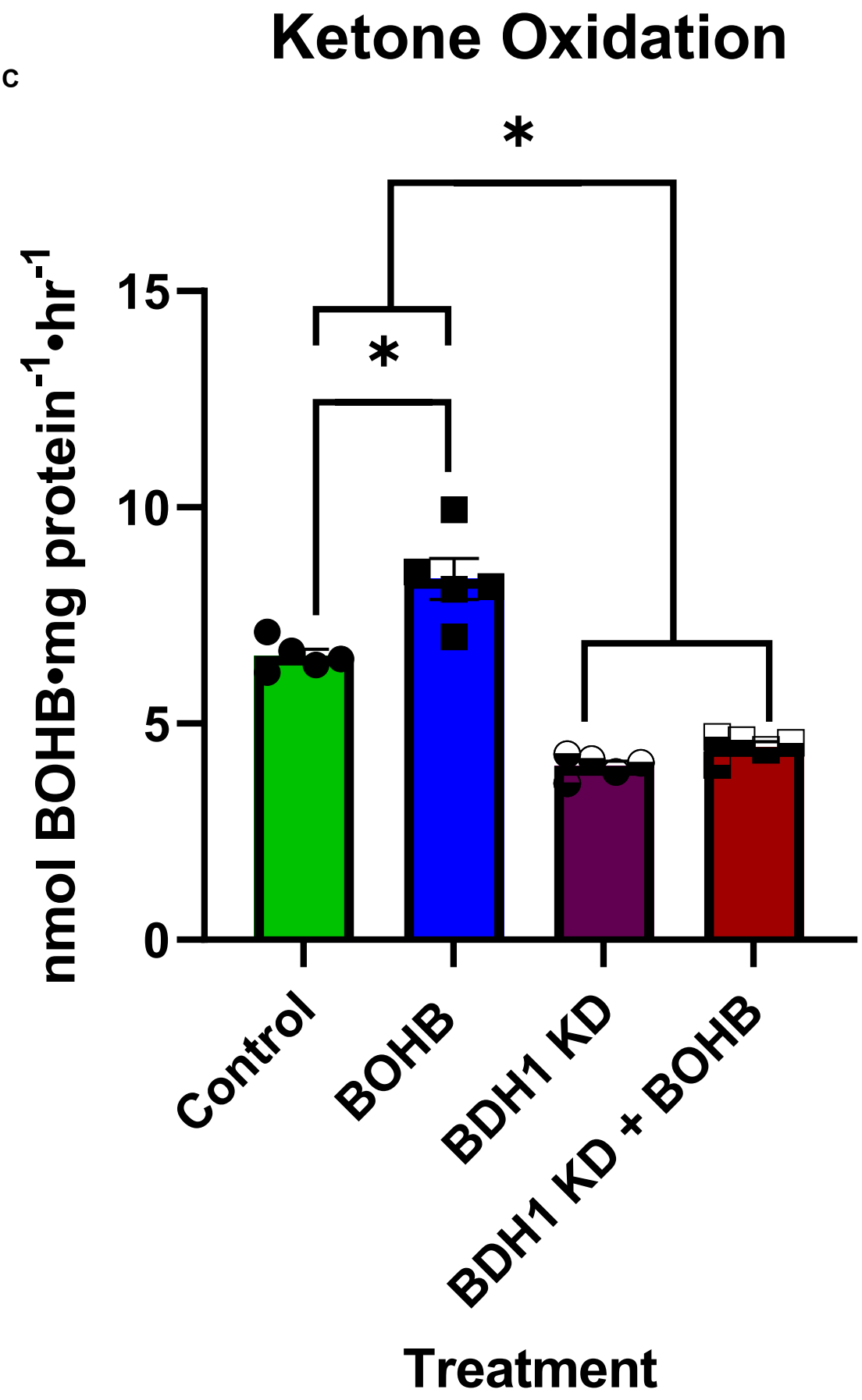
Ketone Oxidation
*
*
nmol BOHB•mg protein-1•hr-1
15
10
5
0
Control
BOHB
BDH1 KD
BDH1 KD + BOHB
Treatment

Figure 3.10. Reduction of the Warburg effect with the addition of ketones did not change when BDH1 was knocked down in proliferating H9c2 cells. Direct measurement of glycolysis (**A**), glucose oxidation (**B**), and ketone oxidation (**C**) in proliferating H9c2 cells treated with either scrambled or BDH1 siRNA in the presence or absence of ketones. n=5-7 for each experimental group. Individual values for each group are presented as a scatter plot with its mean ± SEM. Data were analyzed with Two-way ANOVA followed by Tukey's for multiple comparisons. *p < 0.05.

3.2.4 ATP production and % contribution of BDH1 knockdown in proliferating cells ± ketones

ATP production was similar to the knockdown of BDH1 in the presence or absence of ketones (Figure 3.11A). How the different metabolic processes contribute to ATP production differed depending on the treatment group (Figure 3.11B). The contribution of glycolysis was reduced in proliferating cells and BDH1 knockdown cells treated with ketones. The contribution of ATP from ketone oxidation was not statistically lower in BDH1 knockdown cells compared to controls. Still, it trended downwards, with a significant reduction compared to control cells treated with ketones. Glucose oxidation's contribution to ATP production was reduced in both control and BDH1 knockdown cells treated with ketones.

A

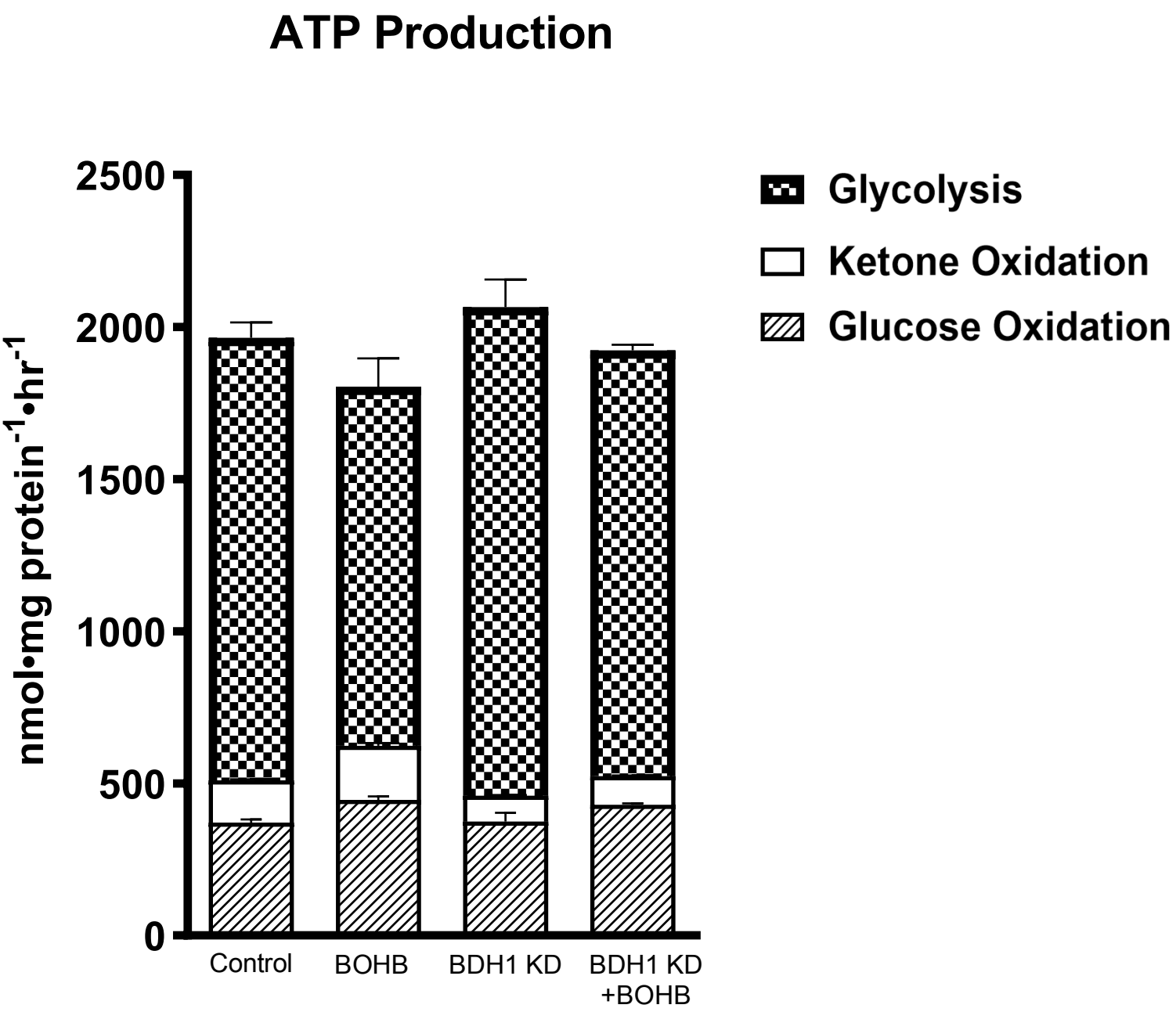
ATP Production
2500
2000
1500
1000
500
0
nmol•mg protein-1•hr-1
Glycolysis
Ketone Oxidation
Glucose Oxidation
Control
BOHB
BDH1 KD
BDH1 KD +BOHB

B

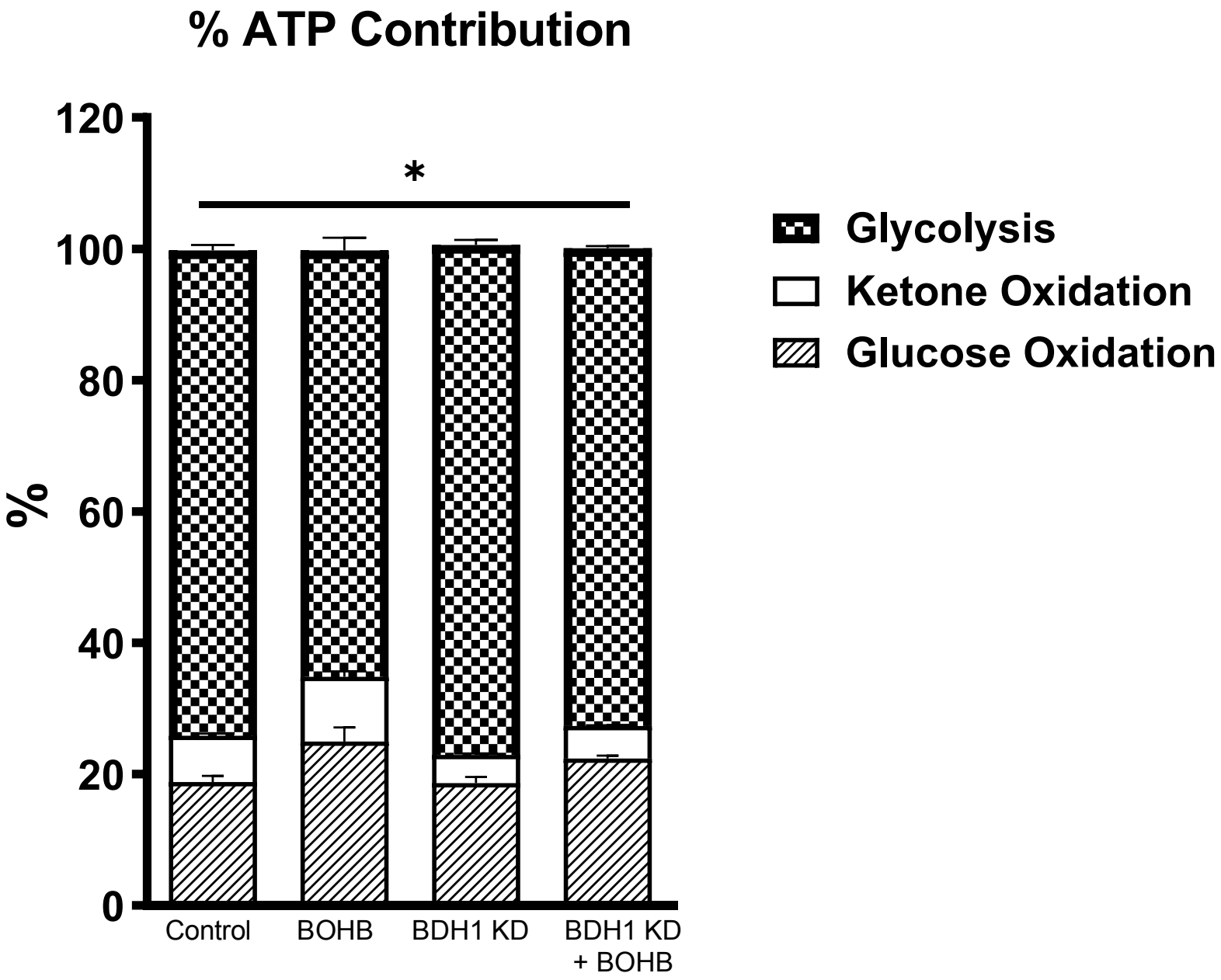
% ATP Contribution
120
100
80
60
40
20
0
%
*
Control
BOHB
BDH1 KD
BDH1 KD + BOHB
Glycolysis
Ketone Oxidation
Glucose Oxidation

Figure 3.11. ATP production/contribution of proliferating H9c2 cells with BDH1 knockdown. Total ATP production (**A**) and the percent ATP contribution (**B**) in proliferating H9c2 cells treated with BDH1 siRNA in the presence or absence of ketones. n= 5-7 for each experimental group. Data were analyzed with Two-way and One-way ANOVA followed by Tukey's for multiple comparisons. *p < 0.05.

3.3 siRNA knockdown of HDAC2 in proliferating cells ± BOHB

3.3.1 Optimization of siRNA knockdown of HDAC2

To determine the optimal concentration of BDH1 siRNA to use in this series of experiments, I evaluated three concentrations initially: 30nM, 50nM and 80nM for 48 hours. These concentrations for 48 hours led to a dramatic reduction in cell viability, and samples could not be obtained from this experiment. Next, I used the company's suggested concentration (15nM) as well as 30nM and 50nM and adjusted the incubation for 24 and 36 hours. None of the concentrations at 24 hours led to a significant reduction in HDAC2 expression, examined via western blot analysis. For the 36-hour incubation, both 30nM and 50nM led to significant knockdown. Since 50nM for 36 hours was the best knockdown observed, this was the concentration chosen for the experiment (Figure 3.12A).

A

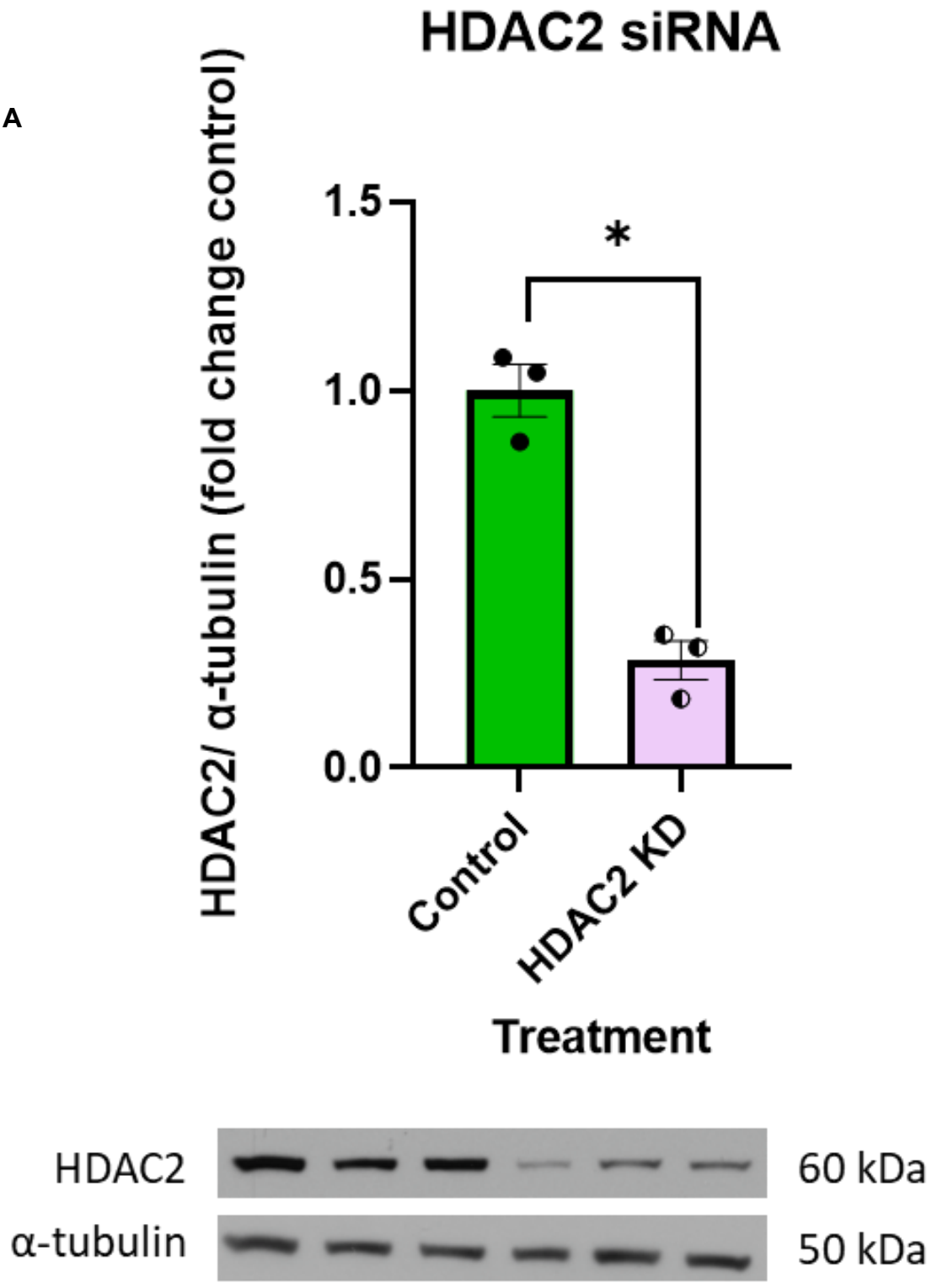
HDAC2 siRNA
HDAC2/ α-tubulin (fold change control)
1.5
1.0
0.5
0.0
*
Control
HDAC2 KD
Treatment
HDAC2
α-tubulin
60 kDa
50 kDa

Figure 3.12. Optimization was done to determine the best concentration of siRNA needed to knock down the HDAC2 enzyme expression. HDAC2 expression (**A**). n=3 for each experimental group. Individual values for each group are presented as a scatter plot with its mean ± SEM. Data were analyzed with a paired t-test. Samples collected from separate flasks at the end of culture or metabolic incubation. *p < 0.05.

3.3.2 HDAC2 Knockdown in proliferating cells ± ketones

HDAC2 expression was markedly reduced in proliferating cells treated with HDAC2 siRNA in the presence and absence of ketones. In order to further validate the HDAC knockdown, an increase sample number is required, and obtaining these results are currently in progress.

A

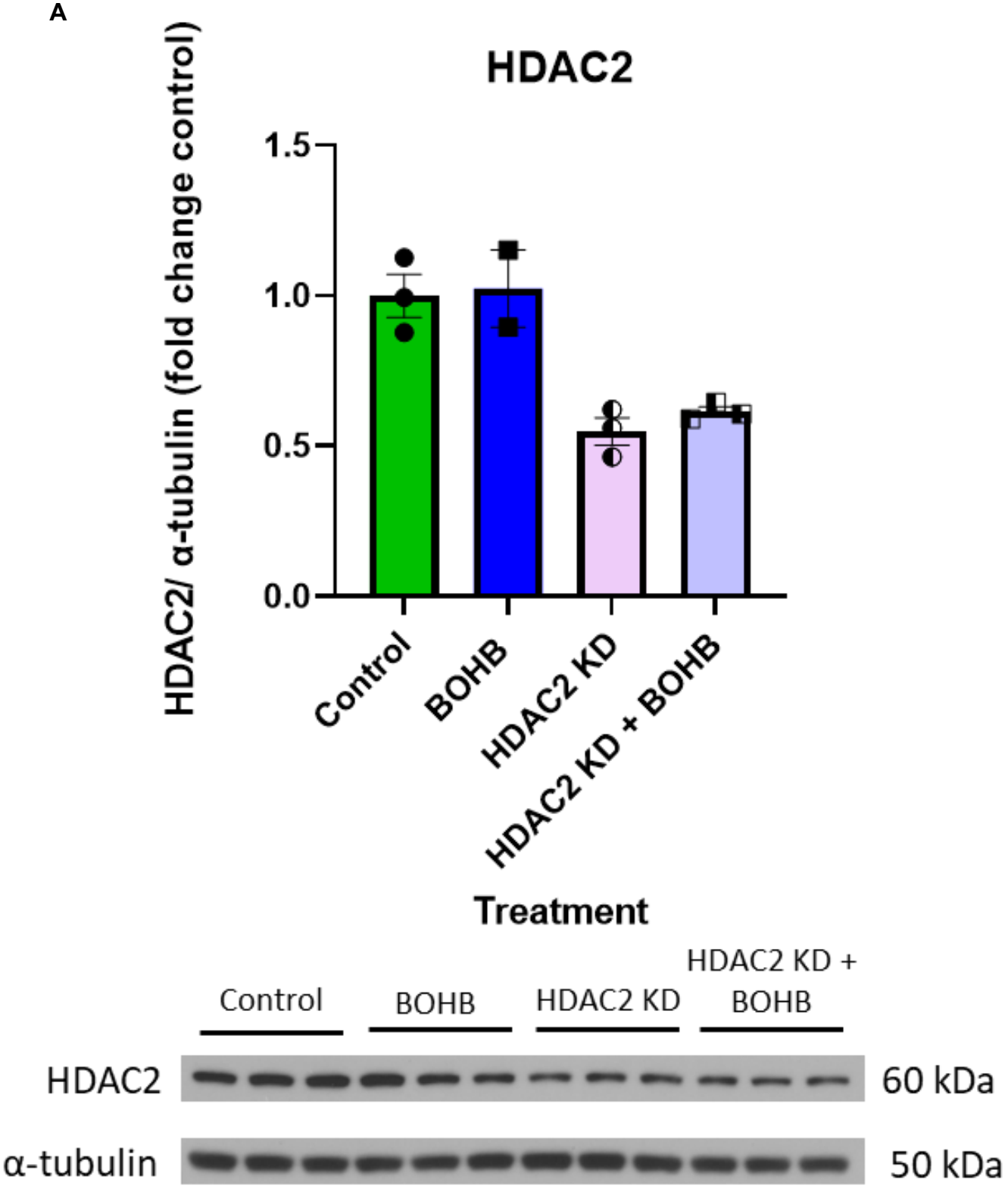
HDAC2
HDAC2/ α-tubulin (fold change control)
1.5
1.0
0.5
0.0
Control
BOHB
HDAC2 KD
HDAC2 KD + BOHB
Treatment
Control
BOHB
HDAC2 KD
HDAC2 KD + BOHB
HDAC2
60 kDa
α-tubulin
50 kDa

Figure 3.13 HDAC2 was knocked down with siRNA treatment of proliferating H9c2 cells ± ketones. HDAC2 protein expression (**A**). n=2-3 for each experimental group. Individual values for each group are presented as a scatter plot with its mean ± SEM. Data were analyzed with Two-way and One-way ANOVA followed by Tukey's for multiple comparisons. Samples collected from separate flasks at the end of culture or metabolic incubation. *$p < 0.05$.

3.3.3 Metabolic measurements of HDAC2 knockdown in proliferating cells ± BOHB

Unlike the previous experiments in sections 3.1 and 3.2, glycolytic rates were not reduced in the control proliferating cells in the presence of ketones (Figure 3.14A). Interestingly, knocking down HDAC2 in the absence of ketones leads to an increase in glycolysis. However, in the presence of ketones, glycolysis was reduced to rates similar to that of the controls (Figure 3.14A). Ketone oxidation was reduced with the knockdown of HDAC2, with no observed changes in the control of HDAC2 knockdown when treated with ketones (Figure 3.14B). Conversely, glucose oxidation was increased with the HDAC2 knockdown, with no changes due to ketones (Figure 3.14B).

A

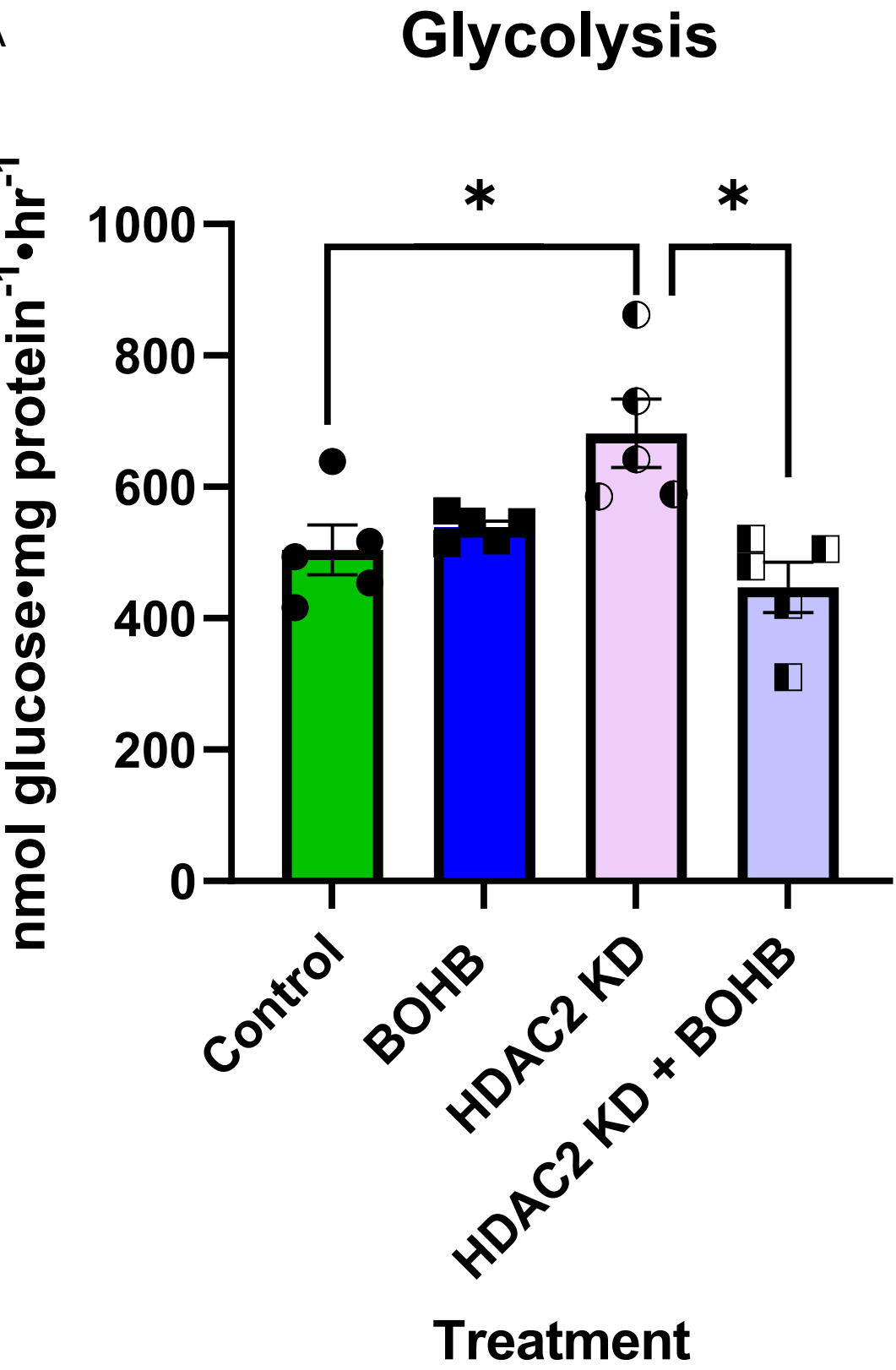
Glycolysis
nmol glucose•mg protein-1•hr-1
1000
800
600
400
200
0
*
*
Control
BOHB
HDAC2 KD
HDAC2 KD + BOHB
Treatment

B

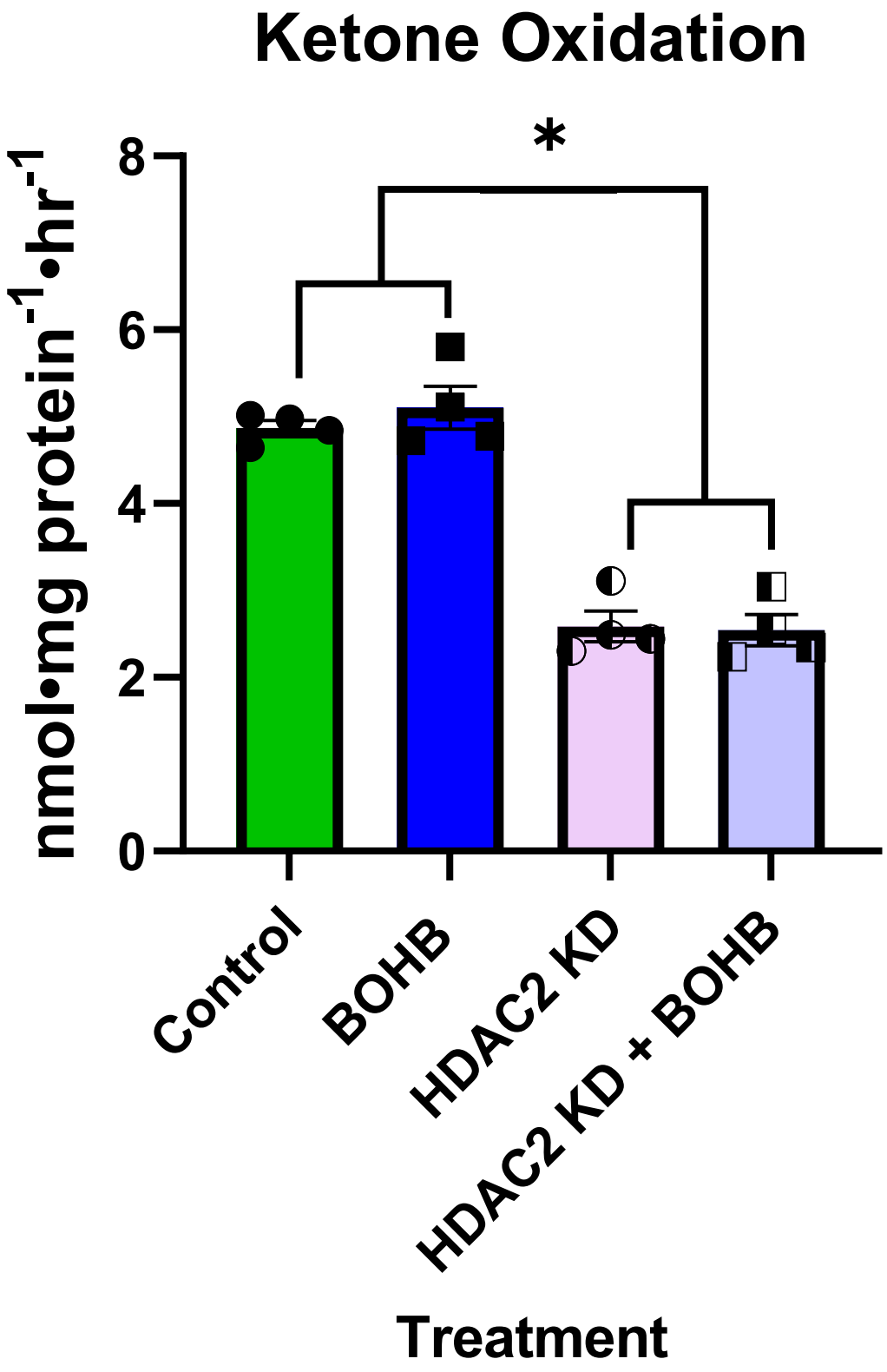
Ketone Oxidation
*
nmol•mg protein-1•hr-1
8
6
4
2
0
Control
BOHB
HDAC2 KD
HDAC2 KD + BOHB
Treatment

Glucose Oxidation

B

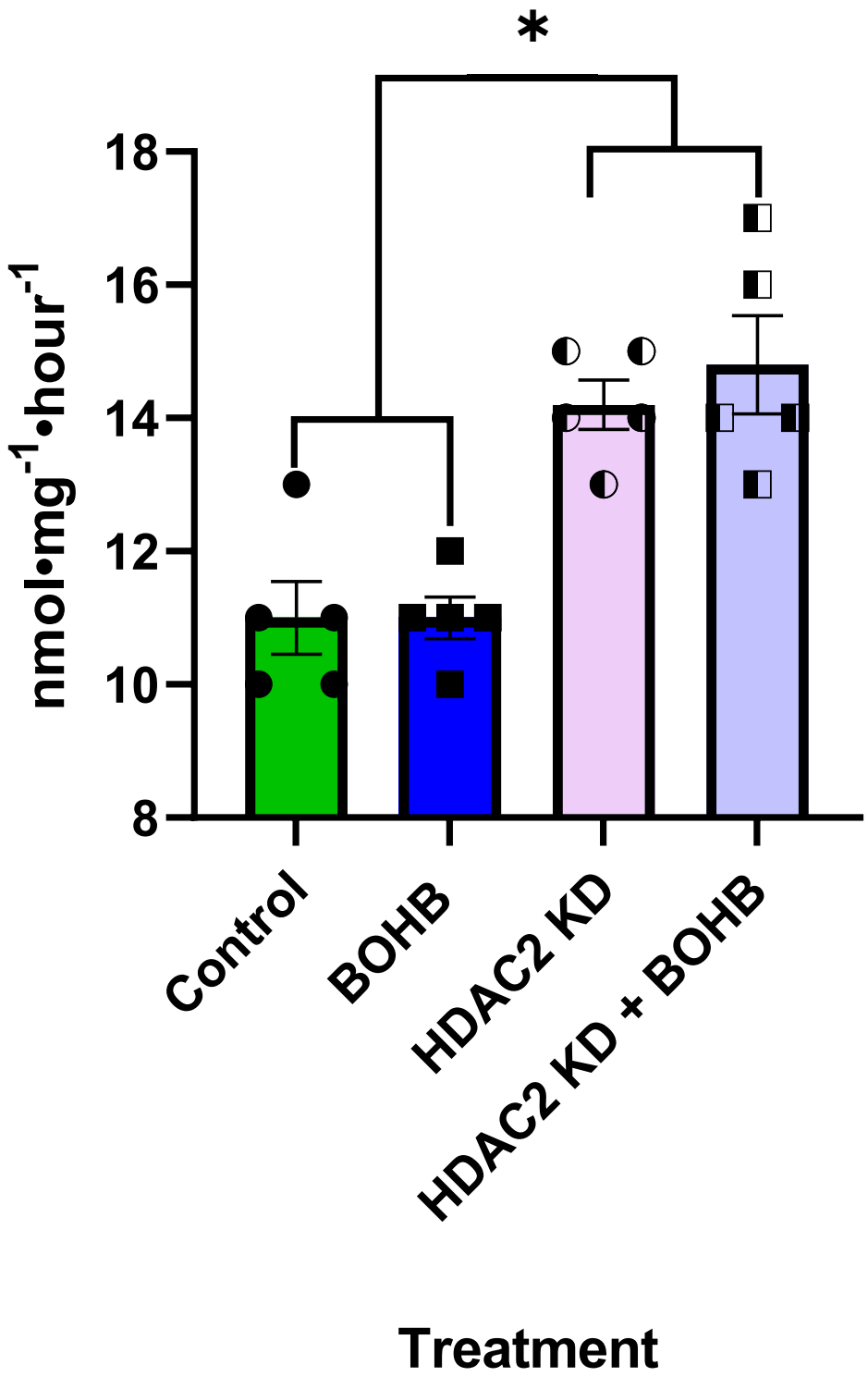

Figure 3.14. Metabolism is altered in proliferating H9c2 cells with the knockdown of HDAC2. Direct measurement of glycolysis (**A**), ketone oxidation (**B**) and glucose oxidation (**B**) in proliferating H9c2 cells treated with either scrambled or HDAC2 siRNA in the presence or absence of ketones. n=4-5 for each experimental group. Individual values for each group are presented as a scatter plot with its mean ± SEM. Data were analyzed with Two-way ANOVA followed by Tukey's for multiple comparisons. *p < 0.05.

3.3.4 ATP production and % contribution of HDAC2 knockdown in proliferating cells ± ketones

ATP production was increased with the HDAC2 knockdown due to an increase in glycolysis. However, in the presence of ketones, this increase in ATP production was not seen (Figure 3.15A). How the different metabolic processes contribute to ATP production was different depending on the treatment group (Figure 3.15B). Under HDAC2 knockdown ± BOHB, ketone oxidation contributed substantially less than in control cells ± BOHB. Glycolysis contributed more to ATP production in HDAC2 knockdown cells in the absence of ketones than in other treatments. In HDAC2 knockdown cells treated with ketones, glucose oxidation contributed more to ATP production than other groups.

A

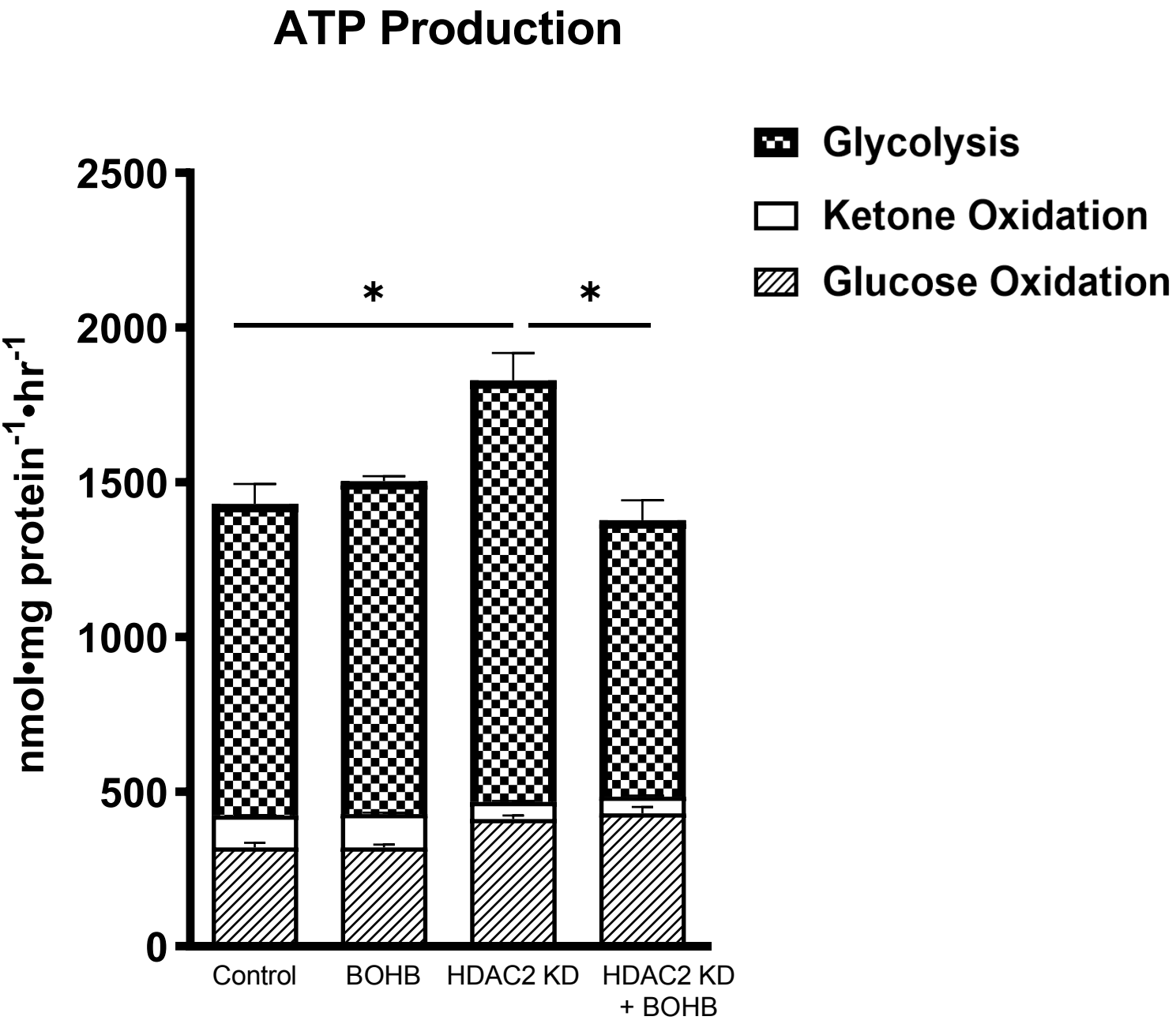
ATP Production
Glycolysis
Ketone Oxidation
Glucose Oxidation
2500
2000
1500
1000
500
0
nmol•mg protein-1•hr-1
*
*
Control
BOHB
HDAC2 KD
HDAC2 KD + BOHB

B

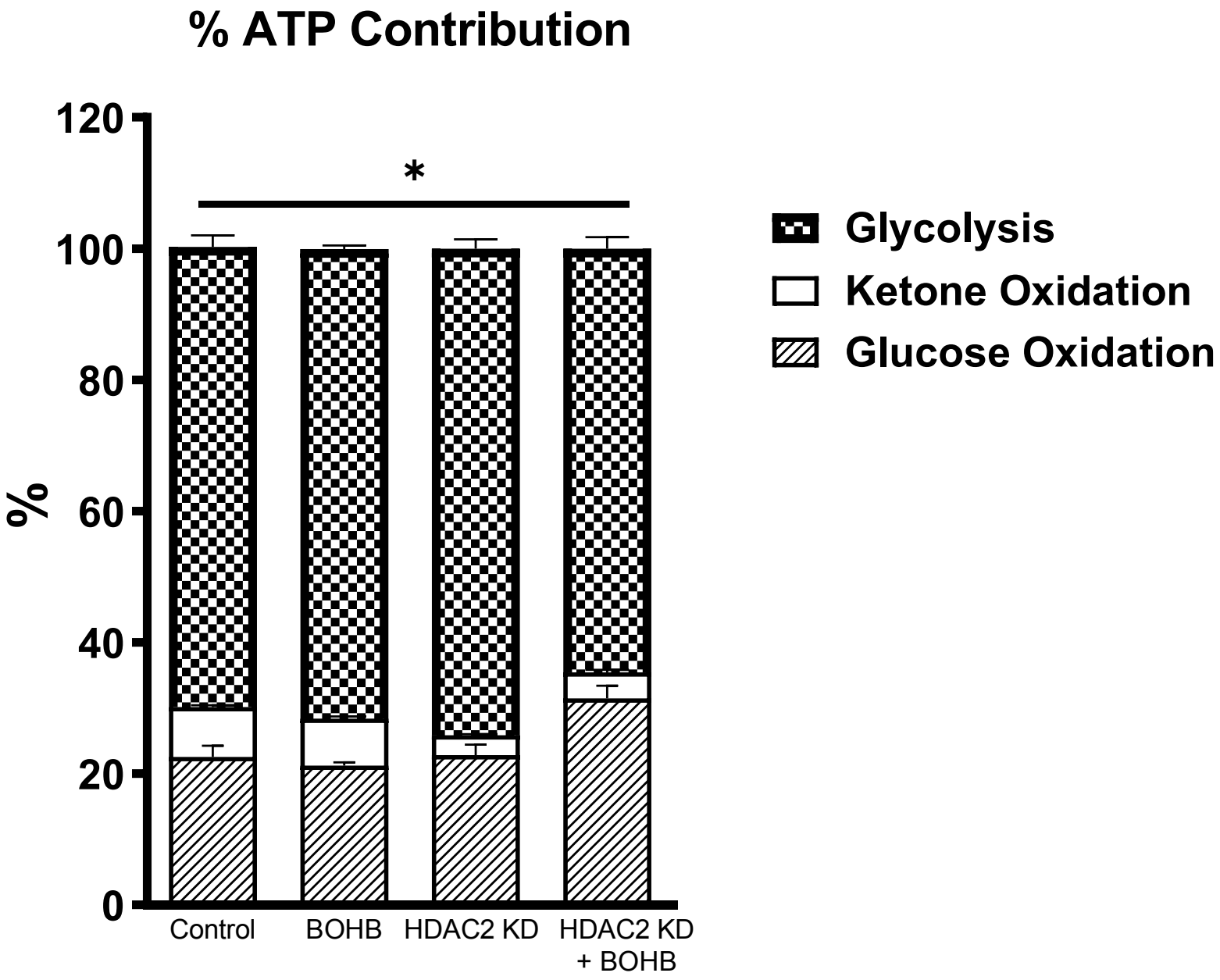
% ATP Contribution
120
100
80
60
40
20
0
%
*
Glycolysis
Ketone Oxidation
Glucose Oxidation
Control
BOHB
HDAC2 KD
HDAC2 KD + BOHB

Figure 3.15. **ATP production/contribution of proliferating H9c2 cells with HDAC2 knockdown.** Total ATP production (**A**) and the percent ATP contribution (**B**) in proliferating H9c2 cells treated with HDAC2 siRNA in the presence or absence of ketones. n= 4-5 for each experimental group. Data were analyzed with Two-way and One-way ANOVA followed by Tukey's for multiple comparison. *$p < 0.05$

CHAPTER 4: Discussion

4.1 Findings

This study provides a number of important novel findings. There are five main outcomes that I will highlight. First, through direct measures, I was able to determine the metabolic profile of differentiated H9c2 cells, such that there is a decrease in the Warburg effect with differentiation to a more cardiomyocyte phenotype. Second, I observed that ketones are associated with increased markers of cardiomyocyte maturation in proliferating H9c2 cells. Third, I found that ketones reduce the Warburg effect through a reduction in glycolysis in proliferating H9c2 cells. Fourth, knocking down BDH1 in proliferating H9c2 cells does not alter the ketone-induced reduction in the Warburg effect seen in proliferating H9c2 cells. Lastly, I observed increased glycolysis when HDAC2 is knocked down; this increase is prevented with the treatment of proliferating H9c2 cells with ketones.

4.1.1 Justification of the in vitro *model used*

Studying the differentiation of cardiomyocytes in cell lines, such as the H9c2 cells, used in this study, allows for several benefits, which includes avoiding animal sacrifice and increased ease in altering the cellular environment. Other models, such as the use hiPSC-CMs, could have been used in this study. However, we decided to use H9c2 cells as they are easy to culture and experiments using these cell lines are highly reproducible. One important attribute of H9c2 cells that we wanted to consistently reproduce are their ability

to transition from proliferating cells to differentiated non-proliferating cardiomyocytes. This phenomenon is relevant when compared to the maturing heart, as fetal cardiomyocytes exhibit proliferating capacity, which is quickly dissolved in the post-birth (post-natal) period (149). As such, it was first important to characterize the maturation of H9c2 cells undergoing the differentiation process. Morphologically, I observed key attributes of cardiomyocyte differentiation, as the H9c2 cell became elongated with the treatment of RA compared with proliferating cells (Figure 3.1A, B). I also observed increases in key markers associated with cardiomyocyte maturation, such as cardiac troponin T, SERCA2A and PGC-1α (Figure 3.1C-E) when differentiating H9c2 cells.

4.1.2 Metabolism of differentiated H9c2 cells

Although a few studies have sought to understand the energy metabolism of H9c2, both in the undifferentiated proliferating state and differentiated state, to the best of our understanding, none have done so through the direct measurement of major energetic pathways as done in this current study. Rather, other studies have reported analysis using indirect techniques such as quantifying protein and genetic markers associated with metabolism, principal component analysis, metabolite studies using nuclear magnetic resonance (NMR) spectroscopy and oxygen consumption assays (24,150–152). Moreover, none of these other studies assessed energy metabolism in the presence of fatty acids or physiologically relevant levels of bovine serum albumin needed to bind these fatty acids. Notably, only one study, to my knowledge, has directly studied fatty acid oxidation to observe the effects of 48-hour fatty acid treatment on neonatal cardiomyocytes. However, this study did not use physiologically relevant levels of energy

substrates, did not asses any other relevant metabolic pathways, nor did it study any maturational changes with its protocol (93). Of note, it seems that only two studies have aimed to characterize the metabolic transition of H9c2 from an undifferentiated to a differentiated state using RA (24,152). To my knowledge, my studies are the first to directly measure energy metabolism pathways in proliferating and differentiated H9c2 cells in the presence of physiologically reflective metabolic substrates. I found a dramatic reduction in glycolysis in differentiated H9c2 compared to proliferating cells (Figure 3.3A). As such, proliferating H9c2 demonstrate a phenomena typically seen in highly proliferating cells, the Warburg effect (11), in which there are high rates of glycolysis uncoupled from glucose oxidation. This is further demonstrated by the fact that glycolysis is the main contributor to ATP production (>60%) in proliferating cells (Figure 3.6B). This Warburg effect is then reduced when H9c2 cells differentiate to a cardiomyocyte phenotype. This is accompanied by an increase in coupling between glycolysis and glucose oxidation, as can be seen by a reduction in glucose oxidation rates in conjunction to the decrease in glycolysis (Figure 3.3B). In differentiated cells there is also a reduction in the ratio of phosphorylated PDH to total PDH, further confirming an increase in the coupling between glycolysis and glucose oxidation. This aligns with previous literature in H9c2 differentiation studies where an increase in glycolytic flux, as seen by NMR spectroscopy in proliferating cells, whereas differentiated H9c2 cells have increased oxidative rates (152). This also corresponds with what is seen in the heart during the newborn period, in which there is a switch from relying primarily on glycolysis to oxidative metabolism (3). While my results do not show absolute increases in oxidative metabolic pathways with differentiation, I did observe that oxidative metabolism contributes

relatively more to ATP production in differentiated H9c2 cells (Figure 3.6B). This aligns with an increase in isocitrate dehydrogenase (IDH), a key enzyme in the TCA cycle responsible for converting isocitrate to α-ketoglutarate. My study shows an increase in IDH in differentiated H9c2 cells (Figure 3.3F). An increase in IDH indicates that the TCA cycle is better utilized in differentiated cells than in proliferating cells.

The three key enzymes supporting the Warburg effect are PFKFB3, PKM2 and G6PD. Given that PFKFB3 is expression is high in rapidly proliferating cells such as seen in cancer cells and endothelial cells, and the inhibition or downregulation of PFKFB3 has antiglycolytic effects that reduce tumorigenicity, our expectation was to see a reduction in PFKFB3 with differentiation (63,65,153,154). However, there were no changes in PFKFB3 expression in this study between proliferating and differentiated cells (Figure 3.3H). Next, I looked at PKM2, which is mainly expressed in proliferating cells the, unlike the isoform PKM1 which is mainly expressed in adult cells (43,48). In PKM2 deletion studies, myocardial size and cardiomyocyte quantity is reduced (55). Whether enhanced or lowered PKM2 is important in inducing proliferation post-MI has produced controversial results. Magadum et al., (55) suggests that an increase in PKM2 is related to an increase in proliferation and cardiomyocyte regeneration, whereas Hauck et al. (155) suggest the opposite, in which a reduction in PKM2 expression would be more beneficial for cardiomyocyte regeneration post-MI. Notably, neither of these studies demonstrate whether their results were aligned with the dimer or tetramer conformation of PKM2. This is relevant, as the tetramer conformation of PKM2 is more similar to PKM1 in being associated with a decrease in the tumorgenicity (50,51). Interestingly, I observed that

PKM2 expression is increased in differentiated H9c2 cells (Figure 3.3I), however whether this increase is associated with dimeric or tetrameric conformation is unknown at present. Lastly, I examined G6PD, which has been shown to be important in regulating proliferation in both cancerous and non-cancerous cells, as several knockdown studies of G6PD have observed deficiencies in growth and development (67–71). Intriguingly, within the context of the heart, G6PD has been shown to have a protective effect against ROS-induced injury (77,78). Under conditions where the heart exhibits a more fetal-like/proliferative metabolic profile, such as in a hypertrophic state, there is a detectable decrease in G6PD (79). Much like what would be expected from an adult cardiomyocyte, I observed an increase in G6PD expression in differentiated H9c2 cells compared to proliferating cells (Figure 3.3G).

Circulating ketones are known to increase in the newborn period, when the heart undergoes dramatic changes, including changes in metabolism (128). To the best of my knowledge, changes in ketone oxidation have not been studied or reported in the context of the newborn heart, nor has it been studied in differentiating H9c2 cells. However, it has been shown that the adult heart can metabolize ketones as a major source of energy (156) and that there are increases in ketone metabolism in the failing heart, a response that is most likely adaptive (157). In the current study, I did not see any changes in ketone oxidation in differentiated cells compared to proliferating H9c2 cells (Figure 3.4A). However, ketone oxidation contributed more to ATP production in differentiated cells than in proliferating H9c2 cells (Figure 3.6B). Despite no changes in ketone oxidation rates, there was an increase in BDH1 protein expression, a key enzyme in ketone oxidation, in

differentiated H9c2 cells (Figure 3.4B). The E2F pathway is important in regulating cardiac metabolism in the post-natal period (158). When this pathway is disrupted by E2F6, there is a reduction in glycolysis associated with an increase in BDH1 protein and gene expression in neonatal cardiomyocytes (158). The increases in BDH1 that was observed with differentiation are potentially due to the reduction in glycolysis seen in differentiated cells (Figure 3.3A) and may be related to changes in E2F6.

Class I HDACs, such as HDAC2 are global repressors of transcription which is important to embryonic development, particularly to the development of the heart (131). Global deletion of HDAC2 leads to the uncontrolled proliferation of ventricular cardiomyocytes, ultimately causing perinatal lethality (131). As such I hypothesized that in differentiated H9c2 cells, in which these cells lose their proliferative capacity, there would be a reduction in HDAC2. Indeed, in my studies I saw a reduction of HDAC2 protein expression in differentiated H9c2 cells (Figure 3.4C). Conversely, HDAC2 knockdown and inhibition have been associated with a reduction in proliferation in cancer studies (132,159). In cardiac hypertrophy studies, in which the metabolism of the heart is similar to the fetal-like state, the inhibition of HDAC2 prevented the re-expression of fetal genes in cardiomyocytes and reduced cardiac hypertrophy. Interestingly, the decrease in HDAC2 expression that I observed, was associated with a decrease in Foxo3a in differentiated H9c2 cells (Figure 3.4D). This was unexpected as several studies indicate that Foxo3a is upregulated by HDAC2 knockdown and inhibition, and that increased Foxo3a is associated with improved cardiac hypertrophy (160–162). Studies in HDAC2 deficient hearts have shown a reduction in phosphorylated Foxo3a, but not show total Foxo3a.

Therefore, I propose that assessing Foxo3a phosphorylation may be a more relevant target to observe (135).

It is well established that in the newborn period, in which the heart undergoes a maturation process, the reductions in glycolysis are associated with an increase in fatty acid oxidation (3,17). Interestingly, a PPARα induced increase in fatty acid oxidation, as measured by indirect extracellular flux or Seahorse KF measurements, leads to a brief increase in proliferation in cardiomyocytes before promoting hypertrophic growth and maturation (163). Moreover, supplementing hiPSC-CMs with fatty acids allows for a more mature phenotype including cell enlargement, improved calcium handling, increasing oxidative capacity, and allowing for great force generation (164). To the best of my knowledge fatty acid oxidation has not been directly examined in cardiomyocyte differentiation. In this study, although I saw lower rates of fatty acid oxidation in differentiated H9c2, I also saw incredibly low rates in both proliferating and differentiated H9c2 cells (Figure 3.5A). This is further evidenced when looking at the contribution to ATP production, in which the contribution from fatty acid oxidation is negligible (Figure 3.6B). Interestingly, despite there being no increase in fatty acid oxidation, key enzymes of fatty acid oxidation control, PPARα and CPT1A, are increased in differentiated H9c2 cells compared to proliferating cells (Figure 3.5 C-D). Increases in PPARα are associated with an increase in fatty acid oxidation (96,97,165). Further an increase in PPARα has been show to be cardioprotective in hypertrophy neonatal hearts (85). Interestingly, CPT1 seems to increase in the newborn period, however this does not seem to be integral to the increases seen in fatty acid oxidation after birth (102). I also saw an increase in ATGL in

differentiated cells (Figure 3.5G). This may indicate an increase in triacylglycerol turnover and endogenous palmitate oxidation (165); however, there was no change in palmitate uptake (Figure 3.5B).

Overall, when characterizing the metabolic profile of differentiated H9c2 cells, I observed a decrease in total ATP production (Figure 3.6A). This is potentially due to the fact that these cells do not possess the ability to contract and are no longer largely proliferative. As a result, there is a reduction in the requirement of ATP for these differentiated H9c2 cells, and so overall ATP production is reduced. Promisingly, we can see that in differentiated H9c2 cells, there is a switch from relying mainly on glycolysis for ATP production to having the majority of ATP contributed from oxidative metabolism (Figure 3.6B).

4.1.3 Maturation and metabolism of proliferating cells treated with ketones

Given that in the post-birth period there is an increase in circulating ketones (128), I aimed to see how both proliferating and differentiating H9c2 responded to ketone treatment in order to elucidate what role this may play in cardiomyocyte maturation. Several studies examining the effects of ketones on cancer cell lines have observed an anti-tumour and anti-proliferative effect when treating cancer cells with ketones or subjecting animals to a ketogenic diet (121,122). Conversely, a recent publication has shown that ketones increase the proliferation of endothelial cells, contributing to an increase in angiogenesis (166). While I did not observe any changes in proliferation, in terms of quantifying cell numbers, with the addition of ketones to proliferating H9c2 cells

(Figure 3.2A), I did see an increase in SERCA2 and PGC-1α, key markers of cardiomyocyte maturation, with the addition of ketones (Figure 3.1 D, E). This upregulation of cardiomyocyte maturation markers was seen only in proliferating cells treated with ketones, but not in differentiated H9c2 cells which were unaffected by the addition of ketones. This indicates that ketones may lead to the differentiation towards a more mature cardiomyocyte phenotype in proliferating H9c2 cells, as these markers are typically upregulated in differentiated H9c2 cells, as seen by others and this current study (24).

Furthermore, as was observed in the differentiated H9c2 cells, proliferating H9c2 cells treated with ketones also exhibited a reduction in glycolysis (Figure 3.3A). Importantly, this reduction in glycolysis was not as dramatic as the decreases seen with differentiated H9c2 cells. As previously mentioned, this is indicative of a reduced Warburg effect and aligns with previous literature in cancer research, indicating that the use of the ketogenic diet in cancer therapies targets the Warburg effect (123,167). When analyzing key enzymes in glucose metabolism, only one of the proteins examined, G6PD, seemed to change with the addition of ketones. Similar to differentiated H9c2 cells, proliferating cells treated with ketones experience an increase in G6PD expression (Figure 3.3G). Although in typical proliferating cells G6P is seen to decrease with differentiation (67–71), other studies have shown that G6PD is cardio protective (77,78). Moreover, it is reduced in hearts with more fetal like metabolic profiles, such as hypertrophied hearts (79). Therefore, the reduction in the Warburg effect may be due to regulation of the PPP, of which G6PD is a key enzyme.

Despite there being no changes in ketone oxidation, there did appear to be a trend towards increased ketone oxidation in both proliferating and differentiated H9c2 cells treated with ketones (Figure 3.4A). This is most likely due to an increase in substrate availability leading to increased ketone oxidative rates. Ketones are not only a energy substrate, but also contribute to cell signaling pathways. Most relevant here is that ketones are endogenous inhibitors of HDACs (118,133). Cancer literature has shown that the ketone induced HDAC2 inhibition can attenuate the growth of tumours (168). In the current study, I did not see any decreases in HDAC2 expression when proliferating H9c2 cells were treated with ketones (Figure 3.4C). Interestingly there was a decrease in Foxo3a expression in these ketones treated proliferating cells (Figure 3.4D). This decrease in Foxo3a was also seen in the differentiated H9c2 cells, however HDAC2 inhibition is typically associated with increase Foxo3a activity (160–162). Importantly, neither HADC2 nor Foxo3a activity were directly measured in this study, so a further exploration of direct activity may be warranted.

Fatty acid oxidation and associated enzymes related to fatty acid oxidation were not changed in proliferating cells when treated with ketones (Figure 3.5A-G). However, given the reduction in glycolytic rates, I did observe an overall decrease in ATP production in proliferating cells treated with ketones (Figure 3.6A). This follows a similar, but not as extensive, trend as what is seen in differentiated H9c2 cells. Moreover, there was increased contribution of ATP from oxidative metabolism compared to proliferating cells cultured in the absence of ketones. Together, it appears that adding ketones to

proliferating cells during culture seems to initiate the process towards differentiating H9c2 cells to a more mature cardiac phenotype, as evidenced by the results discussed above. This is in contrast to results by Xu et al., (169), who showed that culturing H9c2 cells and other cardiomyocytes with BOHB leads to a increase in cardiac fibrosis and apoptosis and inhibits mitochondrial biogenesis, which is ultimately harmful to the cardiomyocyte. However key differences exist between my study and Xu et al (169). In this current study I treated the cells for approximately 72 hours in the presence of 1mM BOHB; Xu et al (169) use 5mM for 24 hours. Potentially this acute treatment with a high concentration of BOHB may be responsible for the negative outcomes compared to the longer treatment timeline at lower concentration of BOHB that was done in my study.

4.1.4 Metabolism of proliferating cells treated with ketones with the knockdown of BDH1

Given that ketones seem to influence cellular differentiation, I wanted to further explore the mechanism of this activity. First, in order to reduce the amount of BOHB that can go through ketone oxidation, I knocked down BDH1, a key enzyme that regulates ketone oxidation (Figure 3.9A). BDH1 knockdown has been studied extensively in the context of cancer. The results from these studies have been variable. Some studies have shown that knocking out BDH1 leads to decrease in proliferation (170), and a decrease BDH1 is associated with better anti-tumor effects of the ketogenic diet (171). Others have reported the opposite in which a BDH1 knockdown increases the proliferation of cancer cells (172). In the adult heart, the knockdown or knockout of BDH1 does not lead to major change under physiological conditions, however once the heart is under stress many issues are

exacerbated, indicating that ketone metabolism is a safety defence (173). This further supported by the evidence that overexpression of BDH1 improves outcomes in heart failure (174). BDH1 also appears to be protective against cardiac pathologies in infants (158,175). Previous studies have knocked down BDH1 in H9c2 cells. When studying heart failure with preserved ejection fraction, Deng et al. found that BOHB improved mitochondrial function, which was enhanced by BDH1 knockdown; this indicates that BOHB exerts an improvement in mitochondrial function independent of ketone oxidation (176). The findings of this study are important as improved mitochondrial function is a characteristic of a more mature cardiomyocyte. Conversely, Xu et al. found that the ketogenic diet inhibits mitochondrial biogenesis (169). When I knocked down BDH1 in proliferating H9c2 cells in the current study, as expected there was an observed reduction in ketone oxidation (Figure 3.10C). Interestingly, glycolytic rates were the same between control cells and BDH1 knocked down cells (Figure 3.10A). Furthermore, the reduction in glycolysis seen with the addition of ketones in the control cells was also observed in BDH1 knockdown cells treated with ketones. This indicates that the changes in the Warburg effect seen in proliferating H9c2c cells treated with ketones is not mediated through BDH1 and subsequently, due to changes in ketone oxidation.

4.1.5 Metabolism of proliferating cells treated with ketones with the knockdown of HDAC2

Given that BDH1 knockdown did not alter the ketone induced reduction in the Warburg effect, I next wanted to explore the cell signaling mechanisms of BOHB. Namely, I explored BOHBs putative effect as a endogenous HDAC2 inhibitor, and how proliferating

H9c2 cell metabolism is influenced by the knockdown of HDAC2. In cancer cells, knocking down HDAC2 is associated with an increase in differentiation and reduced proliferation (132). Under conditions of cardiac hypertrophy, knocking down HDAC2 leads to an increase in hypertrophy and an increase in cardiomyocyte proliferation (135). Furthermore, abnormalities in maturation, such as a down regulation of sarcomere and calcium handling genes, and abnormal sarcomere structure with HDAC2 deficiencies (135) have been observed and reported. The combined loss of both HDAC1 and HDAC2, leads to perinatal lethality and cardiac defects (131). Overall, several studies have shown that HDAC2 is essential to proper cardiac development (135,169,177,178). In the current study, the knockdown of HDAC2 is associated with an increase in glycolysis compared to control H9c2 cells (3.14A). As previously described, increased glycolysis is typically associated with proliferation and a less mature phenotype, which aligns with other literature in regards to the effects of knocking down HDAC2 (135). Interestingly, this increase was ameliorated with the addition of ketones, back to levels that is comparable to that of the control cells (Figure 3.14A). This is in line with Xu et al., who showed that the knock down of HDAC2 in the presence of BOHB led to a increase in mitochondrial biogenesis and a reduction in glycolysis (169). Intriguingly we also saw an increase in glucose oxidation with the knockdown, which was not affected by the addition of ketones (Figure 3.14C). This further indicates that the Warburg effect is decreased with the addition of ketones in HDAC2 knockdown cells, as there seems to be an increased coupling between glycolysis and glucose oxidation. Lastly, I also looked at ketone oxidation, and found that there was reduction in ketone oxidation with the knockdown of HDAC2, which was not affected by the addition of ketones (Figure 3.14B). Overall, it

appears that ATP production is increased in HDAC2 deficient H9c2 cells (Figure 3.15A), mainly due to an increase in glycolysis. This increase was returned to normal levels with addition of ketones. There is not enough data to understand the exact mechanism, however we can surmise that HDAC is important to the regulation of the Warburg effect in proliferating H9c2 cells.

4.2 Limitation & Future Directions

There are several limitations and short/long term future directions for this project.

1. First a foremost, there are still several biomarkers that need to be evaluated with a higher sample size in order to confirm the validity of our results. Additionally, particularly for the BDH1 knockdown and HDAC2 knockdown, several biomarkers need to be assessed via western blot analysis, such as PGC-1α, SERCA2, and G6PD; all of which were increased in the proliferating cells treated with ketones in a similar fashion to what was seen in differentiated H9c2 cells

2. As mentioned, studying the phosphorylation of Foxo3a may be a more relevant indicator of Foxo3a activation in relation to HDAC2 levels. Therefore, in the future, in order to better understand changes in HDAC2 signaling immunoblotting for phosphorylated Foxo3a should be done in addition to total Foxo3a.

3. For the HDAC2 knockdown study I noticed that the control glycolytic rates are lower than previously observed, and there are no changes in glycolysis due to

ketones in the cells treated with scrambled control. As such we would like to further validate these results by replicating the experiment. Additionally, sample number is not high enough to confirm the HDAC2 knockdown in the experimental groups, so further western blotting of HDAC2 is needed to validate the knockdown.

4. Our current method of studying cellular proliferation is not very refined. In the future, I think that a valuable experiment to strengthen these experiments would be to use a different method to assess cell proliferation. While there are certain assays, such as the MTT assay that are popular when studying proliferation, this technique uses the indirect measurement of metabolic activity in order to inform researchers of their cell line's proliferative capacity. Given that this study has directly studied metabolism, this is potentially redundant. Ki67, however is a nuclear antigen that acts a marker of active cell proliferation (179). Therefore, a more accurate measure of proliferation might be studying changes in Ki67 over times may to inform how proliferation changes with the addition of ketones in H9c2 cells.

5. We are unsure of PKM2 activity, and whether or not the increase expression that we observed in differentiated H9c2 cells was of the dimeric or tetrameric conformation. Therefore, it may be valuable to do further experiments in order to study PKM2 activity and elucidate which conformation of PKM2 is being upregulated.

6. In this project, we have used a single cell line, H9c2 cells. In order to further validate the finding of this study, it would be prudent to also repeat these experiments in other cell lines such as AC16 cells which also have the capacity to be studied in proliferating and differentiated states. Other models that may utilized are hiPSC-CMs, as we can also study the differentiating transition from highly proliferative cells to cells with a matured cardiomyocyte phenotype in this model.

7. Once we complete our *in vitro* study, evaluating the role of ketones in cardiomyocyte maturation, in animal models, such as previous reported experiments done in newborn rabbits (3), would be beneficial to produce more translational data. However, there is significant value in exploring this topic *in vitro* first as we can elucidate the mechanism that is most important to explore to limit the amount of animal sacrificed overall.

8. The use of the H9c2 cell line presents some general limitations as well. Firstly, while studies have shown that H9c2 cells share many characteristics and responses to stimuli as neonatal cardiomyocytes (150), they do not have an important characteristic of cardiomyocytes - the ability to contract. This limitation is potentially why in the current study as we see the dramatic reduction in ATP production in differentiated H9c2 cells (Figure 3.6A). Therefore, this model may present limitations when trying to compare transition from fetal cardiomyocytes to matured newborn cardiomyocytes. Despite this limitation, other studies as well as the current study show that differentiated H9c2 cells do share important

characteristics of matured cardiomyocytes, such as an increase in proteins associated with calcium handling and mitochondrial biogenesis, those of which are responsible to drive the increase in contractile force in the developing heart (24,27). Importantly, it should be noted that the differentiation protocol produces a heterogenous cell populations (24). Given that the process of differentiation is ongoing, there are cells at various stages of differentiation within each group of samples. However, we ensure that a significant amount of differentiation has occurred with each experiment through the analysis of several different cardiomyocyte maturation markers.

While there are a few limitations of this study and future experiments that should be done to better validate these results, the current data does allow for important insights when studying cardiomyocyte maturation.

4.3 Conclusion

By directly measuring the energy metabolic profile of proliferating and differentiated H9c2 cells in the presence or absence of ketones I found that differentiating H9c2 cells lead to a decrease in the Warburg effect, primarily due to a decrease in glycolysis. Furthermore, treating proliferating H9c2 cells with ketones, a substrate that increases in the newborn period, also leads to reduction in the Warburg effect due to a decrease in glycolysis. This reduction in the Warburg effect was associated with an increase in cardiomyocyte maturation markers in proliferating H9c2 cells treated with ketones. While the knockdown

of BDH1 did not cause any changes in glycolytic rates in proliferating cells in the presence or absence of ketones, the knockdown of HDAC2 lead to an increase in the Warburg effect, implicating this as a potential pathway by which ketones may be exerting their effects.

BIBLIOGRAPHY

1. Persad KL, Lopaschuk GD. Energy Metabolism on Mitochondrial Maturation and Its Effects on Cardiomyocyte Cell Fate. Front Cell Dev Biol. 2022;10:886393.

2. Velayutham N, Agnew EJ, Yutzey KE. Postnatal Cardiac Development and Regenerative Potential in Large Mammals. Pediatr Cardiol. 2019 Oct;40(7):1345–58.

3. Lopaschuk GD, Spafford MA, Marsh DR. Glycolysis is predominant source of myocardial ATP production immediately after birth. American Journal of Physiology-Heart and Circulatory Physiology. 1991 Dec 1;261(6):H1698–705.

4. Abdel-Haleem AM, Lewis NE, Jamshidi N, Mineta K, Gao X, Gojobori T. The Emerging Facets of Non-Cancerous Warburg Effect. Front Endocrinol. 2017 Oct 23;8:279.

5. Lopaschuk GD, Ussher JR, Folmes CDL, Jaswal JS, Stanley WC. Myocardial Fatty Acid Metabolism in Health and Disease. Physiological Reviews. 2010 Jan;90(1):207–58.

6. Folmes CDL, Nelson TJ, Martinez-Fernandez A, Arrell DK, Lindor JZ, Dzeja PP, et al. Somatic Oxidative Bioenergetics Transitions into Pluripotency-Dependent Glycolysis to Facilitate Nuclear Reprogramming. Cell Metabolism. 2011 Aug;14(2):264–71.

7. Kondoh H, Lleonart ME, Nakashima Y, Yokode M, Tanaka M, Bernard D, et al. A High Glycolytic Flux Supports the Proliferative Potential of Murine Embryonic Stem Cells. Antioxidants & Redox Signaling. 2007 Mar;9(3):293–9.

8. Chung S, Dzeja PP, Faustino RS, Perez-Terzic C, Behfar A, Terzic A. Mitochondrial oxidative metabolism is required for the cardiac differentiation of stem cells. Nat Rev Cardiol. 2007 Feb;4(S1):S60–7.

9. Chen C, Liu Y, Liu R, Ikenoue T, Guan KL, Liu Y, et al. TSC–mTOR maintains quiescence and function of hematopoietic stem cells by repressing mitochondrial biogenesis and reactive oxygen species. Journal of Experimental Medicine. 2008 Sep 29;205(10):2397–408.

10. DeBerardinis RJ, Lum JJ, Hatzivassiliou G, Thompson CB. The Biology of Cancer: Metabolic Reprogramming Fuels Cell Growth and Proliferation. Cell Metabolism. 2008 Jan;7(1):11–20.

11. Vander Heiden MG, Cantley LC, Thompson CB. Understanding the Warburg Effect: The Metabolic Requirements of Cell Proliferation. Science. 2009 May 22;324(5930):1029–33.

12. Boroughs LK, DeBerardinis RJ. Metabolic pathways promoting cancer cell survival and growth. Nat Cell Biol. 2015 Apr;17(4):351–9.

13. Schowen RL. Principles of biochemistry 2nd ed. (Lehninger, Albert L.; Nelson, David L.; Cox, Michael M.). J Chem Educ. 1993 Aug;70(8):A223.

14. Shyh-Chang N, Daley GQ, Cantley LC. Stem cell metabolism in tissue development and aging. Development. 2013 Jun 15;140(12):2535–47.

15. Lopaschuk GD, Jaswal JS. Energy Metabolic Phenotype of the Cardiomyocyte During Development, Differentiation, and Postnatal Maturation. Journal of Cardiovascular Pharmacology. 2010 Aug;56(2):130–40.

16. Lopaschuk GD, Collins-Nakai RL, Itoi T. Developmental changes in energy substrate use by the heart. Cardiovascular Research. 1992 Dec 1;26(12):1172–80.

17. Makinde AO, Kantor PF, Lopaschuk GD. Maturation of fatty acid and carbohydrate metabolism in the newborn heart. In: Pierce GN, Izumi T, Rupp H, Grynberg A, editors. Molecular and Cellular Effects of Nutrition on Disease Processes [Internet]. Boston, MA: Springer US; 1998 [cited 2023 Mar 22]. p. 49–56. Available from: http://link.springer.com/10.1007/978-1-4615-5763-0_6

18. Guo Y, Pu WT. Cardiomyocyte Maturation: New Phase in Development. Circ Res. 2020 Apr 10;126(8):1086–106.

19. Medina JM. The Role of Lactate as an Energy Substrate for the Brain during the Early Neonatal Period. Neonatology. 1985;48(4):237–44.

20. Girard J, Ferre P, Pegorier JP, Duee PH. Adaptations of glucose and fatty acid metabolism during perinatal period and suckling-weaning transition. Physiological Reviews. 1992 Apr 1;72(2):507–62.

21. Nose N, Werner RA, Ueda Y, Günther K, Lapa C, Javadi MS, et al. Metabolic substrate shift in human induced pluripotent stem cells during cardiac differentiation: Functional assessment using in vitro radionuclide uptake assay. International Journal of Cardiology. 2018 Oct;269:229–34.

22. Nakano H, Minami I, Braas D, Pappoe H, Wu X, Sagadevan A, et al. Glucose inhibits cardiac muscle maturation through nucleotide biosynthesis. eLife. 2017 Dec 12;6:e29330.

23. Yang P, Chen X, Kaushal S, Reece EA, Yang P. High glucose suppresses embryonic stem cell differentiation into cardiomyocytes: High glucose inhibits ES cell cardiogenesis. Stem Cell Res Ther. 2016 Dec;7(1):187.

24. Branco AF, Pereira SP, Gonzalez S, Gusev O, Rizvanov AA, Oliveira PJ. Gene Expression Profiling of H9c2 Myoblast Differentiation towards a Cardiac-Like Phenotype. PLoS One. 2015;10(6):e0129303.

25. Attardi G, Schatz G. Biogenesis of mitochondria. Annu Rev Cell Biol. 1988;4:289–333.

26. Mayor F, Cuezva JM. Hormonal and Metabolic Changes in the Perinatal Period. Neonatology. 1985;48(4):185–96.

27. Stanley WC, Recchia FA, Lopaschuk GD. Myocardial Substrate Metabolism in the Normal and Failing Heart. Physiological Reviews. 2005 Jul;85(3):1093–129.

28. Lai L, Leone TC, Zechner C, Schaeffer PJ, Kelly SM, Flanagan DP, et al. Transcriptional coactivators PGC-1α and PGC-lβ control overlapping programs required for perinatal maturation of the heart. Genes Dev. 2008 Jul 15;22(14):1948–61.

29. Lehman JJ, Barger PM, Kovacs A, Saffitz JE, Medeiros DM, Kelly DP. Peroxisome proliferator–activated receptor γ coactivator-1 promotes cardiac mitochondrial biogenesis. J Clin Invest. 2000 Oct 1;106(7):847–56.

30. Leone TC, Lehman JJ, Finck BN, Schaeffer PJ, Wende AR, Boudina S, et al. PGC-1α Deficiency Causes Multi-System Energy Metabolic Derangements: Muscle Dysfunction, Abnormal Weight Control and Hepatic Steatosis. Vidal-Puig A, editor. PLoS Biol. 2005 Mar 15;3(4):e101.

31. Lelliott CJ, Medina-Gomez G, Petrovic N, Kis A, Feldmann HM, Bjursell M, et al. Ablation of PGC-1β Results in Defective Mitochondrial Activity, Thermogenesis, Hepatic Function, and Cardiac Performance. Barsh GS, editor. PLoS Biol. 2006 Nov 7;4(11):e369.

32. Martin OJ, Lai L, Soundarapandian MM, Leone TC, Zorzano A, Keller MP, et al. A Role for Peroxisome Proliferator-Activated Receptor γ Coactivator-1 in the Control of Mitochondrial Dynamics During Postnatal Cardiac Growth. Circ Res. 2014 Feb 14;114(4):626–36.

33. Schaper J, Meiser E, Stämmler G. Ultrastructural morphometric analysis of myocardium from dogs, rats, hamsters, mice, and from human hearts. Circ Res. 1985 Mar;56(3):377–91.

34. Dai DF, Danoviz ME, Wiczer B, Laflamme MA, Tian R. Mitochondrial Maturation in Human Pluripotent Stem Cell Derived Cardiomyocytes. Stem Cells International. 2017;2017:1–10.

35. Venkatesh S, Baljinnyam E, Tong M, Kashihara T, Yan L, Liu T, et al. Proteomic analysis of mitochondrial biogenesis in cardiomyocytes differentiated from human

induced pluripotent stem cells. American Journal of Physiology-Regulatory, Integrative and Comparative Physiology. 2021 Apr 1;320(4):R547–62.

36. Liu Y, Bai H, Guo F, Thai PN, Luo X, Zhang P, et al. PGC-1α activator ZLN005 promotes maturation of cardiomyocytes derived from human embryonic stem cells. Aging. 2020 Apr 28;12(8):7411–30.

37. Folmes CDL, Nelson TJ, Dzeja PP, Terzic A. Energy metabolism plasticity enables stemness programs. Annals NY Academy of Science. 2012 Apr;1254(1):82–9.

38. Cho YM, Kwon S, Pak YK, Seol HW, Choi YM, Park DJ, et al. Dynamic changes in mitochondrial biogenesis and antioxidant enzymes during the spontaneous differentiation of human embryonic stem cells. Biochemical and Biophysical Research Communications. 2006 Oct;348(4):1472–8.

39. Hansson J, Rafiee MR, Reiland S, Polo JM, Gehring J, Okawa S, et al. Highly Coordinated Proteome Dynamics during Reprogramming of Somatic Cells to Pluripotency. Cell Reports. 2012 Dec;2(6):1579–92.

40. Simsek T, Kocabas F, Zheng J, DeBerardinis RJ, Mahmoud AI, Olson EN, et al. The Distinct Metabolic Profile of Hematopoietic Stem Cells Reflects Their Location in a Hypoxic Niche. Cell Stem Cell. 2010 Sep;7(3):380–90.

41. Takubo K, Nagamatsu G, Kobayashi CI, Nakamura-Ishizu A, Kobayashi H, Ikeda E, et al. Regulation of Glycolysis by Pdk Functions as a Metabolic Checkpoint for Cell Cycle Quiescence in Hematopoietic Stem Cells. Cell Stem Cell. 2013 Jan;12(1):49–61.

42. Pfeiffer T, Schuster S, Bonhoeffer S. Cooperation and Competition in the Evolution of ATP-Producing Pathways. Science. 2001 Apr 20;292(5516):504–7.

43. Christofk HR, Vander Heiden MG, Harris MH, Ramanathan A, Gerszten RE, Wei R, et al. The M2 splice isoform of pyruvate kinase is important for cancer metabolism and tumour growth. Nature. 2008 Mar;452(7184):230–3.

44. Lunt SY, Vander Heiden MG. Aerobic Glycolysis: Meeting the Metabolic Requirements of Cell Proliferation. Annu Rev Cell Dev Biol. 2011 Nov 10;27(1):441–64.

45. Varum S, Momčilović O, Castro C, Ben-Yehudah A, Ramalho-Santos J, Navara CS. Enhancement of human embryonic stem cell pluripotency through inhibition of the mitochondrial respiratory chain. Stem Cell Research. 2009 Sep;3(2–3):142–56.

46. Fukushima A, Zhang L, Huqi A, Lam VH, Rawat S, Altamimi T, et al. Acetylation contributes to hypertrophy-caused maturational delay of cardiac energy metabolism. JCI Insight. 2018 May 17;3(10):e99239.

47. Tormos KV, Anso E, Hamanaka RB, Eisenbart J, Joseph J, Kalyanaraman B, et al. Mitochondrial Complex III ROS Regulate Adipocyte Differentiation. Cell Metabolism. 2011 Oct;14(4):537–44.

48. Garnett ME, Dyson RD, Dost FN. Pyruvate Kinase Isozyme Changes in Parenchymal Cells of Regenerating Rat Liver. Journal of Biological Chemistry. 1974 Aug;249(16):5222–6.

49. Ikeda Y, Noguchi T. Allosteric Regulation of Pyruvate Kinase M2 Isozyme Involves a Cysteine Residue in the Intersubunit Contact. Journal of Biological Chemistry. 1998 May;273(20):12227–33.

50. Ashizawa K, Willingham MC, Liang CM, Cheng SY. In vivo regulation of monomer-tetramer conversion of pyruvate kinase subtype M2 by glucose is mediated via fructose 1,6-bisphosphate. Journal of Biological Chemistry. 1991 Sep;266(25):16842–6.

51. Kung C, Hixon J, Choe S, Marks K, Gross S, Murphy E, et al. Small Molecule Activation of PKM2 in Cancer Cells Induces Serine Auxotrophy. Chemistry & Biology. 2012 Sep;19(9):1187–98.

52. Parnell KM, Foulks JM, Nix RN, Clifford A, Bullough J, Luo B, et al. Pharmacologic Activation of PKM2 Slows Lung Tumor Xenograft Growth. Molecular Cancer Therapeutics. 2013 Aug 1;12(8):1453–60.

53. Anastasiou D, Yu Y, Israelsen WJ, Jiang JK, Boxer MB, Hong BS, et al. Pyruvate kinase M2 activators promote tetramer formation and suppress tumorigenesis. Nat Chem Biol. 2012 Oct;8(10):839–47.

54. Li T, Han J, Jia L, Hu X, Chen L, Wang Y. PKM2 coordinates glycolysis with mitochondrial fusion and oxidative phosphorylation. Protein Cell. 2019 Aug;10(8):583–94.

55. Magadum A, Singh N, Kurian AA, Munir I, Mehmood T, Brown K, et al. Pkm2 Regulates Cardiomyocyte Cell Cycle and Promotes Cardiac Regeneration. Circulation. 2020 Apr 14;141(15):1249–65.

56. Pilkis SJ, El-Maghrabi MR, Pilkis J, Claus TH, Cumming DA. Fructose 2,6-bisphosphate. A new activator of phosphofructokinase. Journal of Biological Chemistry. 1981 Apr;256(7):3171–4.

57. Pilkis SJ, Claus TH, Kurland IJ, Lange AJ. 6-PHOSPHOFRUCTO-2-KINASE/FRUCTOSE-2,6-BISPHOSPHATASE: A METABOLIC SIGNALING ENZYME. Annu Rev Biochem. 1995 Jun;64(1):799–835.

58. Uyeda K, Furuya E, Luby LJ. The effect of natural and synthetic D-fructose 2,6-bisphosphate on the regulatory kinetic properties of liver and muscle phosphofructokinases. Journal of Biological Chemistry. 1981 Aug;256(16):8394–9.

59. Ros S, Schulze A. Balancing glycolytic flux: the role of 6-phosphofructo-2-kinase/fructose 2,6-bisphosphatases in cancer metabolism. Cancer Metab. 2013 Dec;1(1):8.

60. Novellasdemunt L, Obach M, Millán-Ariño L, Manzano A, Ventura F, Rosa JL, et al. Progestins activate 6-phosphofructo-2-kinase/fructose-2,6-bisphosphatase 3 (PFKFB3) in breast cancer cells. Biochemical Journal. 2012 Mar 1;442(2):345–56.

61. Nissler K, Petermann H, Wenz I, Brox D. Fructose 2,6-bisphosphate metabolism in Ehrlich ascites tumour cells. J Cancer Res Clin Oncol. 1995 Dec;121(12):739–45.

62. Hue L, Rousseau GG. Fructose 2,6-bisphosphate and the control of glycolysis by growth factors, tumor promoters and oncogenes. Advances in Enzyme Regulation. 1993 Jan;33:97–110.

63. Seo M, Kim JD, Neau D, Sehgal I, Lee YH. Structure-Based Development of Small Molecule PFKFB3 Inhibitors: A Framework for Potential Cancer Therapeutic Agents Targeting the Warburg Effect. Tyagi AK, editor. PLoS ONE. 2011 Sep 21;6(9):e24179.

64. Clem B, Telang S, Clem A, Yalcin A, Meier J, Simmons A, et al. Small-molecule inhibition of 6-phosphofructo-2-kinase activity suppresses glycolytic flux and tumor growth. Molecular Cancer Therapeutics. 2008 Jan 1;7(1):110–20.

65. De Bock K, Georgiadou M, Schoors S, Kuchnio A, Wong BW, Cantelmo AR, et al. Role of PFKFB3-Driven Glycolysis in Vessel Sprouting. Cell. 2013 Aug;154(3):651–63.

66. Dobrina A, Rossi F. Metabolic properties of freshly isolated bovine endothelial cells. Biochimica et Biophysica Acta (BBA) - Molecular Cell Research. 1983 Apr;762(2):295–301.

67. Deng P, Li K, Gu F, Zhang T, Zhao W, Sun M, et al. LINC00242/miR-1-3p/G6PD axis regulates Warburg effect and affects gastric cancer proliferation and apoptosis. Mol Med. 2021 Dec;27(1):9.

68. Li D, Zhu Y, Tang Q, Lu H, Li H, Yang Y, et al. A New G6PD Knockdown Tumor-Cell Line with Reduced Proliferation and Increased Susceptibility to Oxidative Stress. Cancer Biotherapy and Radiopharmaceuticals. 2009 Feb;24(1):81–90.

69. Tian WN, Braunstein LD, Pang J, Stuhlmeier KM, Xi QC, Tian X, et al. Importance of Glucose-6-phosphate Dehydrogenase Activity for Cell Growth. Journal of Biological Chemistry. 1998 Apr;273(17):10609–17.

70. Yang HC, Chen TL, Wu YH, Cheng KP, Lin YH, Cheng ML, et al. Glucose 6-phosphate dehydrogenase deficiency enhances germ cell apoptosis and causes defective embryogenesis in Caenorhabditis elegans. Cell Death Dis. 2013 May 2;4(5):e616–e616.

71. Longo L. Maternally transmitted severe glucose 6-phosphate dehydrogenase deficiency is an embryonic lethal. The EMBO Journal. 2002 Aug 15;21(16):4229–39.

72. Richardson AD, Yang C, Osterman A, Smith JW. Central carbon metabolism in the progression of mammary carcinoma. Breast Cancer Res Treat. 2008 Jul;110(2):297.

73. Kletzien RF, Harris PKW, Foellmi LA. Glucose-6-phosphate dehydrogenase: a “housekeeping” enzyme subject to tissue-specific regulation by hormones, nutrients, and oxidant stress. FASEB j. 1994 Feb;8(2):174–81.

74. Yang, Wu, Yen, Liu, Hwang, Stern, et al. The Redox Role of G6PD in Cell Growth, Cell Death, and Cancer. Cells. 2019 Sep 8;8(9):1055.

75. Pandolfi PP, Sonati F, Rivi R, Mason P, Grosveld F, Luzzatto L. Targeted disruption of the housekeeping gene encoding glucose 6-phosphate dehydrogenase (G6PD): G6PD is dispensable for pentose synthesis but essential for defense against oxidative stress. The EMBO Journal. 1995 Nov;14(21):5209–15.

76. Zhang Z, Liew CW, Handy DE, Zhang Y, Leopold JA, Hu J, et al. High glucose inhibits glucose-6-phosphate dehydrogenase, leading to increased oxidative stress and β-cell apoptosis. FASEB j. 2010 May;24(5):1497–505.

77. Wu G, Lupton JR, Turner ND, Fang YZ, Yang S. Glutathione Metabolism and Its Implications for Health. The Journal of Nutrition. 2004 Mar;134(3):489–92.

78. Jain M, Cui L, Brenner DA, Wang B, Handy DE, Leopold JA, et al. Increased Myocardial Dysfunction After Ischemia-Reperfusion in Mice Lacking Glucose-6-Phosphate Dehydrogenase. Circulation. 2004 Feb 24;109(7):898–903.

79. Li B, Wang X, Yu M, Yang P, Wang W. G6PD, bond by miR-24, regulates mitochondrial dysfunction and oxidative stress in phenylephrine-induced hypertrophic cardiomyocytes. Life Sciences. 2020 Nov;260:118378.

80. Folmes CDL, Dzeja PP, Nelson TJ, Terzic A. Metabolic Plasticity in Stem Cell Homeostasis and Differentiation. Cell Stem Cell. 2012 Nov;11(5):596–606.

81. Mandal S, Lindgren AG, Srivastava AS, Clark AT, Banerjee U. Mitochondrial Function Controls Proliferation and Early Differentiation Potential of Embryonic Stem Cells. Stem Cells. 2011 Mar 1;29(3):486–95.

82. Bracha AL, Ramanathan A, Huang S, Ingber DE, Schreiber SL. Carbon metabolism–mediated myogenic differentiation. Nat Chem Biol. 2010 Mar;6(3):202–4.

83. Schell JC, Wisidagama DR, Bensard C, Zhao H, Wei P, Tanner J, et al. Control of intestinal stem cell function and proliferation by mitochondrial pyruvate metabolism. Nat Cell Biol. 2017 Sep;19(9):1027–36.

84. Gray LR, Tompkins SC, Taylor EB. Regulation of pyruvate metabolism and human disease. Cell Mol Life Sci. 2014 Jul;71(14):2577–604.

85. Lam VH, Zhang L, Huqi A, Fukushima A, Tanner BA, Onay-Besikci A, et al. Activating PPARα Prevents Post–Ischemic Contractile Dysfunction in Hypertrophied Neonatal Hearts. Circ Res. 2015 Jun 19;117(1):41–51.

86. Soonpaa MH, Kim KK, Pajak L, Franklin M, Field LJ. Cardiomyocyte DNA synthesis and binucleation during murine development. American Journal of Physiology-Heart and Circulatory Physiology. 1996 Nov 1;271(5):H2183–9.

87. Ahuja P, Sdek P, MacLellan WR. Cardiac Myocyte Cell Cycle Control in Development, Disease, and Regeneration. Physiological Reviews. 2007 Apr;87(2):521–44.

88. Itoi T, Lopaschuk GD. The Contribution of Glycolysis, Glucose Oxidation, Lactate Oxidation, and Fatty Acid Oxidation to ATP Production in Isolated Biventricular Working Hearts from 2-Week-Old Rabbits. Pediatr Res. 1993 Dec;34(6):735–41.

89. Kolwicz SC, Purohit S, Tian R. Cardiac Metabolism and its Interactions With Contraction, Growth, and Survival of Cardiomyocytes. Circ Res. 2013 Aug 16;113(5):603–16.

90. Saddik M, Lopaschuk GD. Myocardial triglyceride turnover and contribution to energy substrate utilization in isolated working rat hearts. Journal of Biological Chemistry. 1991 May;266(13):8162–70.

91. Huss JM, Kelly DP. Nuclear Receptor Signaling and Cardiac Energetics. Circulation Research. 2004 Sep 17;95(6):568–78.

92. Finck B. The PPAR regulatory system in cardiac physiology and disease. Cardiovascular Research. 2007 Jan 15;73(2):269–77.

93. van der Lee KAJM, Vork MM, De Vries JE, Willemsen PHM, Glatz JFC, Reneman RS, et al. Long-chain fatty acid-induced changes in gene expression in neonatal cardiac myocytes. Journal of Lipid Research. 2000 Jan;41(1):41–7.

94. Brandt JM, Djouadi F, Kelly DP. Fatty Acids Activate Transcription of the Muscle Carnitine Palmitoyltransferase I Gene in Cardiac Myocytes via the Peroxisome Proliferator-activated Receptor α. Journal of Biological Chemistry. 1998 Sep;273(37):23786–92.

95. Mascaró C, Acosta E, Ortiz JA, Marrero PF, Hegardt FG, Haro D. Control of Human Muscle-type Carnitine Palmitoyltransferase I Gene Transcription by Peroxisome Proliferator-activated Receptor. Journal of Biological Chemistry. 1998 Apr;273(15):8560–3.

96. Gulick T, Cresci S, Caira T, Moore DD, Kelly DP. The peroxisome proliferator-activated receptor regulates mitochondrial fatty acid oxidative enzyme gene expression. Proc Natl Acad Sci USA. 1994 Nov 8;91(23):11012–6.

97. Leone TC, Weinheimer CJ, Kelly DP. A critical role for the peroxisome proliferator-activated receptor α (PPARα) in the cellular fasting response: The PPARα-null mouse as a model of fatty acid oxidation disorders. Proc Natl Acad Sci USA. 1999 Jun 22;96(13):7473–8.

98. Gilde AJ, van der Lee KAJM, Willemsen PHM, Chinetti G, van der Leij FR, van der Vusse GJ, et al. Peroxisome Proliferator-Activated Receptor (PPAR) α and PPARβ/δ, but not PPARγ, Modulate the Expression of Genes Involved in Cardiac Lipid Metabolism. Circulation Research. 2003 Mar 21;92(5):518–24.

99. Panadero M, Herrera E, Bocos C. Peroxisome proliferator-activated receptor-α expressionin rat liver during postnatal development. Biochimie. 2000 Aug;82(8):723–6.

100. Lopaschuk GD, Belke DD, Gamble J, Toshiyuki I, Schönekess BO. Regulation of fatty acid oxidation in the mammalian heart in health and disease. Biochimica et Biophysica Acta (BBA) - Lipids and Lipid Metabolism. 1994 Aug;1213(3):263–76.

101. Mcmillin JB, Wang DC, Witters LA, Buja LM. Kinetic Properties of Carnitine Palmitoyltransferase I in Cultured Neonatal Rat Cardiac Myocytes. Archives of Biochemistry and Biophysics. 1994 Aug;312(2):375–84.

102. Lopaschuk GD, Witters LA, Itoi T, Barr R, Barr A. Acetyl-CoA carboxylase involvement in the rapid maturation of fatty acid oxidation in the newborn rabbit heart. Journal of Biological Chemistry. 1994 Oct;269(41):25871–8.

103. Lopaschuk GD, Gamble J. The 1993 Merck Frosst Award. Acetyl-CoA carboxylase: an important regulator of fatty acid oxidation in the heart. Can J Physiol Pharmacol. 1994 Oct 1;72(10):1101–9.

104. Dyck JRB, Barr AJ, Barr RL, Kolattukudy PE, Lopaschuk GD. Characterization of cardiac malonyl-CoA decarboxylase and its putative role in regulating fatty acid oxidation. American Journal of Physiology-Heart and Circulatory Physiology. 1998 Dec 1;275(6):H2122–9.

105. Saddik M, Gamble J, Witters LA, Lopaschuk GD. Acetyl-CoA carboxylase regulation of fatty acid oxidation in the heart. Journal of Biological Chemistry. 1993 Dec;268(34):25836–45.

106. Grahame Hardie D. Regulation of fatty acid synthesis via phosphorylation of acetyl-CoA carboxylase. Progress in Lipid Research. 1989 Jan;28(2):117–46.

107. Hardie DG. Regulation of fatty acid and cholesterol metabolism by the AMP-activated protein kinase. Biochimica et Biophysica Acta (BBA) - Lipids and Lipid Metabolism. 1992 Feb;1123(3):231–8.

108. Jäger S, Handschin C, St.-Pierre J, Spiegelman BM. AMP-activated protein kinase (AMPK) action in skeletal muscle via direct phosphorylation of PGC-1α. Proc Natl Acad Sci USA. 2007 Jul 17;104(29):12017–22.

109. Dyck JRB, Berthiaume LG, Thomas PD, Kantor PF, Barr AJ, Barr R, et al. Characterization of rat liver malonyl-CoA decarboxylase and the study of its role in regulating fatty acid metabolism. Biochemical Journal. 2000 Sep 1;350(2):599–608.

110. Yatscoff MA, Jaswal JS, Grant MR, Greenwood R, Lukat T, Beker DL, et al. Myocardial Hypertrophy and the Maturation of Fatty Acid Oxidation in the Newborn Human Heart. Pediatr Res. 2008 Dec;64(6):643–7.

111. Sakamoto J, Barr RL, Kavanagh KM, Lopaschuk GD. Contribution of malonyl-CoA decarboxylase to the high fatty acid oxidation rates seen in the diabetic heart. American Journal of Physiology-Heart and Circulatory Physiology. 2000 Apr 1;278(4):H1196–204.

112. Yang X, Pabon L, Murry CE. Engineering Adolescence: Maturation of Human Pluripotent Stem Cell–Derived Cardiomyocytes. Circ Res. 2014 Jan 31;114(3):511–23.

113. Robertson C, Tran DD, George SC. Concise Review: Maturation Phases of Human Pluripotent Stem Cell-Derived Cardiomyocytes. Stem Cells. 2013 May 1;31(5):829–37.

114. Mummery CL, Zhang J, Ng ES, Elliott DA, Elefanty AG, Kamp TJ. Differentiation of Human Embryonic Stem Cells and Induced Pluripotent Stem Cells to Cardiomyocytes: A Methods Overview. Circ Res. 2012 Jul 20;111(3):344–58.

115. Drawnel FM, Boccardo S, Prummer M, Delobel F, Graff A, Weber M, et al. Disease Modeling and Phenotypic Drug Screening for Diabetic Cardiomyopathy using Human Induced Pluripotent Stem Cells. Cell Reports. 2014 Nov;9(3):810–20.

116. Horikoshi Y, Yan Y, Terashvili M, Wells C, Horikoshi H, Fujita S, et al. Fatty Acid-Treated Induced Pluripotent Stem Cell-Derived Human Cardiomyocytes Exhibit Adult Cardiomyocyte-Like Energy Metabolism Phenotypes. Cells. 2019 Sep 17;8(9):1095.

117. Miao S, Zhao D, Wang X, Ni X, Fang X, Yu M, et al. Retinoic acid promotes metabolic maturation of human Embryonic Stem Cell-derived Cardiomyocytes. Theranostics. 2020;10(21):9686–701.

118. Newman JC, Verdin E. Ketone bodies as signaling metabolites. Trends in Endocrinology & Metabolism. 2014 Jan;25(1):42–52.

119. Bartelds B, Gratama JWC, Knoester H, Takens J, Smid GB, Aarnoudse JG, et al. Perinatal changes in myocardial supply and flux of fatty acids, carbohydrates, and ketone bodies in lambs. American Journal of Physiology-Heart and Circulatory Physiology. 1998 Jun 1;274(6):H1962–9.

120. Newman JC, Verdin E. β-hydroxybutyrate: Much more than a metabolite. Diabetes Research and Clinical Practice. 2014 Nov;106(2):173–81.

121. Ferrere G, Tidjani Alou M, Liu P, Goubet AG, Fidelle M, Kepp O, et al. Ketogenic diet and ketone bodies enhance the anticancer effects of PD-1 blockade. JCI Insight. 2021 Jan 25;6(2):e145207.

122. Singh S, Pandey S, Bhatt AN, Chaudhary R, Bhuria V, Kalra N, et al. Chronic Dietary Administration of the Glycolytic Inhibitor 2-Deoxy-D-Glucose (2-DG) Inhibits the

Growth of Implanted Ehrlich's Ascites Tumor in Mice. Huang C, editor. PLoS ONE. 2015 Jul 2;10(7):e0132089.

123. Weber DD, Aminazdeh-Gohari S, Kofler B. Ketogenic diet in cancer therapy. Aging. 2018 Feb 11;10(2):164–5.

124. Li X, Higashida K, Kawamura T, Higuchi M. Alternate-Day High-Fat Diet Induces an Increase in Mitochondrial Enzyme Activities and Protein Content in Rat Skeletal Muscle. Nutrients. 2016 Apr 6;8(4):203.

125. Sparks LM, Xie H, Koza RA, Mynatt R, Hulver MW, Bray GA, et al. A High-Fat Diet Coordinately Downregulates Genes Required for Mitochondrial Oxidative Phosphorylation in Skeletal Muscle. Diabetes. 2005 Jul 1;54(7):1926–33.

126. Jensen J, Rustad PI, Kolnes AJ, Lai YC. The Role of Skeletal Muscle Glycogen Breakdown for Regulation of Insulin Sensitivity by Exercise. Front Physio [Internet]. 2011 [cited 2023 Mar 23];2. Available from: http://journal.frontiersin.org/article/10.3389/fphys.2011.00112/abstract

127. Hasan-Olive MM, Lauritzen KH, Ali M, Rasmussen LJ, Storm-Mathisen J, Bergersen LH. A Ketogenic Diet Improves Mitochondrial Biogenesis and Bioenergetics via the PGC1α-SIRT3-UCP2 Axis. Neurochem Res. 2019 Jan;44(1):22–37.

128. Bougneres PF, Lemmel C, Ferré P, Bier DM. Ketone body transport in the human neonate and infant. J Clin Invest. 1986 Jan 1;77(1):42–8.

129. Haberland M, Montgomery RL, Olson EN. The many roles of histone deacetylases in development and physiology: implications for disease and therapy. Nat Rev Genet. 2009 Jan;10(1):32–42.

130. Gregoretti I, Lee YM, Goodson HV. Molecular Evolution of the Histone Deacetylase Family: Functional Implications of Phylogenetic Analysis. Journal of Molecular Biology. 2004 Apr;338(1):17–31.

131. Montgomery RL, Davis CA, Potthoff MJ, Haberland M, Fielitz J, Qi X, et al. Histone deacetylases 1 and 2 redundantly regulate cardiac morphogenesis, growth, and contractility. Genes Dev. 2007 Jul 15;21(14):1790–802.

132. Jurkin J, Zupkovitz G, Lagger S, Grausenburger R, Hagelkruys A, Kenner L, et al. Distinct and redundant functions of histone deacetylases HDAC1 and HDAC2 in proliferation and tumorigenesis. Cell Cycle. 2011 Feb;10(3):406–12.

133. Mierziak J, Burgberger M, Wojtasik W. 3-Hydroxybutyrate as a Metabolite and a Signal Molecule Regulating Processes of Living Organisms. Biomolecules. 2021 Mar 9;11(3):402.

134. Razeghi P, Young ME, Alcorn JL, Moravec CS, Frazier OH, Taegtmeyer H. Metabolic Gene Expression in Fetal and Failing Human Heart. Circulation. 2001 Dec 11;104(24):2923–31.

135. Trivedi CM, Luo Y, Yin Z, Zhang M, Zhu W, Wang T, et al. Hdac2 regulates the cardiac hypertrophic response by modulating Gsk3β activity. Nat Med. 2007 Mar;13(3):324–31.

136. Fukushima A, Alrob OA, Zhang L, Wagg CS, Altamimi T, Rawat S, et al. Acetylation and succinylation contribute to maturational alterations in energy metabolism in the newborn heart. American Journal of Physiology-Heart and Circulatory Physiology. 2016 Aug 1;311(2):H347–63.

137. Watkins SJ, Borthwick GM, Arthur HM. The H9C2 cell line and primary neonatal cardiomyocyte cells show similar hypertrophic responses in vitro. In Vitro CellDevBiol-Animal. 2011 Feb;47(2):125–31.

138. Marelli AJ, Mackie AS, Ionescu-Ittu R, Rahme E, Pilote L. Congenital Heart Disease in the General Population: Changing Prevalence and Age Distribution. Circulation. 2007 Jan 16;115(2):163–72.

139. Kimes B, Brandt B. Properties of a clonal muscle cell line from rat heart. Experimental Cell Research. 1976 Mar 15;98(2):367–81.

140. Ménard C, Pupier S, Mornet D, Kitzmann M, Nargeot J, Lory P. Modulation of L-type calcium channel expression during retinoic acid-induced differentiation of H9C2 cardiac cells. J Biol Chem. 1999 Oct 8;274(41):29063–70.

141. Lampert MA, Orogo AM, Najor RH, Hammerling BC, Leon LJ, Wang BJ, et al. BNIP3L/NIX and FUNDC1-mediated mitophagy is required for mitochondrial network remodeling during cardiac progenitor cell differentiation. Autophagy. 2019 Jul 3;15(7):1182–98.

142. Sharow KA, Temkin B, Asson-Batres MA. Retinoic acid stability in stem cell cultures. Int J Dev Biol. 2012;56(4):273–8.

143. Uddin GM, Karwi QG, Pherwani S, Gopal K, Wagg CS, Biswas D, et al. Deletion of BCATm increases insulin-stimulated glucose oxidation in the heart. Metabolism. 2021 Nov;124:154871.

144. Karwi QG, Wagg CS, Altamimi TR, Uddin GM, Ho KL, Darwesh AM, et al. Insulin directly stimulates mitochondrial glucose oxidation in the heart. Cardiovasc Diabetol. 2020 Dec 7;19:207.

145. Salway JG. Metabolism at a Glance, 4th Edition | Wiley [Internet]. [cited 2023 Feb 28]. Available from: https://www.wiley.com/en-in/Metabolism+at+a+Glance%2C+4th+Edition-p-9780470674710

146. Bradford MM. A rapid and sensitive method for the quantitation of microgram quantities of protein utilizing the principle of protein-dye binding. Anal Biochem. 1976 May 7;72:248–54.

147. Komatsu S. Western Blotting Using PVDF Membranes and Its Downstream Applications. Methods Mol Biol. 2015;1312:227–36.

148. Mahmood T, Yang PC. Western blot: technique, theory, and trouble shooting. N Am J Med Sci. 2012 Sep;4(9):429–34.

149. Porrello ER, Mahmoud AI, Simpson E, Hill JA, Richardson JA, Olson EN, et al. Transient Regenerative Potential of the Neonatal Mouse Heart. Science. 2011 Feb 25;331(6020):1078–80.

150. Kuznetsov AV, Javadov S, Sickinger S, Frotschnig S, Grimm M. H9c2 and HL-1 cells demonstrate distinct features of energy metabolism, mitochondrial function and sensitivity to hypoxia-reoxygenation. Biochimica et Biophysica Acta (BBA) - Molecular Cell Research. 2015 Feb;1853(2):276–84.

151. Lima MF, Amaral AG, Moretto IA, Paiva-Silva FJTN, Pereira FOB, Barbas C, et al. Untargeted Metabolomics Studies of H9c2 Cardiac Cells Submitted to Oxidative Stress, β-Adrenergic Stimulation and Doxorubicin Treatment: Investigation of Cardiac Biomarkers. Front Mol Biosci. 2022 Jun 29;9:898742.

152. Pereira SL, Ramalho-Santos J, Branco AF, Sardão VA, Oliveira PJ, Carvalho RA. Metabolic Remodeling During H9c2 Myoblast Differentiation: Relevance for In Vitro Toxicity Studies. Cardiovasc Toxicol. 2011 Jun;11(2):180–90.

153. Cieślar-Pobuda A, Jain MV, Kratz G, Rzeszowska-Wolny J, Ghavami S, Wiechec E. The expression pattern of PFKFB3 enzyme distinguishes between induced-pluripotent stem cells and cancer stem cells. Oncotarget. 2015 Oct 6;6(30):29753–70.

154. Thirusangu P, Ray U, Sarkar Bhattacharya S, Oien DB, Jin L, Staub J, et al. PFKFB3 regulates cancer stemness through the hippo pathway in small cell lung carcinoma. Oncogene. 2022 Aug 12;41(33):4003–17.

155. Hauck L, Dadson K, Chauhan S, Grothe D, Billia F. Inhibiting the Pkm2/b-catenin axis drives in vivo replication of adult cardiomyocytes following experimental MI. Cell Death Differ. 2021 Apr;28(4):1398–417.

156. Ho KL, Karwi QG, Wagg C, Zhang L, Vo K, Altamimi T, et al. Ketones can become the major fuel source for the heart but do not increase cardiac efficiency. Cardiovascular Research. 2021 Mar 21;117(4):1178–87.

157. Lopaschuk GD, Karwi QG, Ho KL, Pherwani S, Ketema EB. Ketone metabolism in the failing heart. Biochimica et Biophysica Acta (BBA) - Molecular and Cell Biology of Lipids. 2020 Dec;1865(12):158813.

158. Major JL, Dewan A, Salih M, Leddy JJ, Tuana BS. E2F6 Impairs Glycolysis and Activates BDH1 Expression Prior to Dilated Cardiomyopathy. Hsieh PCH, editor. PLoS ONE. 2017 Jan 13;12(1):e0170066.

159. Harms KL, Chen X. Histone Deacetylase 2 Modulates p53 Transcriptional Activities through Regulation of p53-DNA Binding Activity. Cancer Research. 2007 Apr 1;67(7):3145–52.

160. Skurk C, Izumiya Y, Maatz H, Razeghi P, Shiojima I, Sandri M, et al. The FOXO3a Transcription Factor Regulates Cardiac Myocyte Size Downstream of AKT Signaling. Journal of Biological Chemistry. 2005 May;280(21):20814–23.

161. Peng S, Zhao S, Yan F, Cheng J, Huang L, Chen H, et al. HDAC2 Selectively Regulates FOXO3a-Mediated Gene Transcription during Oxidative Stress-Induced Neuronal Cell Death. J Neurosci. 2015 Jan 21;35(3):1250–9.

162. Shimazu T, Hirschey MD, Newman J, He W, Shirakawa K, Le Moan N, et al. Suppression of Oxidative Stress by β-Hydroxybutyrate, an Endogenous Histone Deacetylase Inhibitor. Science. 2013 Jan 11;339(6116):211–4.

163. Cao T, Liccardo D, LaCanna R, Zhang X, Lu R, Finck BN, et al. Fatty Acid Oxidation Promotes Cardiomyocyte Proliferation Rate but Does Not Change Cardiomyocyte Number in Infant Mice. Front Cell Dev Biol. 2019 Mar 22;7:42.

164. Yang X, Rodriguez ML, Leonard A, Sun L, Fischer KA, Wang Y, et al. Fatty Acids Enhance the Maturation of Cardiomyocytes Derived from Human Pluripotent Stem Cells. Stem Cell Reports. 2019 Oct;13(4):657–68.

165. Ong KT, Mashek MT, Bu SY, Greenberg AS, Mashek DG. Adipose triglyceride lipase is a major hepatic lipase that regulates triacylglycerol turnover and fatty acid signaling and partitioning. Hepatology. 2011 Jan;53(1):116–26.

166. Weis E, Puchalska P, Nelson AB, Taylor J, Moll I, Hasan SS, et al. Ketone body oxidation increases cardiac endothelial cell proliferation. EMBO Mol Med. 2022 Feb 18;14(4):e14753.

167. Klement RJ. Beneficial effects of ketogenic diets for cancer patients: a realist review with focus on evidence and confirmation. Med Oncol. 2017 Aug;34(8):132.

168. Jones P, Altamura S, De Francesco R, Paz OG, Kinzel O, Mesiti G, et al. A Novel Series of Potent and Selective Ketone Histone Deacetylase Inhibitors with Antitumor Activity in Vivo. J Med Chem. 2008 Apr 1;51(8):2350–3.

169. Xu S, Tao H, Cao W, Cao L, Lin Y, Zhao SM, et al. Ketogenic diets inhibit mitochondrial biogenesis and induce cardiac fibrosis. Sig Transduct Target Ther. 2021 Feb 9;6(1):54.

170. Zhang Z, Bi X, Lian X, Niu Z. BDH1 promotes lung cancer cell proliferation and metastases by PARP1-mediated autophagy. J Cellular Molecular Medi. 2023 Apr;27(7):939–49.

171. Zhang J, Jia PP, Liu QL, Cong MH, Gao Y, Shi HP, et al. Low ketolytic enzyme levels in tumors predict ketogenic diet responses in cancer cell lines in vitro and in vivo. Journal of Lipid Research. 2018 Apr;59(4):625–34.

172. Han F, Zhao H, Lu J, Yun W, Yang L, Lou Y, et al. Anti-Tumor Effects of BDH1 in Acute Myeloid Leukemia. Front Oncol. 2021 Jun 4;11:694594.

173. Horton JL, Davidson MT, Kurishima C, Vega RB, Powers JC, Matsuura TR, et al. The failing heart utilizes 3-hydroxybutyrate as a metabolic stress defense. JCI Insight. 2019 Feb 21;4(4):e124079.

174. Uchihashi M, Hoshino A, Okawa Y, Ariyoshi M, Kaimoto S, Tateishi S, et al. Cardiac-Specific Bdh1 Overexpression Ameliorates Oxidative Stress and Cardiac Remodeling in Pressure Overload–Induced Heart Failure. Circ: Heart Failure. 2017 Dec;10(12):e004417.

175. Greenwell AA, Gopal K, Altamimi TR, Saed CT, Wang F, Tabatabaei Dakhili SA, et al. Barth syndrome-related cardiomyopathy is associated with a reduction in myocardial glucose oxidation. American Journal of Physiology-Heart and Circulatory Physiology. 2021 Jun 1;320(6):H2255–69.

176. Deng Y, Xie M, Li Q, Xu X, Ou W, Zhang Y, et al. Targeting Mitochondria-Inflammation Circuit by β-Hydroxybutyrate Mitigates HFpEF. Circ Res. 2021 Jan 22;128(2):232–45.

177. Zhang H, He Y, Zhang G, Li X, Yan S, Hou N, et al. HDAC2 is required by the physiological concentration of glucocorticoid to inhibit inflammation in cardiac fibroblasts. Can J Physiol Pharmacol. 2017 Sep;95(9):1030–8.

178. Kee HJ, Eom GH, Joung H, Shin S, Kim JR, Cho YK, et al. Activation of Histone Deacetylase 2 by Inducible Heat Shock Protein 70 in Cardiac Hypertrophy. Circulation Research. 2008 Nov 21;103(11):1259–69.

179. Schlüter C, Duchrow M, Wohlenberg C, Becker MH, Key G, Flad HD, et al. The cell proliferation-associated antigen of antibody Ki-67: a very large, ubiquitous nuclear protein with numerous repeated elements, representing a new kind of cell cycle-maintaining proteins. Journal of Cell Biology. 1993 Nov 1;123(3):513–22.